

Development of a test procedure to study the effect of unilateral load on the posture and trunk biomechanics during walking (Gait) using nonlinear methods

by

Vikas Yadav

A thesis submitted to the Graduate Faculty of
Auburn University
in partial fulfillment of the
Requirements for the Degree of
Master of Science

Auburn, Alabama
December 14, 2013

Keywords: Variability, Range of Motion, Approximate Entropy, Correlation Dimension,
Mean and Median Frequency

Approved by

P. K. Raju, Chair, Thomas Walter Distinguished Professor of Mechanical Engineering
M. Ram Gudavalli, Associate Professor and Director of Biomechanics Core, Palmer College of
Chiropractic
Dan Marghitu, Professor of Mechanical Engineering

Abstract

Low back pain is a common musculoskeletal disorder that affects 80 percentages of people at some point in their lives. In the United States it is the most common cause of job-related disability, a leading contributor to missed work and health care expenditures related to low back pain can be substantial. In recent years, the United States has been facing skyrocketing health care cost, with health care expenditures reaching \$1.2 trillion and accounting for 13.6 percentage of the gross domestic product.

The aim of this study was to develop a test procedure to study the effect of carrying a unilateral load or laptop bag or briefcase on the posture and trunk biomechanics when walking (Gait). The objective was to quantify movements of the trunk during walking using traditional and non-linear methods. The study was approved by the Institutional Review Boards (IRB) of Auburn University, AL as well as the Palmer College of Chiropractic, IA. Nine participants were recruited from the population of the Palmer College of Chiropractic students and employees. All volunteers signed IRB approved informed consent. Data were recorded from 8 healthy participants after being screened for eligibility by licensed clinicians during walking. Participants were asked to walk back and forth at their comfortable speed carrying loads on one hand on the right hand side of 0,5,10, 15, 20, and 25 pounds on a wooden walking platform (5 ft * 8 ft) for a maximum of 30 steps/cycles. Participants walked with self-selected speed to ensure that any potential discomfort is minimized during walking. Motion data were recorded from T1, L1, L3,

and S1 vertebrae at a frequency of 120 Hz. Range of Motion (ROM), Correlation Dimension (CoD), and Approximate Entropy (ApEn) was determined using custom written MatLab programs. EMG data were recorded from six muscle groups bilaterally (right and left): Erector Spinae, Multifidus, Latissimus Dorsi, Internal Obliques, External Obliques and Rectus Abdominis at a frequency of 1200 Hz. For EMG, root mean square EMG values, Mean and Median Frequency of the EMG data were calculated to see the effect of increasing load on muscle fatigue using custom developed MatLab program. Ground reaction force data were collected using a force plate. Vertical ground reaction forces, 1st peak force (Fz1), 2nd Peak force (Fz3) and minimum force (Fz2) between 1st peak and 2nd peak forces were calculated during gait cycle.

The ROM values varied from 2.6 – 3.2 deg. for Lumbar LB, 6.7- 8.7 deg. for Thoracic LB. ApEn values ranged from 0.20-0.40 for Lumbar motion and 0.30– 0.50 for Thoracic motion. No significant difference ($p>0.05$) were found for ROM values and ApEn values for lumbar LB and Thoracic LB as the load increased from 0 lb to 25 lb. And the CoD values ranged from 1.20 – 1.40 for lumbar LB and 1.20-1.30 for Thoracic LB. No significant difference ($p>0.05$) were found for CoD values for Thoracic LB but for Lumbar LB, significant difference ($p<0.05$) were found for CoD values as load increased from 0lb to 25 lb. Normalized GRF (Fz1, Fz2 and Fz3) increased during walking with increased load. No significant difference ($p>0.05$) were found for mean and median frequencies values from muscles activity during walking as load increased from 0lb to 25 lb.

In conclusion, both traditional linear and nonlinear tools were applied successfully to study the spinal motion and trunk muscle activation during walking with increased loads. Our finding revealed that variability of spinal motion did not change significantly during walking as

load increased. Also significance difference ($P < 0.05$) were found for vGRF parameters during walking as load increased. The EMG results (Mean and Median Frequency) indicated that fatigue was not induced during walking in participant's muscles as load increased which might have helped them provide required neuromuscular response to increasing loads.

Future studies are needed to consider some recommendations for obtaining more meaningful data based on healthy subjects. This developed test procedure can apply on low back pain participants may provide results helpful for low back pain treatment. Data acquisition part needs to be smoother. Wireless EMG electrodes and motion sensor can be used to avoid noise in data captured because of wires sway during walking. The test procedure developed from this study need to be fine tuned before it can be applied on larger population.

Acknowledgments

I would like to express my deep gratitude to my academic advisor, Dr. P. K. Raju, for providing me with the opportunity to work under him on this project. I would also like to thank Dr. M. Ram Gudavalli for being a co-advisor and great mentor and guide during my work at Palmer Center for Chiropractic Research, IA. Also, a special thank you to Dr. Dan Marghitu for all the help they have provided to me during my study period at Auburn University. I would also like to special thanks to Dr. Xia Ting who provided valuable technical help during my work at Palmer Center for Chiropractic Research, IA. I would also like to express my deep gratitude to all clinician and other staff who provided valuable help during my work at Palmer Center for Chiropractic Research, IA. I also appreciate the help provided by Ms. Anna Hewlett in IRB process and editing the draft of the thesis.

I would like to thank my parents, Mr. Jai Bhagwan and Mrs. Nirmala Devi, as well as my family, for having faith in me and providing love, encouragement and moral support. I would also like to thank all my friends and colleagues for their priceless friendship and support.

I gratefully acknowledge the financial support during my studies from grant #'s U19AT004663 and U19AT004137 National Center for Complementary and Alternative Medicine (NCCAM), National Institutes of Health. The investigation was conducted in a facility constructed with support from Research Facilities Improvement Program Grant number C06 RR15433-01 from the National center for Research Resources, National Institutes of Health.

Table of Contents

Abstract	ii
Acknowledgments	iii
List of Tables	vii
List of Figures	ix
List of Abbreviations	xiii
Chapter 1 Introduction	1
1.1 Low Back Pain	1
1.2 Variability	2
1.3 Quantification of Variability.....	3
1.3.1 Linear Methods	3
1.3.2 Nonlinear Methods.....	4
1.4 Spinal motion during walking.....	8
1.5 Ground Reaction Forces (GRF) during walking carrying loads.....	12
1.6 EMG measurements during walking carrying loads.....	15
1.7 Objective.....	20
Chapter 2 Anatomy of Human Spine	21
2.1 The Vertebral Column	21
2.1.1 Thoracic Vertebrae.....	23
2.1.2 Lumbar Vertebrae	24

2.1.3 Sacrum Vertebrae.....	25
2.2 Low Back Muscles.....	26
2.2.1 Erector Spinae.....	26
2.2.2 Multifidus.....	27
2.2.3 Latissimus Dorsi	28
2.3 Abdominal Muscles	29
2.3.1 External Obliques.....	29
2.3.2 Internal Obliques.....	29
2.3.3 Rectus Abdominis.....	31
Chapter 3 Methods and Techniques Used	33
3.1 Subjects Selection	34
3.2 Inclusion/Exclusion Criteria	36
3.3 Preparation	37
3.4 Data Acquisition	37
3.5 Data Analysis	41
3.5.1 Motion Data Analysis	41
3.5.1.1 Time series	41
3.5.1.2 State Space	44
3.5.1.3 Time Lag	47
3.5.1.4 Embedding Dimension	49
3.5.1.5 Correlation Dimension	50
3.5.1.6 Quantify Correlation Dimension.....	52
3.5.1.7 Approximate Entropy	57

3.5.1.8 Calculation of Approximate Entropy	57
3.5.2 EMG Data Analysis	60
3.5.2.1 Identifying Muscles activation	60
3.5.2.2 Fast Fourier Analysis.....	60
3.5.2.3 Power spectral density	62
3.5.2.4 Sampling Frequency	63
3.5.2.5 Mean and Median Frequency of SEMG signals	64
3.5.3 Ground Reaction Force (GRF).....	65
Chapter 4 Results	68
4.1 Ground Reaction Force	68
4.2 EMG.....	75
4.3 Approximate Entropy (ApEn).....	85
4.4 Correlation Dimension (CoD).....	91
4.5 ROM	93
Chapter 5 Discussion	96
Chapter 6 Conclusions	109
References	111
Appendix	118

List of Tables

Table 1 Demographics Data.....	36
Table 2 EMG Sensor Placement.....	40
Table 3 Vertical GRF (N) during walking carrying different loads	69
Table 4 Normalized vGRF during walking carrying different loads	69
Table 5 Average Time during different phases of gait	73
Table 6 Muscles recruitment during Walking by number of participants	76
Table 7 Mean (SD) values of Mean Frequencies during walking with increasing loads	83
Table 8. p-values for mean frequency.....	83
Table 9. Mean (SD) values of Median Frequencies during walking with increasing loads	84
Table 10. p-values for medianFrequency.....	85
Table 11. ApEn values for Lumbar FE, LB, and ROT	86
Table 12. one-way ANOVA test for ApEn values for Lumbar FE, LB & ROT vs increasing loads	88
Table 13. ApEn values for Thoracic FE, LB, and ROT	89
Table 14. one-way ANOVA test for ApEn values for Thoracic FE, LB & ROT vs increasing loads	90
Table 15. mean (SD) of CoD for lumbar LB and Thoracic LB during walking with increased loads from all subjects	91
Table 16. one-way ANOVA test for CoD values for Lumbar LB vs increasing loads	92

Table 17. one-way ANOVA test for CoD values for Thoracic LB vs increasing loads.....	92
Table 18. mean (SD) values for ROM for Lumbar LB and Thoracic LB during walking with increased loads	93
Table 19. p-values for ROM.....	95

List of Figures

Figure 1 The Vertebral Column (Wikipedia.com).....	21
Figure 2 Thoracic Vertebra (Wikipedia.com).....	23
Figure 3 Lumbar Vertebra (Wikipedia.com)	24
Figure 4 Sacrum Vertebra (Wikipedia.com).....	25
Figure 5 Erector Spinae (Wikipedia.com)	26
Figure 6 Multifidus (Wikipedia.com).....	28
Figure 7 Latissimus Dorsi (Wikipedia.com).....	28
Figure 8 Abdominal Muscles (Wikipedia.com).....	30
Figure 9 sEMG and motion sensors attached to back muscles and vertebrae ...	39
Figure 10 sEMG sensors attached to abdominal muscles.....	39
Figure 11 Participant with Load	40
Figure 12 Time series for Sine Curve	43
Figure 13 Time series for Walking with 25 lb load for Lumbar LB for subject 4.....	43
Figure 14 Time series for Walking with 25 lb load for Thoracic LB for subject 4	44
Figure 15 Example of standard phase space	45
Figure 16 Phase space plot for periodic, chaotic, and random time series.	46
Figure 17 Pseudo phase space plot of experimental data	47
Figure 18 Time lag during walking without any loads for Lumbar LB for subject 4.....	49
Figure 19 Embedding Dimnesion during walking for Lumbar LB for subject 4	50

Figure 20 CoD during walking without load for Thoracic LB for subject 4	52
Figure 21 Identifying qualifying neighbors from (a) point 1 and (b) point 2	53
Figure 22 Correlation Sum vs. Radius for increasing Embedding Dimension.....	55
Figure 23 Hypothetical behavior of correlation dimension with increase in embedding dimension, for chaotic as compared to random data.....	56
Figure 24 FFT of a periodic sine curve.....	61
Figure 25 FFT of experimental motion data.....	62
Figure 26 PSD for ES Left during walking with 10 lbs for participants 7....	63
Figure 27 Ground Reaction Force.....	65
Figure 28 Identification of the four functional phases	66
Figure 29 GRF vs % Gait Cycle	67
Figure 30 1 st peak Force a) vGRF (N) and b) Normalized vGRF during walking carrying varying loads	70
Figure 31 2 nd peak Force a) vGRF (N) and b) Normalized vGRF during walking carrying varying loads.....	71
Figure 32 3 rd peak Force a) vGRF (N) and b) Normalized vGRF during walking carrying varying loads.....	72
Figure 33 vGRF (N) vs. % Gait Cycle during walking carrying varying loads	74
Figure 34 ES Left – Mean Frequencies and Median Frequencies during walking with varying loads	77
Figure 35 ES Right - Mean Frequencies and Median Frequencies during walking with varying loads.....	77
Figure 36 EO Left - Mean Frequencies and Median Frequencies during walking with varying loads	78
Figure 37 EO Right - Mean Frequencies and Median Frequencies during walking with varying loads	78

Figure 38 IO Left - Mean Frequencies and Median Frequencies during walking with varying loads	79
Figure 39 IO Right - Mean Frequencies and Median Frequencies during walking with varying loads	79
Figure 40 RA Left - Mean Frequencies and Median Frequencies during walking with varying loads	80
Figure 41 RA Right - Mean Frequencies and Median Frequencies during walking with varying loads	80
Figure 42 LD Left - Mean Frequencies and Median Frequencies during walking with varying loads	81
Figure 43 LD Right - Mean Frequencies and Median Frequencies during walking with varying loads	81
Figure 44 MF Left - Mean Frequencies and Median Frequencies during walking with varying loads	82
Figure 45 MF Right - Mean Frequencies and Median Frequencies during walking with varying loads	82
Figure 46 ApEn results for Lumbar Flexion Extension during increasing loads	86
Figure 47 ApEn results for Lumbar Lateral Bending during increasing loads.....	87
Figure 48 ApEn results for Lumbar Rotation during increasing loads.....	87
Figure 49 ApEn results for Thoracic FE.....	89
Figure 50 ApEn results for Thoracic LB	89
Figure 51 ApEn results for Thoracic ROT	90
Figure 52 CoD results for Lumbar LB.....	91
Figure 53 CoD results for Thoracic LB.....	92
Figure 54 ROM vs. Loads a) Lumbar LB Right Step b) Lumbar LB Left Step.....	94
Figure 55 ROM vs. Loads a) Thoracic LB Right Step b) Thoracic LB Left Step.....	95
Figure 56 Mean and Median Frequency results for LD Left muscle for participant 5 during walking.....	103

Figure 57 Mean and Median Frequency results for ES Right muscle for participant 8 during walking.....104

Figure 58 vGRF profile.....106

List of Abbreviations

ApEn	–	Approximate Entropy
CoD	–	Correlation Dimension
EO	–	External Obliques
ES	–	Erector Spinae
FE	–	Flexion Extension
IO	–	Internal Obliques
LB	–	Lateral Bending
LD	–	Latissimus Dorsi
MF	–	Multifidus
RA	–	Rectus Abdominis
ROT	–	Rotation
sEMG	–	Surface Electromyography
vGRF	–	Vertical Ground Reaction Forces

CHAPTER 1

INTRODUCTION

1.1. Low back pain

Low back pain is a common musculoskeletal disorder that affects 80% of people at some point in their lives [29]. In the United States it is the most common cause of job-related disability, a leading contributor to missed work and health care expenditures related to low back pain can be substantial. In recent years, the United States has been facing skyrocketing health care cost, with health care expenditures reaching \$1.2 trillion and accounting for 13.6% of gross domestic product [2, 60].

Although, most occurrences of low back pain go away within a few days, others take much longer to resolve or lead to more serious conditions. Low back pain can be caused by injury or over use of muscles, ligament and joints and may be triggered by repeated vibration or motion during athletics or every day activities. Most of the time; it is due to a sprain or strain in the muscles and soft tissues of the back and aging is often a factor. Low back pain is categorized as either acute, sub chronic or chronic. Acute low back pain last from few days to several weeks and is generally mechanical in nature. It may be caused by a sports injury, work around the house or in the garden, or a sudden jolt such as a car accident or other stress on spinal bones and tissues. Symptoms may range from muscle ache to shooting or stabbing pain, limited flexibility and/or range of motion, or an inability to stand straight. Low back pain that lasts for 2 to 3

months is considered sub-chronic. Low back pain that lasts for more than 3 months is considered chronic. It is often progressive and the cause can be difficult to determine [2].

Roy [73] highlighted the clinical need for an objective technique to assess the muscle dysfunction associated with chronic lower back pain went on to examine the reliability and validity of his proposed technique by testing both chronic low back pain patients and control subjects without back pain. Median frequency parameters of the EMG power density spectrum were monitored to quantify localized muscle fatigue and Roy reported high reliability estimates for repeated trials. He observed significant differences (P less than 0.05) in median frequency parameters between lower back pain patients and control subjects for specific combinations of contractile force level and muscle site tested and Median Frequency parameters correctly classified lower back pain and control subjects using a two-group discriminate analysis procedure [73].

Life is becoming ever more hectic nowadays and laptop computers have become essential tools for many people with both professional and students using them every day. Carrying a laptop unilaterally on a regular basis may seriously affect on body characteristics; laptop bags are generally single strap bags, carried over one shoulder and the weight of the laptop can cause considerable low back pain and strain on the shoulder muscles as well as restricting blood flow, and pinching nerves. Carrying a laptop bag daily for long periods of time can cause poor walking posture placing strain on several different parts of the body especially the back. This may be particularly important of younger people: a study conducted at Auburn University reported that book bags that are too heavy for their wearers may threaten developing spines [1].

1.2. Variability

Variability is a central characteristic of all human movement and is the result of random processes. As Giakas et al. [42] said “Variability is a natural phenomenon associated with any movement over repeated trials”. Some degree of variation is inherent within all biological systems and can be characterized as the normal changes that occur in motor performance across multiple repetitions of tasks. The variability in kinematic, kinetic and temporal variables can be computed using both traditional and non-traditional approaches. Goldberger and colleagues suggested that every healthy system has a certain amount of variability that is not random but contains order, and can be characterized via nonlinear descriptors. Consequently, nonlinear methods have increasingly been used to describe complex conditions that cannot be well characterized by linear tools [42]. Range, standard deviation, variance, and coefficient of variance are commonly used measures variability analyses. Range is the difference between the largest and smallest observations; variance is the mean of the squared deviations of a set of measurements, and standard deviation is the square root of the variance. Coefficient of variation is defined as the ratio of the standard deviation to the mean and is given as a percentage. Not surprisingly, people suffering from low back pain perform differently from people without low back pain during functional tasks.

1.3. Quantification of variability

1.3.1. Linear Methods

Masani [54] investigated the variability of ground reaction forces during treadmill walking at different speeds. Three components of the GRF were recorded for 35 consecutive steps for each leg. Five indexes (the first and second peaks of F_z , the first and second peaks of F_y , and the F_x peak where F_z , F_y and F_x represent the x, y and z component of GRF respectively) were defined. Coefficients of variation were calculated for each of these five

indexes to evaluate the GRF variability for each walking speed. The results showed that the variability of F_z and F_x increased with incremental increases in walking speed, whereas there was a speed (5.5–5.8 km/h) at which variability was at a minimum for the first and second peaks of F_y , and these were related to forward propulsion of the body [54].

Ten year later Simpson studied the effect of vertical load position on the gait and subjective responses of female hikers. Although, load carriage has been linked an enhanced risk of musculoskeletal disorders in the back and upper limbs in hikers. Simpson found that neither high, medium nor low load positions could be preferentially recommended for healthy, experienced, female hikers carrying 30% of their body weight. Instead, the hikers should choose the load position they find the feel most comfortable [53]).

At about the same time, Qu [85] studied the effect of load carriage and fatigue on gait characteristics utilizing both gait variability measures and kinematics measures. This study found that gait width variability, hip range of motion and trunk range of motion increased with fatigue and with a heavy load. These findings clearly illustrate how increasing load and fatigue can affect gait characteristics.

It has been argued that asymmetric loading during walking can increase lower limb joint stress and will also affect dynamic balance. Matsuo investigated balance is affected by asymmetric load-carrying and how loading affects lower limb coordination during gait among different age group. The study showed that the contralateral hip abduction torque increased and ipsilateral hip torque decreased in all participants when carrying an asymmetric load. Those in the oldest group of abducted their shoulders to a greater extent even when walking without a bag [79].

1.3.2. Nonlinear Methods

Nonlinear tools are becoming more popular as a way to examine the variability in human movement as linear models are limited in many cases and are certainly not the best models for understanding the nonlinear human system [23]. The commonly used nonlinear methods include Lyapunov Exponents, Approximate Entropy, and Correlation Dimension. The Lyapunov Exponent approach calculates the rate at which adjacent trajectories converge or diverge in reconstructed state space. Approximate Entropy (ApEn) calculates the predictability of a given time series, and Correlation dimension is quantifies chaos in given time series [23, 46, 51, and 80]. Approximate Entropy measures the logarithmic probability that a series of data points a certain distance apart will exhibit similar relative characteristics on the next incremental comparison within the state space. Two main parameters are needed to calculate ApEn: m , the number of observation windows to be compared and r , the tolerance factor. Generally $m=2$ for all ApEn calculations while r ranges from 0.1 to 0.25 SD of the data. ApEn provides a direct measurement of feedback and connection. A low ApEn value often indicates predictability and high regularity of time series data, whereas a high ApEn value indicates unpredictability and random variation [22, 68, and 69].

Many researchers have investigated human motion using nonlinear tools but although many studies have examined the effect of increased speed on the human gait using nonlinear methods, little research has focused on changes in human gait with different form of loads using nonlinear tools.

Ahsan Khandoker conducted a comparative study on approximate entropy measure and Poincaré plot indexes of minimum foot clearance variability in the elderly during walking. Minimum Foot Clearance (MFC) data was gathered during treadmill walking for 14 healthy

elderly and 10 elderly participants with balance problems and a history of falls (risk of falls) and analysed using a PEAK-2D motion analysis system. ApEn and Poincaré plot indexes of all the MFC data sets were calculated and compared. Khandoker found significant relationships for the mean MFC with ApEn ($r = 0.74$, $p < 0.05$) in the elderly group at risk of falling as compared to the healthy elderly group. The ApEn values in the risk of falls group (mean ApEn = 0.18 ± 0.03) were significantly ($p < 0.05$) higher than in the healthy group (mean ApEn = 0.13 ± 0.13). The higher ApEn values in the risk of fall group could indicate increased irregularities and randomness in their gait patterns and an indication of loss of gait control mechanism. Khandoker suggested that ApEn analysis of MFC might provide a valuable opportunity to initiate pre-emptive measures to avoid injurious falls [22].

Another researcher who used nonlinear analysis methods to analyze gait parameters, Ugo H. Buzzi et al 2003 measured the variability present in time series generated from gait parameters in a comparison of young and elderly females subjects using nonlinear methods. Aging may cause some changes in motor variability during walking which may explain falls in elderly. Buzzi's finding revealed that the Lyapunov exponents differed significantly between the two age groups, with the elderly participants demonstrating significantly larger Lyapunov exponents and correlation dimensions for all the parameters evaluated indicating local instability. Linear measures indicated that the elderly demonstrated significantly higher variability, while the nonlinear analysis revealed that the fluctuations in the time series of certain gait parameters were not random but displayed a deterministic behavior. Buzzi & Ulrich went on to study the dynamic stability of gait cycles as a function of speed and system constraints in children. The stability of the lower extremity segments of preadolescent children (8–10 years old) with and without Down syndrome (DS) were evaluated as the children walked on a motorized treadmill at varying

speeds. Nonlinear dynamics tools, maximum Lyapunov exponent, and approximate entropy were used. Their finding suggested that dynamic stability decreased during walking in all segments for the children with DS and that this could be a consequence of inherently different subsystem constraints compared to their non-DS peers. [80]

Dingwell et al. [34] examined changes in local dynamic stability associated with ground and treadmill walking in healthy adults. Their results showed a poor correlation between nonlinear and traditional measures for both ground and treadmill conditions, suggesting that nonlinear measures quantify different aspects of walking behavior than traditional measures. They argued that traditional discrete measures of variability do not provide an accurate means for assessing the stability of the locomotor system, because they masked stride-to-stride fluctuations, and that nonlinear measures could be more appropriate for addressing questions related to the control of locomotor stability and balance.

England & Granata et al. 2007 investigated the role of walking velocity in stability during normal gait by measuring local dynamic stability using maximum finite-time Lyapunov (λ max) exponents where as smaller λ max indicate more stable walking dynamics. Their results suggested that slower walking velocities lead to increases in stability and this approach may expose more comprehensive information on the behavior of the neurocontroller than variability-based analyses alone.

Justin J Kavanagh et al. [51] examined the effect of walking speed on an individual's lower trunk motion. Subjects performed 5 walking trials at a self-selected pace: slow, preferred and fast. A triaxial accelerometer was used to collect data from the muscles involved. Stride-to-stride acceleration amplitude, regularity and repeatability were examined with RMS acceleration, Approximate Entropy and Coefficient of Multiple determination respectively. The study showed

that RMS acceleration amplitude increased with gait speed in all directions, while the value of Approximate Entropy decreased as the walking velocity increased. Walking at speeds slower than preferred primarily altered lower trunk accelerations in the frontal plane. Despite greater amplitudes of trunk acceleration at fast speeds, the lack of regularity and repeatability differences between the preferred and fast speeds suggested that features of trunk motion are preserved between the same conditions.

James T Cavanaugh et al. [46] examined the short term effect of secondary cognitive task performance on postural control in healthy young adults calculating ApEn values, root mean square (RMS) displacement, and equilibrium scores (ES) from anterior posterior (AP) and medial-lateral (ML) center of pressure (COP) component time series. There was no significant effect of cognitive task for either the ApEn values of COP ML time series, the RMS displacement (AP or ML) or ES and Cavanaugh concluded that utilizing ApEn as a measure for characterizing the temporal dynamics of COP variability shows promise for detecting the immediate, short-term effect of secondary cognitive task performance on postural control during quiet standing, even among healthy subjects whose postural sway in this position is minimal.

Anastasios et al. [23] examined the variability of the ACL deficient knee during walking. Data were collected from 10 subjects (diagnosed with complete ACL rupture using MRI scans volunteered for the ACL deficient group) during walking on a treadmill at a self-selected speed with the variability assessed using ApEn. Their results showed that significantly smaller ApEn values were observed in the subjects with an ACL deficient knee for all speeds ($p=0.022$) and these ApEn values increased significantly with increasing walking speed. The altered properties of the ACL deficient knee, which exhibits more regular and less variable patterns than the

contralateral intact knee, may decrease the adaptability of the system rendering it less able to adjust to perturbations.

1.4. Spinal motion during walking

Many researchers are now focusing on the effect of low back pain on trunk movements, but although there has been considerable research into spinal motion during walking, few studies have looked at spinal motion during walking with different forms of loads. Instead the spine is generally treated as either a whole unit or as a set of different segments, such as the lumbar segment and thoracic segments of the spine. Kinematic and kinetic quantities are usually assumed to be periodic or pseudo periodic based on body characteristics and personal ability to control the lumbar spine. However, with neuromuscular and musculoskeletal pathologies or injuries, these movements may not be periodic and may result in increased instability of the lumbar spine [67]. The effect of age, load amount and load symmetry on lower extremity kinematics during different carrying tasks was studied by Gillette whose subjects carried loads of 0 %, 10% and 20% of their body weight either unilaterally or bilaterally. Reflective markers were used to collect the data and total joint ROM and maximum joint angle were calculated. The child/teenager age groups displayed significantly greater maximum hip extension, hip adduction, and hip internal rotation angles than adults. Although, setting carrying guidelines for the 8-10 year old group appeared to be particularly critical since this age group was tested at lower loads than commonly observed in the field, they still displayed the greatest maximum hip internal rotation angles [47].

Fowler et al. [38] quantified the kinematics of the spine and stature loss induced by asymmetric load carriage. Data were collected from 6 healthy males walking at their self-selected pace for 8500 m with and without a standard RoyalMail bag (model MB36) containing

17.5% of the participant's body mass. The load was reduced gradually during the task. Increased forward leaning (up to 6 degree) and lateral bending of the spine (up to 12 degree) was observed with a load. Thoracic adjustments occurred in the sagittal plane, while changes in the lumbar area occurred in the frontal plane.

Crosbie et al. 1995 & 1997 investigated the patterns and ranges of movement of the lower thoracic and lumbar spinal segments and the pelvis in subjects walking at two self-selected speeds. In this analysis, the spine was divided into lower thoracic, lumbar and pelvic segments and data were recorded using a video-based system. Crosbie observed an increased range of motion in each segment with increased walking speed, although there were few gender-related differences in patterns or ranges of motion and a significant reduction in spinal range of motion with advancing age. He considered that these age-related changes were more likely to be step-length dependent than an intrinsic feature of aging [31, 32].

Malgorzata [62] studied the segmental movement patterns of the spine during normal treadmill walking task with the spine movement of ten healthy subjects has being investigated using an optoelectronic measuring system. In this study, the spine was divided into seven segments, from C7 to S2 and the subjects walked with their normal speed. All data were normalized to percentage of the gait cycle and the normal patterns of the spine segment movements were observed in the sagittal and frontal planes. Malgorzata's results showed that the behavior of the spine can be described as the motion of a stiff element with superimposed small, inter-segmental movements. These small inter-segmental movements were found both in the sagittal and the frontal planes. The small inter-segmental movements could play an important role in reducing of the energy consumption during motion and in maintaining the equilibrium.

Rowe and White developed a new system for the clinical measurement of spinal kinematics during gait and demonstrated its use to measure the motion of lumbar spine during level, free, and speed, walking in a group of ten nurses returning to work following one or more episodes of mild musculoskeletal back pain. Their results implied that the nurses tested had normal gait patterns [72].

Devroey studied the effects of increasing load (0%, 5%, 10%, and 15% of body weight) and changing the placement of the load on the spine (thoracic vs. lumbar placement) during standing and walking in 20 college-aged students by collecting physiological, biomechanical and subjective data. Their results indicated significant increases in thorax flexion; reduced activity of M. erector spinae vs. increased activation of abdominals; and increased heart rate and Borg scores for the heaviest loads. A trend towards increased spinal flexion reduced pelvic anteversion and rectus abdominis muscle activity was observed for the lumbar placement. These findings suggest that carrying loads of 10% of body weight and above should be avoided, since these loads induce significant changes in electromyography, kinematics and subjective scores in the study participants. [30]

Frigo [39] studied the physiological pattern of trunk and shoulders movements during walking in order to provide a reference for further studies on spine deformities. Data were recorded from 18 young, healthy female participants using retroreflective markers positioned on the main spine processes and acromions to be detected by a TV-based motion analysis system. Movements in the main reference planes and in relation to the pelvis were analyzed. Frigo's results showed that the trunk was on average bent forward by 3.4 degree compared to the standing position; of the two physiological curves in the sagittal plane only lordosis changed during walking. In the frontal plane, however, a dynamic spine deformation appeared that was at

a maximum at the heel strike-early stance; the trunk was bent contralaterally of the foot on the ground, while the shoulders remained stable and in the horizontal plane, the shoulders rotated contralaterally to the pelvis. In the sample population, all the segmental movements analyzed were smaller than 5 degree during gait except for the angle of proximal curvature in the frontal plane, shoulder rotation, and the angle between shoulders and pelvis. All the measured angles were far below their possible ranges of motion.

1.5. Ground reaction forces (GRF) while carrying unilateral loads

Carrying an asymmetric load while walking is a common activity and a regular part of daily life. However tasks such as carrying a laptop unilaterally on daily basis may have a deleterious effect on body characteristics. Laptop bags, for example are generally single strap bags designed to be carried over one shoulder. Unilateral load carrying is known to be more hazardous to the musculoskeletal system than a bilateral load and has been shown to cause increased trunk muscle activity (Devita et al. 1991) and greater spinal shear and compressive forces (Marras and Granata et al. 1997), thus potentially contributing to the development of dorsal and low back pain. Such loads can encourage the lateral bending of the spine. The weight of the laptop can cause considerable low back pain, strain on the shoulder muscles, restricting blood flow, and pinching nerves. Carrying a laptop bag day after day for long periods of time can lead to poor posture when walking, placing strain on several different parts of the body, but especially the back. This is particularly a concern in young people. A study conducted at Auburn University reported that book bags that are too heavy for their wearers may threaten developing spines. [1]

Many researchers have studied the effects of carrying a backpack or other athletics bag or unilateral and bilateral load on musculoskeletal pain and altered spinal curvature. [36, 47, 53, 79,

and 85]. People face unilateral load-carrying conditions every day when they carry things in one-hand. There have also been a great many studies focusing on gait at different speed but few studies have combined the two to examine the effect on gait of different loads.

Unilateral load carriage is known to be more hazardous to the musculoskeletal system than bilateral loading. Zhang examined the effect of asymmetric carriage on postures and gait symmetry by recording the ground reaction force (GRF) during walking. Kinematics and GRF for 19 adults were recorded while walking under five load conditions: no load and a dumbbell (weighing 10 and 20% of their body weight) held in either the right or left hand. The vertical ground reaction forces increased with increasing loads. [84]

An [36] examined the gait parameters of young women using various methods to carry a single-strap bag while walking. The bag-carrying methods were no bag, over the shoulder, on the forearm and by hand. An conducted that when carrying a single-strap bag, the over-the-shoulder method has the least effect on gait parameters relative to other bag carrying methods.

The study of ground reaction forces (GRF) during load carriage can provide relevant information about the mechanisms of gait, and provide a measure of the impact forces acting on the foot. Load or weapon carriage is an essential and inevitable part of military life and many studies have looked at how soldiers carry heavy loads [25, 33, 43, and 78]. For example, Birrell reported that rifle carriage during walking significantly affects the ground reaction forces. Data were collected from 15 participants walking with different loads on an 8.4 m walkway. Kinetic data were normalized and expressed as Newton's per unit body mass. Birrell found that both vertical and anteroposterior GRF parameters increase proportionally when load is added in 8 kg increments to a UK standard issue '90 Pattern LCS. A similar study by Majumdar [33] evaluated kinematic responses to existing load carriage operations and provided guidelines for the future

design of heavy military backpacks (BPs) to enhance soldier's performance. Walking trials were recorded using 3-D Motion Analysis System. Significant increases were observed in ankle and hip ROM and trunk forward inclination ($\geq 10^\circ$) with lighter loads, such as a BP (10.7 kg), BP with rifle (14.9 kg) and BP with a light machine gun (17.5 kg), may cause joint injuries. These findings suggest that the existing BP design could be improved for use in low intensity conflict environments and the data gathered could help optimize load carriage and the design of ensembles, especially a more user-friendly heavy BP for military operations.

Wang investigated the influence of load carriage and muscular fatigue on ground reaction forces and ground reaction loading rates during walking. Data were collected from 18 healthy males during the following tasks: unloaded and unfatigued walking, loaded and unfatigued walking, fatiguing exercise, loaded and fatigued walking, and unloaded and fatigued walking. They found that muscular fatigue and load carriage both have a significant effect on peak vertical ground reaction force and loading rate ($p < 0.01$). The resulting large increases in the ground reaction forces and loading rates may contribute to the high incidence of lower extremity overuse injuries in the military. [43]

Kinoshita studied the effects of two different systems on selected biomechanical parameters of the walking gait, while carrying loads of varying magnitude. The three components of the ground- reaction-force were measured for ten trials for each subject condition using a Kistler force platform interfaced to a Tektronix computer. And the components of the ground-reaction-force-time curves examined. Their results revealed that both light and heavy loads substantially modified the normal walking gait pattern and suggested that the double pack system was more effective than the conventional backpack system, especially for carrying heavy load. [44]

The effect of gait speed and load carrying on the reliability of ground reaction forces were studied by Hsiang [76] who collected data from 15 participants walking on a treadmill under fifteen conditions (five load positions X three speeds) by recording the vertical ground reaction forces for a number of consecutive steps. The first four statistical moments (i.e. mean, standard deviation, skewness and kurtosis) of the distributions of several kinetic parameters were calculated based on the series of recorded steps. Hsiang's result suggested that adding a 30-lb load to various parts of the body and increasing the walking speed generally increase the magnitude of WA (Fz1) and PO (Fz3) the mean value of WA also increased as the speed increased from 2 to 4 mph. In addition, WA had the highest value for two-hand carrying and the lowest in the no-load conditions at any speed. Changes in the higher moments suggested that some loading positions and higher speeds reduced the reliability of the execution of gait patterns while other loading positions may actually increase the reliability [76]. In a similar study, Bas Kluitenberg et al. 2012 compared the vertical ground reaction forces during ground and treadmill running.

McCrary compared the VGRF of a group of subjects who had undergone hip arthroplasty with a group of normal control subjects. Data were collected using a treadmill equipped with two force plates (Kistler Instrument Corporation, Amherst, NY) during walking. GRF parameters such as loading force (first peak), push off (2nd peak), loading rate, push off rate and so on were calculated. The first and second peak forces, loading rate, impulse, and stance time were significantly lower, while the time to first peak force was significantly greater on the affected leg of the hip arthroplasty subjects when compared to both their unaffected leg, or to the control group. The hip arthroplasty group also showed greater asymmetry of ground reaction forces than

the control group so bilateral asymmetric limb loading clearly persists well after unilateral hip replacement surgery. [48]

1.6. EMG measurements during walking and carrying weights

Electromyography (EMG) is a technique that is widely used for evaluating and recording the electrical activity produced by skeletal muscles. EMG is performed using an instrument called an electromyograph, to produce a record called an electromyogram. An electromyograph detects the electrical potential generated by muscle cells when these cells are electrically or neurologically activated. The signals can be analyzed to detect medical abnormalities, activation level, and recruitment order or to analyze the biomechanics of human or animal movement. EMG is frequently used to capture muscle activity during different motor tasks. Two kinds of EMG are currently available: surface EMG and intramuscular (needle and fine-wire) EMG. [9]

EMG frequencies can be recorded during functional activities such as walking in order to evaluate muscle functions. Nissan Kunju (2009), Van Gestel (2011), and Joseph Mizrahi found the range for mean and median frequency was in between 60-140 Hz during different functional activities.

Kunju [56] discussed the use of EMG for analyzing different phases of walk by acquiring the surface EMG from the gastrocnemius and soleus muscles of the leg with the subjects walking at two self-selected paces- fast and slow. The median frequency decreased with increasing walking speed in both muscles. The RMS value of the signal amplitude tended to increase from the slow to the fast walk for both muscles in both limbs which can be attributed to the increase in motor activity with increasing speed of movement.

Prosser and Gestel investigated muscle activity during walking in young children with cerebral palsy (CP) compared with children with typical development (TD). They looked the

potential of the muscle activation and mean EMG frequency, recorded during 3D gait analysis (3DGA), in order to evaluate the functional muscle strength. In both muscles a consistent pattern of increasing mean EMG frequency with decreasing muscle strength was observed. It seems likely that both walking velocity and muscle strength have an impact on EMG, but the contribution of muscle strength is always higher. [58, 70]

Joseph [50] studied the EMG activity and fatigue patterns of iliocostalis lumborum and multifidus muscles during a trunk holding test. To reflect the activity level and fatigue rate of the muscles, EMG amplitude (RMS values) and a frequency variable (median frequency [MF]) were measured. He found that monitoring frequency changes in the EMG signals may enable therapists to quantify the fatigue changes of individual muscles during the trunk holding test. The higher fatigue rate shown in the multifidus muscle compared with the iliocostalis lumborum muscle may be due to the higher activity level of the multifidus muscle during the trunk holding contraction. This greater activity of the multifidus muscle during the contraction might be explained by the functional differences between these two muscles.

Sabut (2010) examined the effect of functional electrical stimulation (FES) in the management of drop foot in stroke subjects with surface electromyographic (sEMG) analysis from the tibialis anterior (TA) muscle. Sabut's results revealed an increase in the mean-absolute-value (MAV), and RMS and also improved the amplitude (0.022 to 0.048) and median frequency (MF 71.4 Hz to 82.7 Hz) of the sEMG power spectrum when monitoring the improvement of the tibialis anterior muscle during maximum voluntary contractions [74].

Hong [86 and 87] investigated the effect of prolonged walking with load carriage on muscle activity and fatigue in children. EMG signals from the upper trapezius (UT), lower trapezius (LT) and rectus abdominis (RA) were recorded at several time intervals (0, 5, 10, 15

and 20 min) while carrying different loads and were normalized to the signals collected during maximum voluntary contraction. Power spectral frequency analysis was applied to evaluate muscle fatigue in terms of the shift in median power frequency (MPF). Their results showed that both the 15% and 20% body weight loads significantly increased muscle activity in the lower trapezius. In the upper trapezius, no increase of muscle activity was found within the 20-min period, although, muscle fatigue was observed from 10 min onwards. No increased muscle activity or muscle fatigue was found in rectus abdominis. They concluded that that backpack loads for children should be restricted to no more than 15% of their body weight for walks of up to 20 min duration to avoid muscle fatigue.

Olsen [64] investigated prolonged physical activities that could introduce risks for low back injury due to the adapted neuromuscular response of the system once neuromuscular fatigue is present. Trunk extensor muscles were fatigued in 14 healthy women to observe myoelectric changes in the trunk musculature during walking trials performed before and after fatigue conditions. EMG from the lumbar paraspinal (LP), rectus abdominis (RA), external oblique (EO) muscles were recorded during fatigue conditions and pre and post fatigue walking trials. Their results revealed that LP and RA activity burst peaks shifted in time at contralateral heel contacts ($p < 0.05$) in the 70% condition, while RA amplitude increased ($p < 0.05$) and EO burst peak temporal shifts ($p < 0.05$) were present in the 50% condition.

Escamilla [71] studied the effectiveness of traditional and nontraditional abdominal exercises in activating abdominal and extraneous musculature. Surface EMG were used to capture muscle activity from the upper and lower rectus abdominis, external and internal oblique, rectus femoris, Latissimus dorsi and lumbar paraspinal muscles while each exercise was performed. The Power Wheel, hanging knee-up with straps, and reverse crunch inclined 30

degrees were not only the most effective exercises in activating abdominal musculature but also were the most effective in activating extraneous musculature. However, Escamilla noted that the relatively high rectus femoris muscle activity obtained with the Power Wheel (pike and knee-up), reverse crunch inclined 30 degrees, and bent-knee sit-up may be problematic for some people with low back problems.

Christoph Anders et al. [27] investigated trunk muscle activation during gait at different speeds by using surface EMG to collect data from 15 healthy subjects from five trunk muscles at speeds of 2, 3, 4, 5, and 6 km/h. Anders found that a speed dependent modulation of activation of the trunk muscles occurred within the investigated range of walking speeds.

Walking requires an upset of the delicate balance of the trunk, which is maintained by minimal muscle activity when standing at rest. During ambulation the pelvis undergoes significant translational and rotary motion in the sagittal, coronal and transverse planes. Therefore, the requirements for balancing the trunk by action of the trunk muscles are much more complex than during standing. Edwin Y Hanada [37] studied the abdominal and low back muscle activation amplitudes of older subject with and without chronic low back pain walking on a level surface at self-selected pace. EMG was used to collect data from the back muscles as this provides a useful means for detecting changes in trunk muscle activation during walking. This study focused on neuromuscular alterations in personnel aged between 50-80 years with low back pain in order to develop subject-specific management regimes designed to maintain spinal stability.

1.7. Objective

The purpose of this investigation is to develop a test procedure to study the effect of carrying a unilateral load or laptop bag or briefcase on the posture and trunk biomechanics during walking (Gait) using Traditional and Non-Linear methods.

- Develop a testing procedure methodology during gait carrying increasing loads.
- Measure ground reaction forces, trunk motion and trunk muscles activation when walking carrying increasing loads.
- Analysis of motion data using traditional linear (ROM) and non-linear (approximate entropy and correlation dimension) methods to study the effect of increasing loads on variability or stability during gait.
- Analysis of EMG data to study effect of increasing loads on muscle fatigue.
- Analysis of vertical ground reaction force data.

CHAPTER 2

ANATOMY OF THE HUMAN SPINE

2.1. The vertebral column

The vertebral column, also known as the backbone or spine, is a bony structure found in vertebrates. The human spine consists of a total of 33 bones known as vertebrae, 24 of which are articulating and 9 fused, with the latter combining to form the sacrum and the coccyx. The spine is situated in the dorsal aspect of the torso, separated by intervertebral discs. The vertebrae are mounted in a vertical column and form the main part of the spine, running from the base of the skull to the pelvis. At the base of the spine there is a bony plate called the sacrum which is made of five fused vertebrae. The sacrum forms the back part of the pelvis. At the bottom of the sacrum is a small set of four partly fused vertebrae, the coccyx or tailbone.

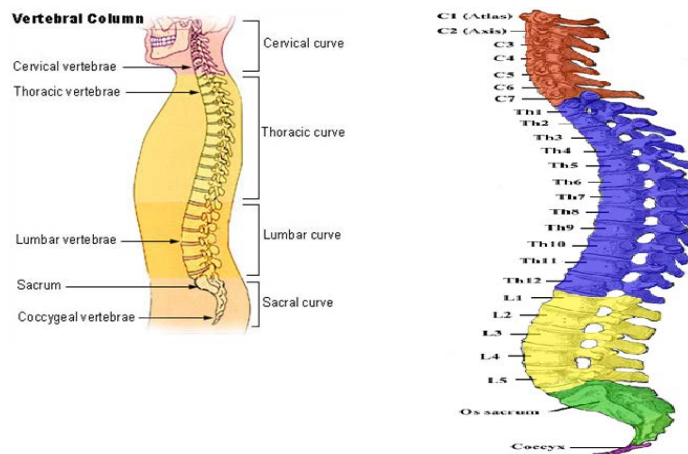


Figure 1: Vertebral Column

The upper, articulated, section of the human spine is composed of three regions: the cervical spine, the thoracic spine and the lumbar spine, grouped as follows: the cervical (7 vertebrae C1-C7), the thoracic (12 vertebrae T1-T12) and the lumbar (5 vertebrae L1-L5), according to the regions they occupy. [3, 4] Viewed laterally, the vertebral column presents several curves that correspond to the different regions of the column, namely the cervical, thoracic, lumbar, and pelvic regions (Figure 1).

The spinal vertebrae are separated from each other by intervertebral discs. These discs are made of collagen fibers and cartilage and provide padding and shock absorption for the vertebrae. Each pair of vertebrae forms a movable unit. The spinal cord runs within the vertebral canal formed by the back parts of the vertebrae. Thirty-one pairs of nerves branch out from the spinal cord through the vertebrae, carrying messages between the brain and every part of the body. Aging, diseases, accidents and muscular imbalances can cause compression and thinning of the intervertebral discs. These results in pressure on the spinal nerves and wear on the bony vertebrae, and these conditions are common sources of back pain.

There are four natural curves in the spine, although the three that comprise the cervical, thoracic, and lumbar portions of the spine are more commonly referred to, the sacrum and coccyx also forms a curved section. The spinal curves provide architectural strength and support for the spine. They distribute the vertical pressure on the spine, and balance the weight of the body. If the spine were absolutely straight, it would be more likely to buckle under the pressure of the weight of the body.

When all the natural curves of the spine are present, the spine is a neutral position. This is its strongest position and usually the safest when exercising. In perfect posture, the curves of the

spine help the body maintain its balance. Human beings evolved to walk and stand in the neutral spine position (Marguerite Ogle, About.com).

2.1.1. Thoracic vertebrae

In vertebrates, the thoracic vertebrae compose the middle segment of the vertebral column, between the cervical vertebrae and the lumbar vertebrae. In humans, these are intermediate in size between those of the cervical and lumbar regions, increasing in size as down the spine with the upper vertebrae being much smaller than those in the lower thoracic region

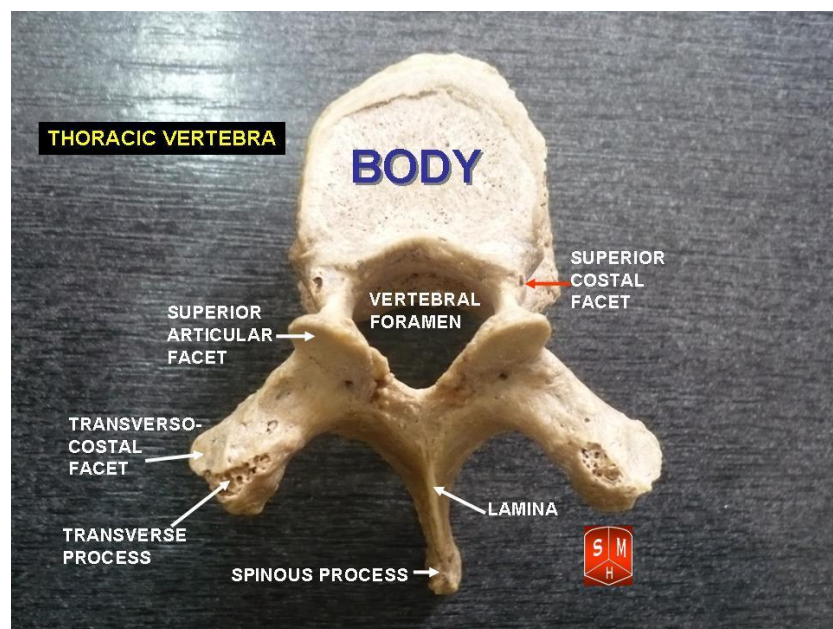


Figure 2: Thoracic Vertebra (Wikipedia.org)

The structure of a typical thoracic vertebra is shown in Figure 2. They are distinguished by the presence of facets on the sides of the bodies for articulation with the heads of the ribs, and facets on the transverse processes of all except the 11th and 12th for articulation with the tubercles of the ribs. The cervical vertebrae run into the cranium and are hence of less interest for

this research. By convention, the human thoracic vertebrae are numbered, with the first one (T1) located closest to the skull and higher numbered vertebrae (T2-T12) proceeding away from the skull and down the spine. [5]

2.1.2. Lumbar Vertebrae

The lumbar vertebrae are the five vertebrae between the rib cage and the pelvis and are the largest segments of the movable part of the vertebral column. They are characterized by the absence of the foramen transversarium within the transverse process, and by the absence of facets on the sides of the body. They are designated L1 to L5, starting at the top (Figure 3).

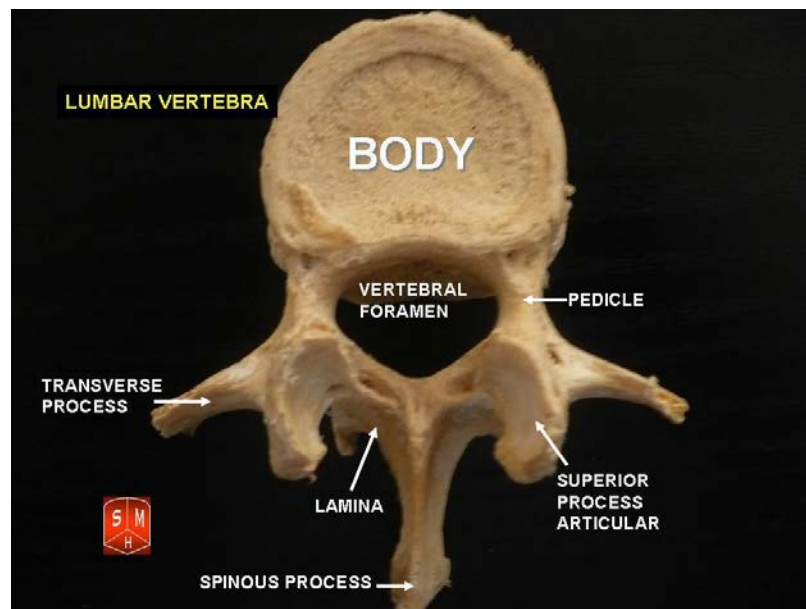


Figure 3: Lumbar Vertebra

Each lumbar vertebra consists of a vertebral body and a vertebral arch. The vertebral arch, consisting of a pair of pedicles and a pair of laminae, encloses the vertebral foramen (opening) and supports seven processes. They allow significant flexion and extension as well as

moderate lateral flexion (side bending). The discs between these vertebrae create a lumbarlordosis (curvature that is concave posteriorly) in the human spine. [6]

2.1.3. Sacrum Vertebrae

The sacrum is a large, triangular bone at the base of the spine and at the upper and back part of the pelvic cavity, where it is inserted like a wedge between the two hip bones. Its upper part connects with the last lumbar vertebra, and the bottom part with the coccyx (tailbone). It consists of five initially unfused vertebrae in most cases that begin to fuse between ages 16–18 and are usually completely fused into a single bone by the age of 34 (Figure 4).

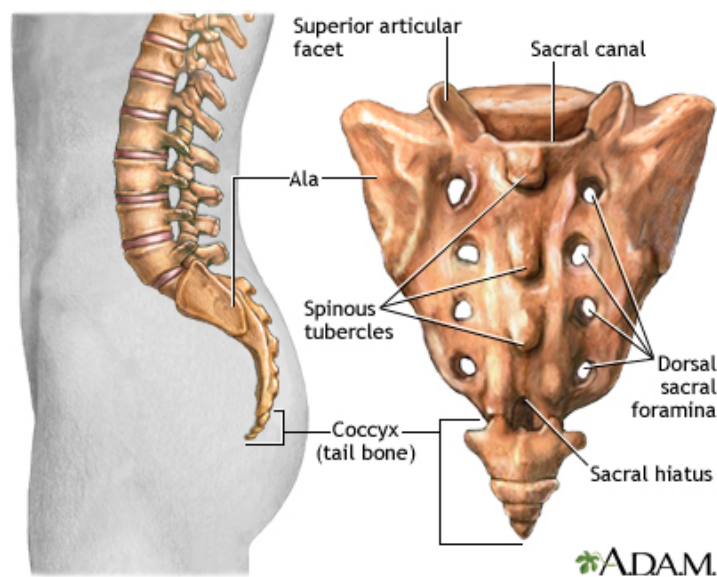


Figure 4: Sacrum Vertebra

The sacrum is curved in upon itself and is placed obliquely (tilted forward). It is kyphotic, i.e. concave facing forward. The base projects forward as the sacral promontory internally, and articulates with the last lumbar vertebra to form the prominent sacrovertebral angle. The central part is curved outward toward the posterior, allowing

greater room for the pelvic cavity. The two lateral projections of the sacrum are called ala (wings), and articulate with the ilium at the L-shaped sacroiliac joints. [7]

2.2. Low Back Muscles:

In this study, six muscle groups have been used to collect Electromyography (EMG) data, as follows:

2.2.1. Erector Spinae

The Erector spinae is a muscle group of the back in humans and animals that extends the vertebral column (bending the spine such that the head moves posteriorly while the chest protrudes anteriorly). It is known as the sacrospinalis in older texts, but a more modern term is extensor spinae.

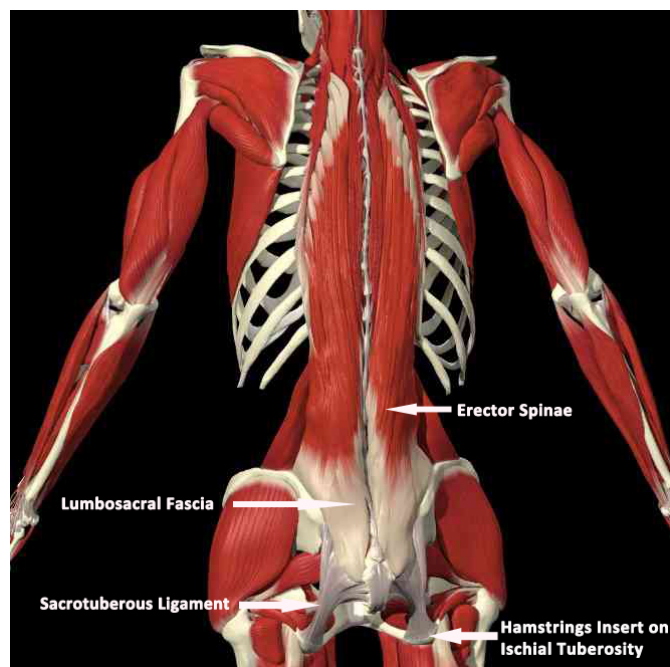


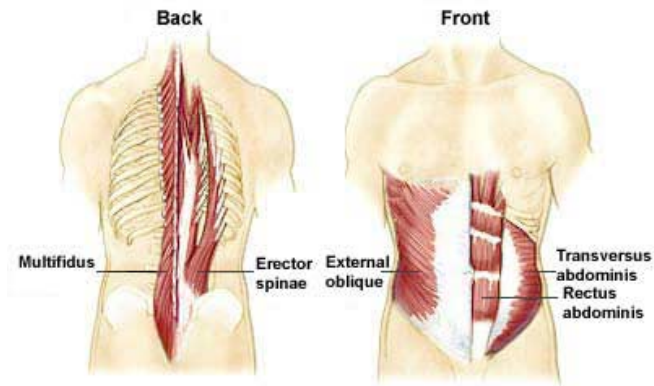
Figure 5: the Erector Spinae muscle

It is not composed of a single muscle, but is instead made up of a bundle of muscles and tendons. It occurs in pairs that run more or less vertically, extending throughout the lumbar, thoracic and cervical regions, and lies in the groove to the side of the vertebral column (Figure 5).

The erector spinae are covered in the lumbar and thoracic regions by the thoracolumbar fascia, and in the cervical region by the nuchal ligament. This large muscular and tendinous mass varies in size and structure in different parts of the vertebral column. In the sacral region it is narrow and pointed, and at its origin chiefly tendinous in structure. In the lumbar region it is larger, and forms a thick fleshy mass which, on being followed upward, is subdivided into three columns that gradually diminish in size as they ascend to be inserted into the vertebrae and ribs. The erector spinae arise from the anterior surface of a broad and thick tendon attached to the medial crest of the sacrum, to the spinous processes of the lumbar and the eleventh and twelfth thoracic vertebrae, and the supraspinous ligament, to the back part of the inner lip of the iliac crests and to the lateral crests of the sacrum, where they blend with the sacrotuberous and posterior sacroiliac ligaments. [8]

2.2.2. Multifidus

The multifidus muscle consists of a number of fleshy and tendinous fasciculi that fill the groove on either side of the spinous processes of the vertebrae from the sacrum to the axis. The multifidus is a very thin muscle. Deep in the spine, it spans three joint segments, and works to stabilize the joints at each segmental level. The stiffness and stability it imparts makes each vertebra work more effectively and slows the degeneration of the joint structures (Figure 6) (Wikipedia.com).



© 2003 Mayo Foundation for Medical Education and Research. All rights reserved.

Figure 6: Multifidus

2.2.3. Latissimus Dorsi

The latissimus dorsi, which is Latin for the 'broadest muscle of the back', is the larger, flat, dorso-lateral muscle on the trunk, posterior to the arm, and partly covered by the trapezius on its median dorsal region (Figure 7).

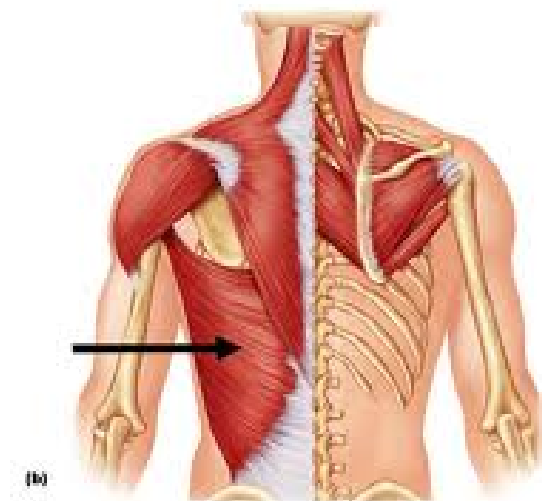


Figure 7: Latissimus Dorsi

The latissimus dorsi is responsible for extension, adduction, transverse extension (also known as horizontal abduction), flexion (from an extended position), and (medial) internal rotation of the shoulder joint. It also has a synergistic role in extension and lateral flexion of the lumbar spine. (Wikipedia.com)

2.3. Abdominus Muscles:

2.3.1. External Oblique

The external oblique muscle (of the abdomen) is the largest and the most superficial (outermost) of the three flat muscles of the lateral anterior abdomen. The external oblique is situated on the lateral and anterior parts of the abdomen. It is broad, thin, and irregularly quadrilateral, its muscular portion occupying the side, its aponeurosis the anterior wall of the abdomen. In most humans (especially females), the oblique is not visible, due to subcutaneous fat deposits and the small size of the muscle (Figure 8).

The external oblique functions to pull the chest downwards and compress the abdominal cavity, which increases the intra-abdominal pressure as in a valsalva maneuver. It also has limited actions in both flexion and rotation of the vertebral column. One side of the obliques contracting can create lateral flexion. It also contributes to compression of abdomen (Wikipedia.com).

2.3.2. Internal Oblique

The internal oblique muscle (of the abdomen) is the intermediate muscle of the abdomen, lying just underneath the external oblique and just above (superficial to) the transverse abdominal muscle.

Its fibers run perpendicular to the external oblique muscle, beginning in the thoracolumbar fascia of the lower back, the anterior two-thirds of the iliac crest (upper part of hip bone) and the lateral half of the inguinal ligament. The muscle fibers run from these points superiomedially (up and towards the midline) to the muscle's insertions on the inferior borders of the 10th through the 12th ribs and the linea alba (abdominal midline seam) (Figure 8).

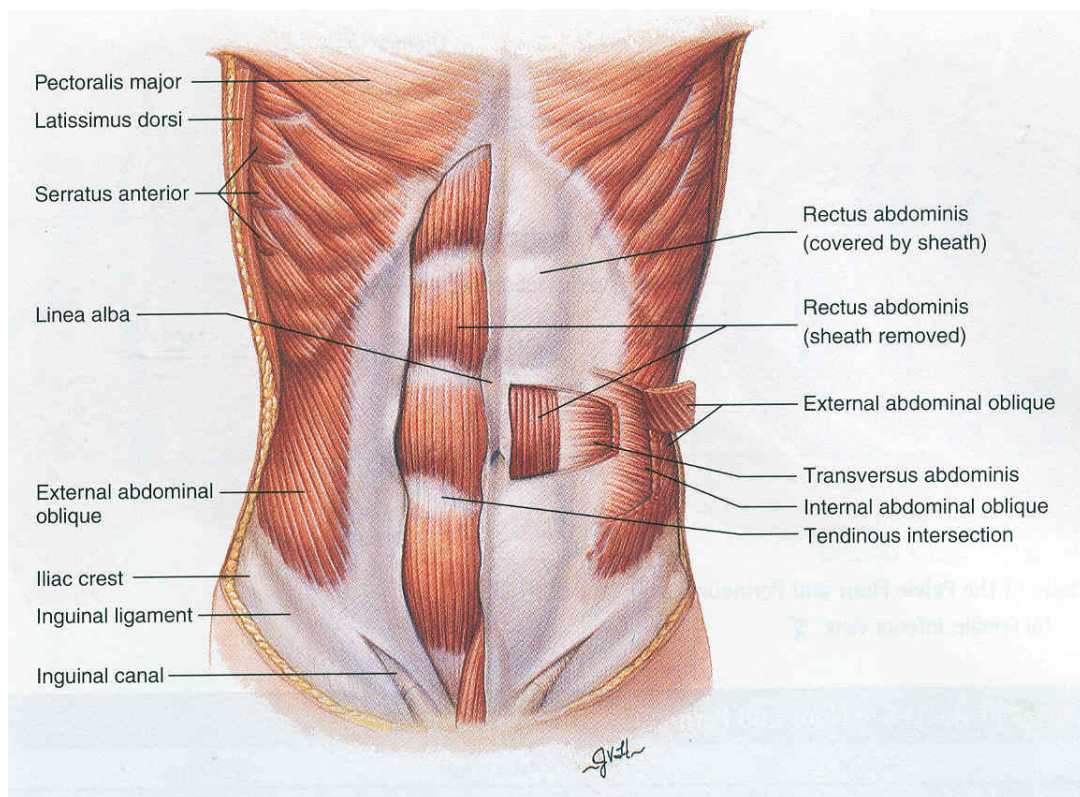


Figure 8: Abdominal Muscles (External Oblique, Internal Oblique and Rectus Abdominus)

The internal oblique performs two major functions. First, it acts as an antagonist (opponent) to the diaphragm, helping to reduce the volume of the thoracic (chest) cavity during exhalation. When the diaphragm contracts, it pulls the lower wall of the chest cavity down to increase the volume of the lungs which then fill with air.

Secondly, its contraction rotates and bends the trunk sideways by pulling the rib cage and midline towards the hip and lower back, of the same side. It acts with the external oblique muscle of the opposite side to achieve this torsional movement of the trunk.

2.3.3. Rectus Abdominus

The rectus abdominis muscle, commonly known as "abs," consists of a pair of muscles running vertically on each side of the anterior wall of the human abdomen. The two parallel muscles are separated by a midline band of connective tissue called the linea alba ("white line") that extends from the pubic symphysis, pubic crest and pubic tubercle inferiorly, to the xiphoid process and costal cartilages of ribs V to VII superiorly (Figure 8).

The rectus abdominis is a long flat muscle that extends along the whole length of the front of the abdomen. The muscle is inserted by three portions of unequal size into the cartilages of the fifth, sixth, and seventh ribs. The upper portion, attached principally to the cartilage of the fifth rib, usually has some fibers of insertion into the anterior extremity of the rib itself. Some fibers are connected to the costoxiphoid ligaments and the side of the xiphoid process.

The rectus abdominis is an important postural muscle that is responsible for flexing the lumbar spine, as when doing a "crunch" The rib cage is brought up to where the pelvis is when the pelvis is fixed, or the pelvis can be brought towards the rib cage (posterior pelvic tilt) when the rib cage is fixed, such as in a leg-hip raise. The two can also be brought together simultaneously when neither is fixed in space. The rectus abdominis assists with breathing and plays an important role in respiration when forcefully exhaling after exercise and in conditions where exhalation is difficult such as emphysema. It also helps in keeping the internal organs

intact and in creating intra-abdominal pressure, such as when exercising or lifting heavy weights, during forceful defecation or parturition (childbirth) (Wikipedia.com).

Escamilla [71] studied the effectiveness of traditional and nontraditional abdominal exercises in activating abdominal and extraneous musculature by using surface EMG to capture muscle activity from the upper and lower rectus abdominis, external and internal oblique, rectus femoris, Latissimus dorsi and lumbar paraspinal muscle while each exercise were performed. The Power Wheel, hanging knee-up with straps, and reverse crunch inclined 30° were the most effective exercises in activating abdominal musculature and also the most effective in activating extraneous musculature. The relatively high rectus femoris muscle activity obtained with the Power Wheel (pike and knee-up), reverse crunch inclined 30°, and bent-knee sit-up may be problematic for some people with low back problems. Dickstein also focused on the EMG activity of the lumbar erector spinae (ES), latissimus dorsi (LD), rectus abdominis (RA), and external oblique (EO) muscles in their study of trunk flexion-extension of post-stroke hemiparetic subjects. (Dickstein et. al. 2004)

Marras and Granata collected ten channels of EMG data from bipolar surface electrodes over the right and left sides of the erector spinae, rectus abdomini, latissimus dorsi, external abdominal obliques, and internal abdominal oblique muscles for their study of spine loading during trunk lateral bending motion. (Marras et. al. 1997)

Similarly, in their study of trunk rotation Ng et. al. 2002 monitored the rectus abdominis, external oblique, internal oblique, latissimus dorsi, iliocostalis lumborum and multifidus muscles in their study of the EMG activity of trunk muscles and torque output during isometric axial rotation exertion (Joseph K.-F Ng et al. 2002).

CHAPTER 3

METHODS AND TECHNIQUES

As the literature review in the previous chapter makes clear, there remains a need for an in-depth analysis of the effect of carrying a unilateral load on posture and trunk biomechanics when walking. We often carry a unilateral load in the form of a laptop bag or briefcase during the course of our everyday lives, but doing so for extended periods of time on a regular basis may have a significant effect on our body characteristics. Laptops are generally transported in a single strap bag carried over one shoulder. The weight of the laptop, which typically weighs up to 7 lbs, along with other items in the bag such as the power cable and any paperwork or books, can cause considerable low back pain and strain on the shoulder muscles, as well as restricting blood flow and pinching nerves. Carrying a laptop bag day after day for long periods of time can cause users to walk with poor posture and place serious strain on several different parts of the body, especially the back. This is particularly critical for younger users; a study conducted at Auburn University reported that book bags that are too heavy for their wearers may threaten developing spines. [1]

The study reported here was therefore designed to study the effect of carrying a unilateral load (maximum 25 lbs) during gait on posture and trunk biomechanics using nonlinear methods. Suitable areas on each participant's low back and spine were chosen for attaching surface electromyography (EMG) sensors and motion sensors, namely the low back, along the lower ribs

on each side and on the abdomen [71] and attached using double sided tape. Participants walked back and forth on a wooden platform at a comfortable walking speed and monitored as they carried varying loads (sand bags) weighing 0, 5, 10, 15, 20, and 25 pounds in one hand at intervals of 30 steps each three separate times. EMG data and motion data were collected using a computer. Individual participants were tested only once for this study.

Approvals were obtained from Institutional Review Boards (IRB) of both Auburn University (Protocol # 12-190EP1207) and Palmer College of Chiropractic, IA (IRB Assurance # 2012G144).

3. Methods:

3.1. Subject selection:

All participants were recruited via word of mouth. Potential participants interested in the study called the research clinic to schedule an appointment or scheduled an appointment in person. Participants attended a baseline visit where they reviewed the informed consent document with a study coordinator and received an eligibility examination. Signed informed consent documents were obtained from each participant following the informed consent process. Consented participants then underwent an eligibility examination to ensure that risks to their health and safety were minimized. All participants were between 18 and 65 years of age and capable of reading and understanding English. Participants who currently, or within the past month, had suffered from a musculoskeletal injury that altered their gait were not eligible for the study. Following clinical evaluation and examination, clinicians verified eligibility status for each participant. Participants who, in the opinion of the examining clinician, were at risk of injury while conducting this test were also deemed ineligible. Enrolled participants did not

experience any pain while performing the test. Gender and ethnicity were representative of those attending the Palmer College of Chiropractic (PCC) and the general population within the Quad Cities area ([Davenport, IA](#), [Bettendorf, IA](#), [Rock Island, IL](#), [Moline, IL](#), and [East Moline, IL](#)) where the clinic is located. Students and employees of PCC and volunteers from the Quad City community were invited to participate in this study. There was no penalty for individuals who did not want to participate. The Informed Consent document (ICD) were kept with each participant's research clinic chart, and a photocopy of the ICD provided to participants

Sample Size –

To ensure success, a biomedical study must have a well-defined problem and an appropriate population, as well as a reliable procedure and instruments and any other necessary resources. In particular, the sample size must be large enough to avoid wasting resources on an inconclusive study but small enough to yield useful results in a timely manner. Also, in experiments involving human or animal subject's ethical issues come into play: an over-populated experiment will expose an unnecessarily high number of participants to potentially hazardous tests, while under-populated studies expose subjects to potentially hazardous tests without advancing the knowledge base. [59]

Finally, the study should be of sufficient size relative to the goal of the study. The present study was a preliminary study, so time and cost were the main constraints. A sample size of ten subjects was considered sufficient for this study; 9 subjects (6 male and 3 female) were actually recruited (Table 1) and Due to bad data from one participant, data analysis were done for 8 participants.

Table 1: Demographic data

	Age (yrs)	Height (cm)	Weight (kg)
Mean (SD)	29.6 (7.4)	173.3 (6.4)	69.3 (6.6)

3.2. Inclusion and exclusion Criteria for the participants:

Inclusion Criteria –

1. Participant must be adults (≥ 18 and ≤ 65) and capable of reading and understanding English language.
2. A signed informed consent document must be obtained for each.

Exclusion Criteria –

1. Participants who currently, or within the past month, had suffered from a musculoskeletal injury causing altered gait.
2. Participants experiencing pain while performing any of the motions required by the testing protocol.
3. Participants identified with a condition, in the opinion of the examining clinician that would compromise collection of EMG or motion sensor data.
4. Participants unable to tolerate or perform the study procedures without symptom aggravation.
5. Participants with an implanted pacemaker, defibrillator or other non-removable metal appliance.
6. Participants suspected of drug or alcohol dependence or abuse by the examining clinician.

7. Participants who were pregnant or seeking to become pregnant.
8. Participants reporting sensitivity to the adhesive.
9. Participants with uncontrolled hypertension.
10. Participants seeking or receiving compensation for any disability.
11. Participants for whom diagnostic procedures were deemed necessary in the opinion of the examining clinician or Case Review Panel.

3.3. Preparation:

Once a participant was deemed eligible and had received their safety review and authorization by a research clinician, the participants were scheduled for a test visit at the Biomechanics lab at PCCR. Preparation of the participant for testing included the identification of anatomical landmarks, and trunk muscle sites at which to attach the surface electromyographic (sEMG) electrodes and motion sensors. EMG activities were recorded using surface electrodes to examine the muscle activity in the low back and along the lower ribs and on the outer abdomen [27, 71]. The anatomical landmarks for the motion sensors were the T1, L1, L3, and S1 vertebrae. Participants wore scrubs and shorts during the test. Surface EMG sensors and motion sensors were attached using double sided tape. The EMG electrode and motion sensor sites were prepared using an alcohol wipe and a mild abrasive pad to allow better sensor contact with the skin. The areas where the electrodes were to be attached were shaved using a disposable razor or sterilized electric razor if necessary with the participant's consent; they could refuse this procedure. During this preparation a brief description of the test procedure was given to the participant.

3.4. Data Acquisition:

For this study, Motion Data, Force Plate Data and EMG data were obtained. EMG sensors measured the electrical activity of the muscles and motion sensors measured the spinal posture and variation during walking. The motion data was obtained using a Liberty 24/8 (Polhemus, Vermont, USA) system at 120 samples per second. A fourth order Butterworth filter with low pass frequency of 20 Hz was used to filter the motion data [27]. The EMG data was recorded using a DELSYS Bagnoli - 12 Channel EMG System at 1200 samples per second. The EMG signals were amplified 1000 times and band passed between 20 Hz and 500 Hz [27, 88]. Force Plate Data was recorded at 120 samples per second. The literature review revealed that different types of EMG systems were used by previous researchers. For example, Christoph [27] used a bipolar surface EMG system (SEMG, 5–700 Hz, Biovision, Wehrheim, Germany). Raw surface EMG was centered and high-pass filtered using 4th-order Butterworth filter with cut-off frequency of 20 Hz to avoid influences from movement artifacts.

Frequencies below 20 Hz do not suffer from noise due to wire sway, whereas frequencies over 500 Hz eliminate the need to compensate for the noise arising due to surface contact between the electrodes and the skin [61]. Motion Monitor 7.0 software (Innovative Sports Training, Inc.) was used to collect both Motion and EMG data.

The sensors were then attached to the skin using double sided tape (Figures 9, 10 and 11). EMG data was obtained from 6 muscles groups, namely Multifidus, Erector Spinae, Latissimus Dorsi, Internal Obliques, External Obliques and Rectus Abdominis (Table 2). The locations for the placement of the sEMG sensors were determined based on previous studies. [27,71 and 83]

Participants warmed up for 2-3 minutes in the Biomechanics lab. During warm up each subject achieved a self selected comfortable walking pace. Once the data acquisition started, participants were asked to walk back and forth at their comfortable speed carrying a load in one

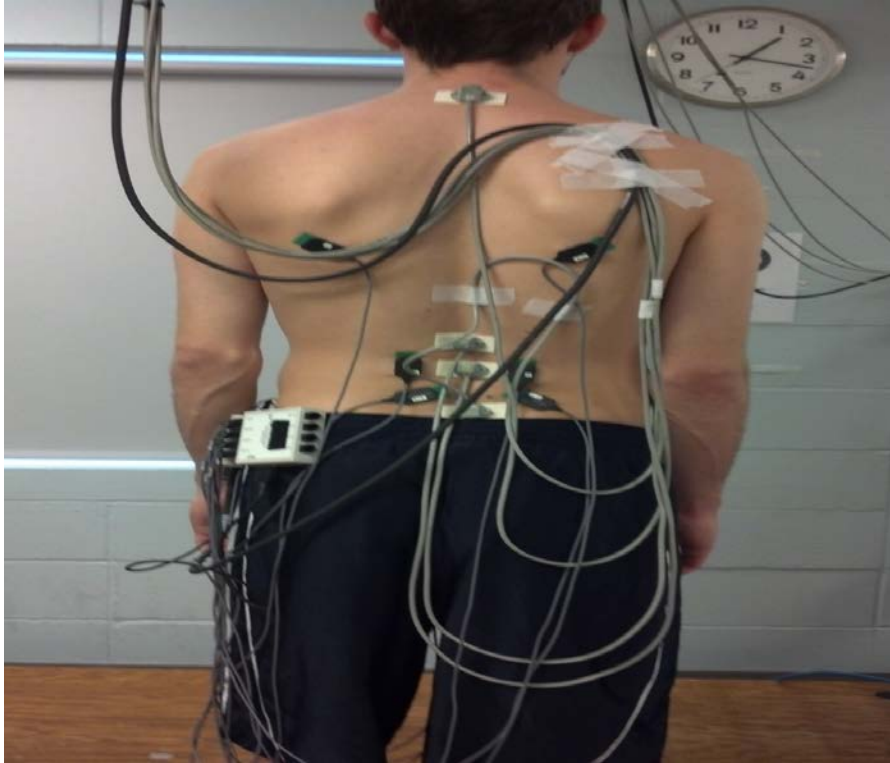


Figure 9: sEMG and motion sensors attached to back muscles and vertebrae respectively

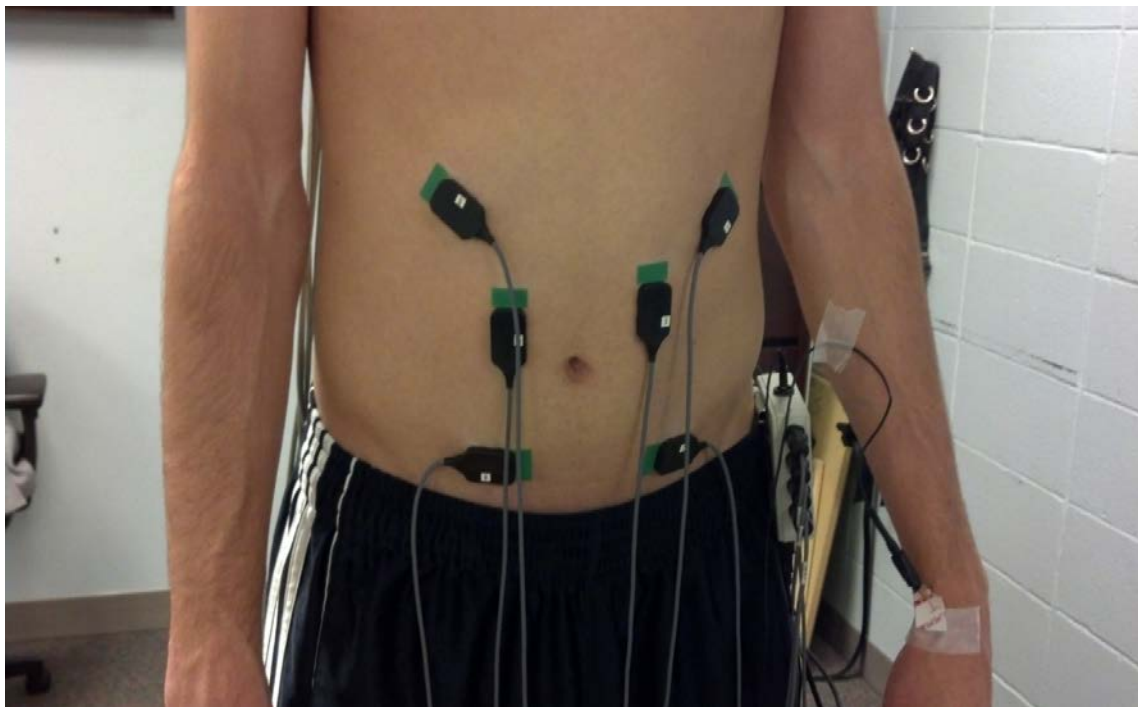


Figure 10: sEMG sensors attached to abdominal muscles



Figure 11: Participant with load

Table 2: EMG sensor placement

Muscle	Side	Location
Erector Spinae	Left	Over the largest muscle mass found by palpation and 4 cm from midline of the spine at the third lumbar vertebrae.
	Right	
Rectus Abdominus	Left	3 cm from the midline of the abdomen and 2 cm above the umbilicus.
	Right	
External Oblique	Left	10 cm from the midline of the abdomen and 4 cm above the ilium at an angle of 45°.
	Right	
Internal Oblique	Left	Positioned horizontally 2 cm inferomedial to the ASIS within a triangle outlined by the inguinal ligament, the lateral border of the rectus sheath, and a line connecting the anterior superior iliac spine (ASISs).
	Right	
Multifidus	Left	Bilaterally at the level of L5 and aligned parallel between the line of the posterior-superior iliac spine (PSIS) and the interspinous space of L1 and L2.
	Right	
Latissimus Dorsi	Left	Positioned obliquely (approximately 25° from horizontal in the inferomedial direction) 4 cm below the inferior angle of the scapula.
	Right	

hand (either right or left hand) weighing 0,5,10, 15, 20, and 25 pounds, in turn, on a wooden walking platform (5 ft × 8 ft) for a maximum of 30 steps/cycle. Participants walked at a self-selected speed to minimize any potential discomfort during walking. Data were collected on the EMG activity of trunk muscles and motion of the trunk and spine using Motion Monitor software on a desktop computer. Three trials were performed for each load. Data were collected for each trial followed by a 2 minute break. The total estimated duration of the test was approximately 1hour. Participants were tested once. The data was then exported from the motion monitors using the preference file created (see Appendix). The data was exported twice, once for motion data and Force Plate data, and then for EMG data.

3.5. Data analysis:

The raw data (EMG and motion) were exported and saved on a password protected network drive. Motion Data were filtered using the motion monitor and EMG data were filtered using the motion monitor and a fourth order Butterworth band pass filter using the MatLab program. The data was saved in separate Excel files for the 0 lb, 5 lb, 10 lb, 15 lb, 20 lb, and 25 lb loads. For the motion data, Range Of Motion (ROM), Correlation Dimension (CoD), and Approximate Entropy (ApEn) were calculated. For EMG, root mean square EMG values, Mean and Median Frequency of the EMG data were calculated using a custom developed MatLab program. For Force Plate Data, 1st peak force (Fz1), 2nd Peak force (Fz3) and minimum force (Fz2) between the 1st peak and 2nd peak forces were calculated.

3.5.1. Motion data:

3.5.1.1. Time series –

In statistics, signal processing, econometrics and mathematical finance, a time series is a sequence of data points measured at successive time instants over uniform time intervals. Time series analyses are then used to extract meaningful statistics and other characteristics from the data. Time series forecasting refers to the use of a model to predict future values based on previously observed values. Time series are usually plotted via line charts [11]. A time series can be represented by a function $x(t)$ where t has the discrete value $t=t_0, t_1, t_2, \dots, t_n$ where the time interval $\Delta t = t_{n+1} - t_n$. The motion data obtained here took the form of a time series. Examples occur in a variety of fields ranging from engineering to economics. Time series analyses may be divided into two classes: frequency-domain methods and time-domain methods. For example, measuring the value of retail sales each month of the year would comprise a time series. Other examples include daily stock market prices or pressure readings from pressure gauges at some factories (Chatfield Chris, 'The Analysis of Time Series: An Introduction'). The best way to see how a physical quantity changes with time is to plot a graph. Figure 12 shows a time series consisting of a simple periodic function, while Figures 13 and 14 show typical examples of the data collected for this study.

Non-linear methods were applied to calculate the chaos in the dynamic system being studied, but before this could be done it was important to ensure that the system is indeed chaotic. Chaos theory is used to study the behavior of dynamical systems that are highly sensitive to initial conditions, an effect which is popularly referred to as the butterfly effect. Small differences in initial conditions yield widely diverging outcomes for chaotic systems, rendering long-term prediction impossible in general [13].

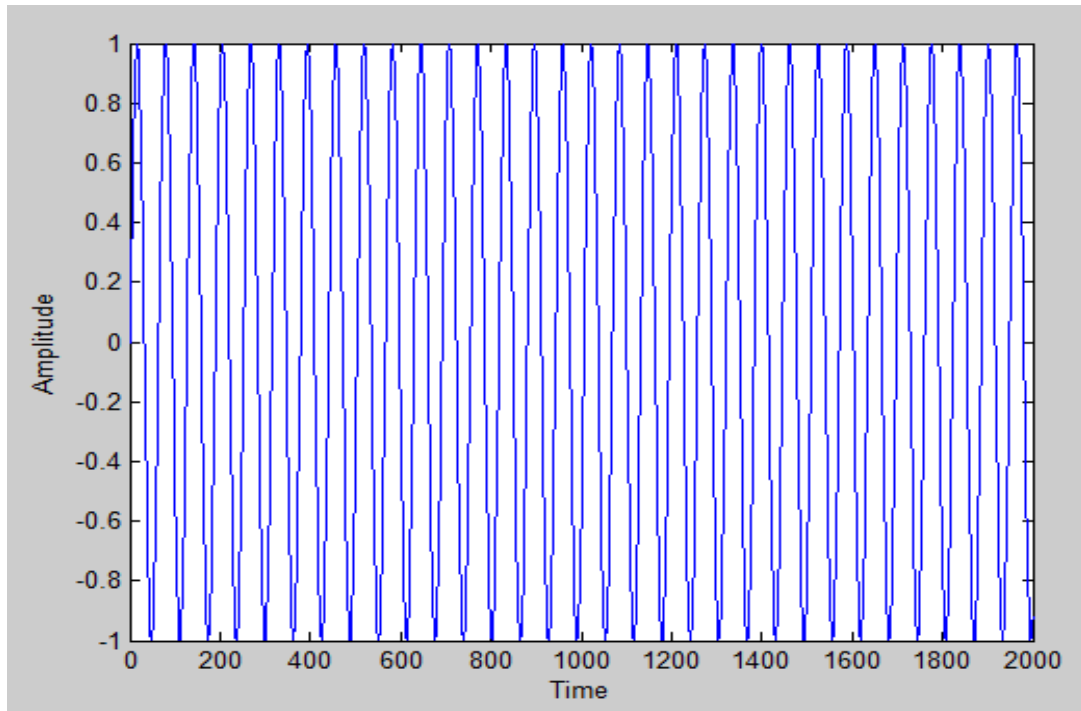


Figure 12: Time series for Sine Curve

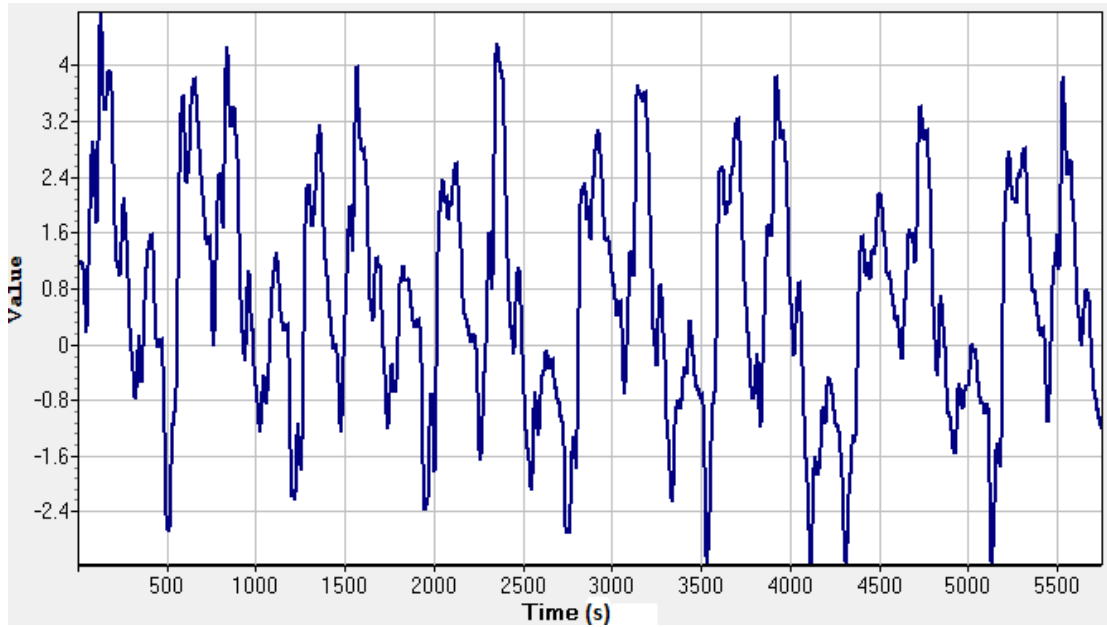


Figure 13: Time series for Walking with 25 lb load for Lumbar LB for subject 4

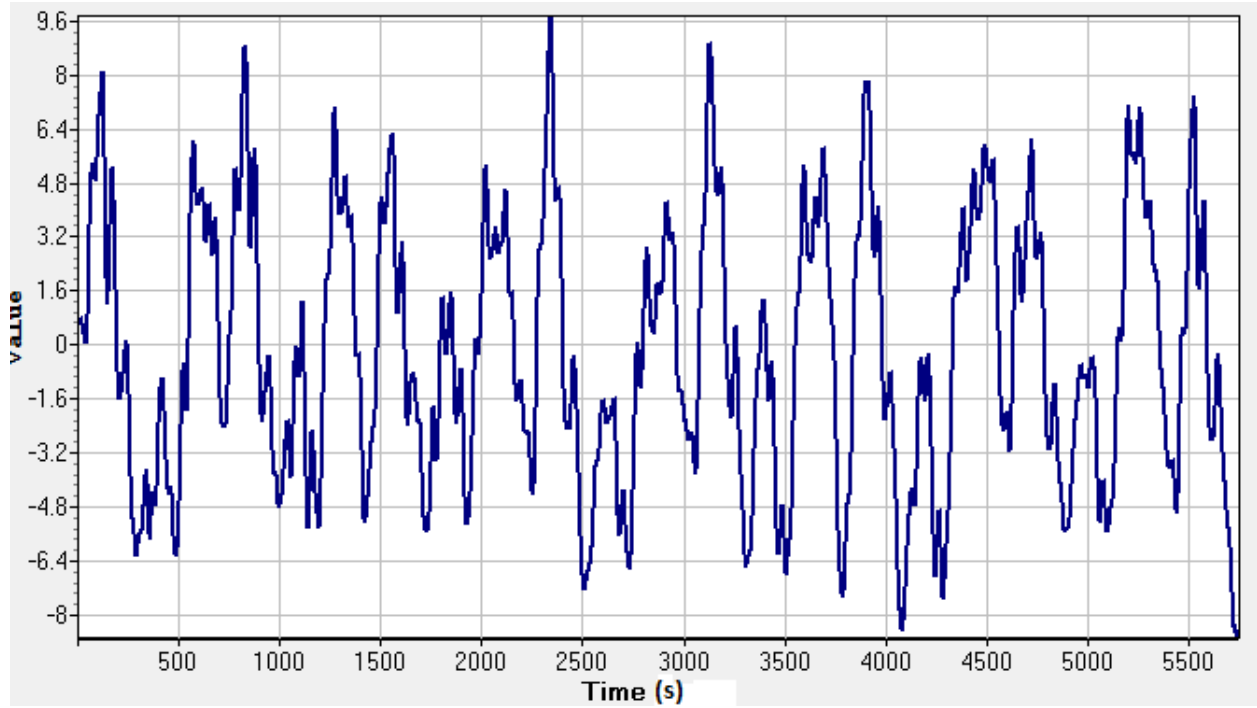


Figure 14: Time series for Walking with 25 lb resistance, Thoracic LB, subject 4

State Space

To examine the dynamic behavior of the time series data, it is first necessary to examine the structural characteristics of a time series by creating a state space where the behavior of the system is embedded. State space is a vector space where a dynamic system such as a moving body during locomotion can be defined at any point. Phase space or a phase plane plot is a representation of the dynamic behavior of a system in state space [77]; phase space or state space is an abstract mathematical space in which coordinates represent the variables needed to specify the phase (or state) of a dynamic system. It includes all the instantaneous states the system can have. To complement the common time-series plot, a phase space plot provides a different view of the evolution of motion. Although some time series can be very long and therefore difficult to show on a single graph, a phase space plot condenses all the data into a manageable space on a

graph. Consequently, chaos theory generally deals with phase space [40] either in the form of standard phase space or pseudo phase space.

3.5.1.1.1. Standard Phase Space

Standard phase space (or phase space) is an abstract space in which coordinates represent the variables needed to specify the state of a dynamic system at a particular time. On a graph, a plotted point neatly and compactly defines the system's condition for some measuring occasion, as indicated by the point's coordinates (values of the variables). For example, a baby's height can be plotted against its weight. Any plotted point represents the state of the baby (a dynamic system) at a particular time, in terms of height and weight. The next plotted point is the same baby's height and weight one time interval later, and so on. Thus, the succession of plotted points shows the growth of the baby over time and comparing successive points shows how height has changed relative to weight, over time t .

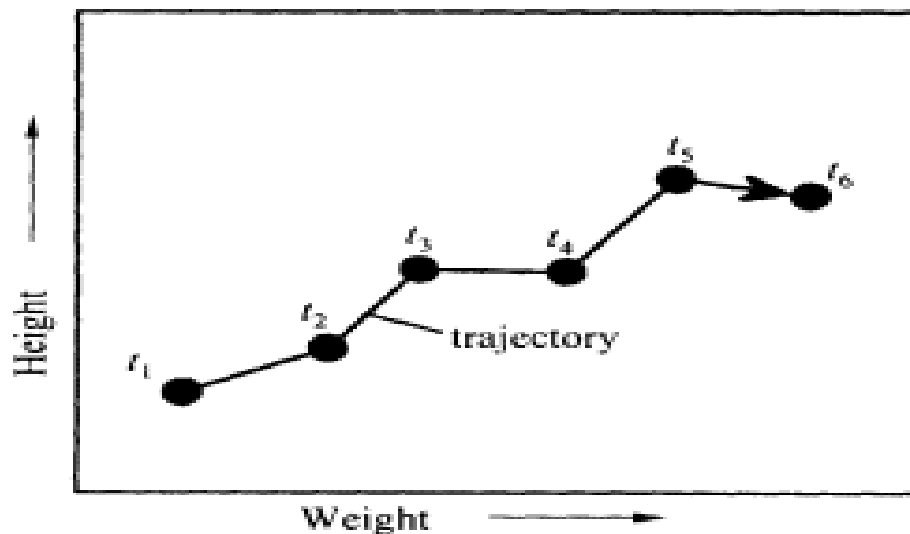
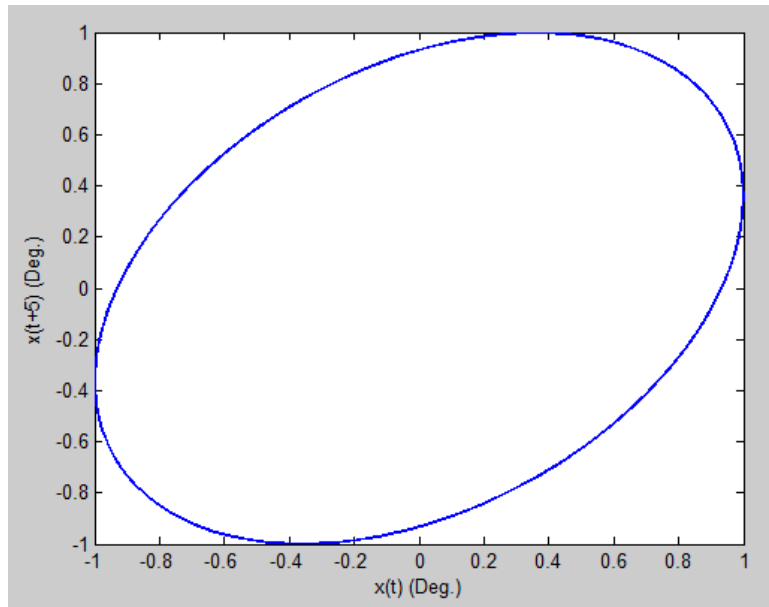
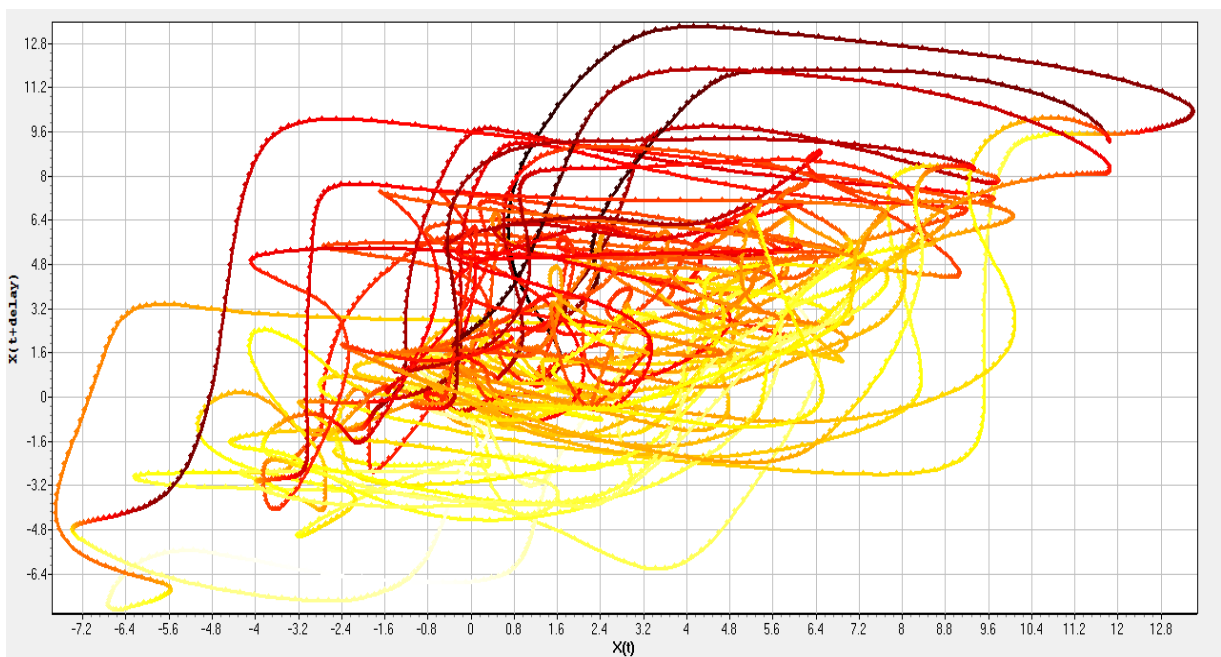


Figure 15: Example of standard phase space



(a)



(b)

Figure 16: Phase space plot (a) for periodic time series, (b) For Thoracic LB during walking at 25 lb for subject 5.

As Figure 16 shows, periodic data give a closed orbit with complete overlapping of the trajectories and absolutely no divergence, but a phase plot of chaotic data gives an elegant

picture that is not apparent when only the time series is observed. The phase space plot of a random series exhibits no clear pattern.

3.5.1.1.2. Pseudo Phase Space

Each axis on a standard phase space graph represents a different variable, as in the example shown in Figure 16. In contrast, a graph of the one-dimensional map plots two successive measurements (x_{t+1} versus x_t) of one measured feature, x (Figure 17). Because x_t and x_{t+1} each have a separate axis on the graph, chaosologists (those who study chaos) think of x_t and x_{t+1} as separate variable ("time-shifted variables") and of their associated plot as a type of phase space. However, this is not a conventional phase space because the axes all represent the same feature (e.g., stock price) rather than different features. Also, each plotted point represents sequential measurements rather than a concurrent measurement. Hence, the graphical space for a one-dimensional map is really a pseudo phase space. Pseudo phase space is an imaginary graphical space in which the axes represent values of a single physical feature, taken at different times. In the most common type of pseudo phase space, different temporal measurements of the variable are taken at uniform time intervals (Garnett P. Williams et al., 1997).

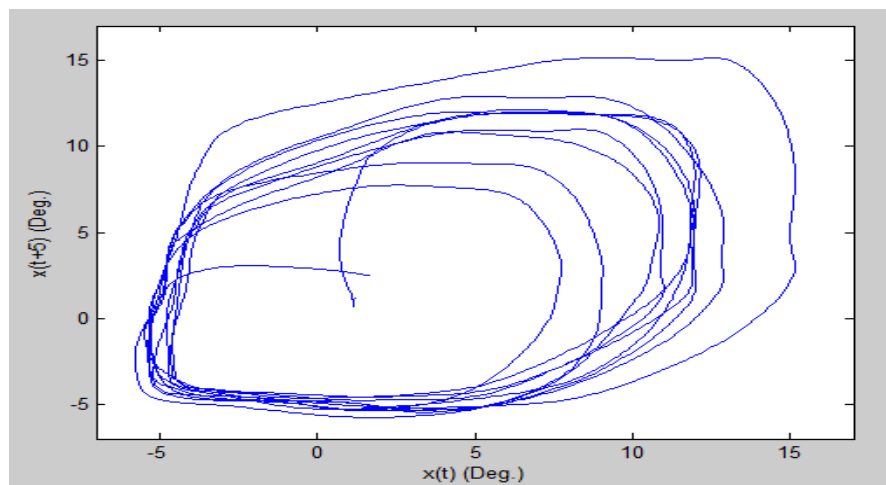


Figure 17: Pseudo phase space plot of experimental data

3.5.1.2. Time Lag:

In order to classify time series with nonlinear tools, it is first necessary to reconstruct a state space where the behavior of the system is embedded. It is essential to quantify an appropriate time delay and embedding dimension for the investigated time series. Investigation of the characteristics of the state space is a powerful tool for examining a dynamic system because it provides information that is not apparent by simply observing the time series [21, 24]. To reconstruct the state space, a state vector must first be created from the time series. This vector was composed of mutually exclusive information about the dynamics of the system (Eq. (1)).

$$y(t) = [x(t), x(t-T_1), x(t-T_2), \dots] \quad (1)$$

where $y(t)$ is the reconstructed state vector, $x(t)$ is the original data, and $x(t - T_i)$ represents the time delayed copies of $x(t)$. The time delay (T_i) for creating the state vector was determined by estimating when information about the state of the dynamic system at $x(t)$ would be different from the information contained in its time-delayed copy. If the time delay chosen is too small then successive points in the state space may be too close together to be sufficiently independent and no additional information about the dynamics of the system would be contained in the state vector. Conversely, if the time delay chosen is too large then information about the dynamics of the system may be lost, resulting in random information [21, 24]. Selection of the appropriate time delay was performed using an average mutual information algorithm; Abarbanel, 1996).

$$I_{x(t), x(t+T)} = \sum P(x(t), x(t+T)) \log_2 \frac{P(x(t), x(t+T))}{P(x(t))P(x(t+T))} \quad (2)$$

where T is the time delay, $x(t)$ is the original data, $x(t + T)$ represents the time delay data, $P(x(t), x(t + T))$ is the joint probability for the measurement of $x(t)$ and $x(t + T)$, $P(x(t))$ is the probability for the measurement of $x(t)$, and $P(x(t + T))$ is the probability for the measurement of

$x(t + T)$. The probabilities were constructed from the frequency of $x(t)$ occurring in the time series. Average mutual information was iteratively calculated for various time delays and the time delay selected was located at the first local minimum of the iterative process (Figure 18) [21, 77]. This selection was based on previous investigations that have determined that the time delay at the first local minimum contains sufficient information about the dynamics of the system to reconstruct the state vector [21].

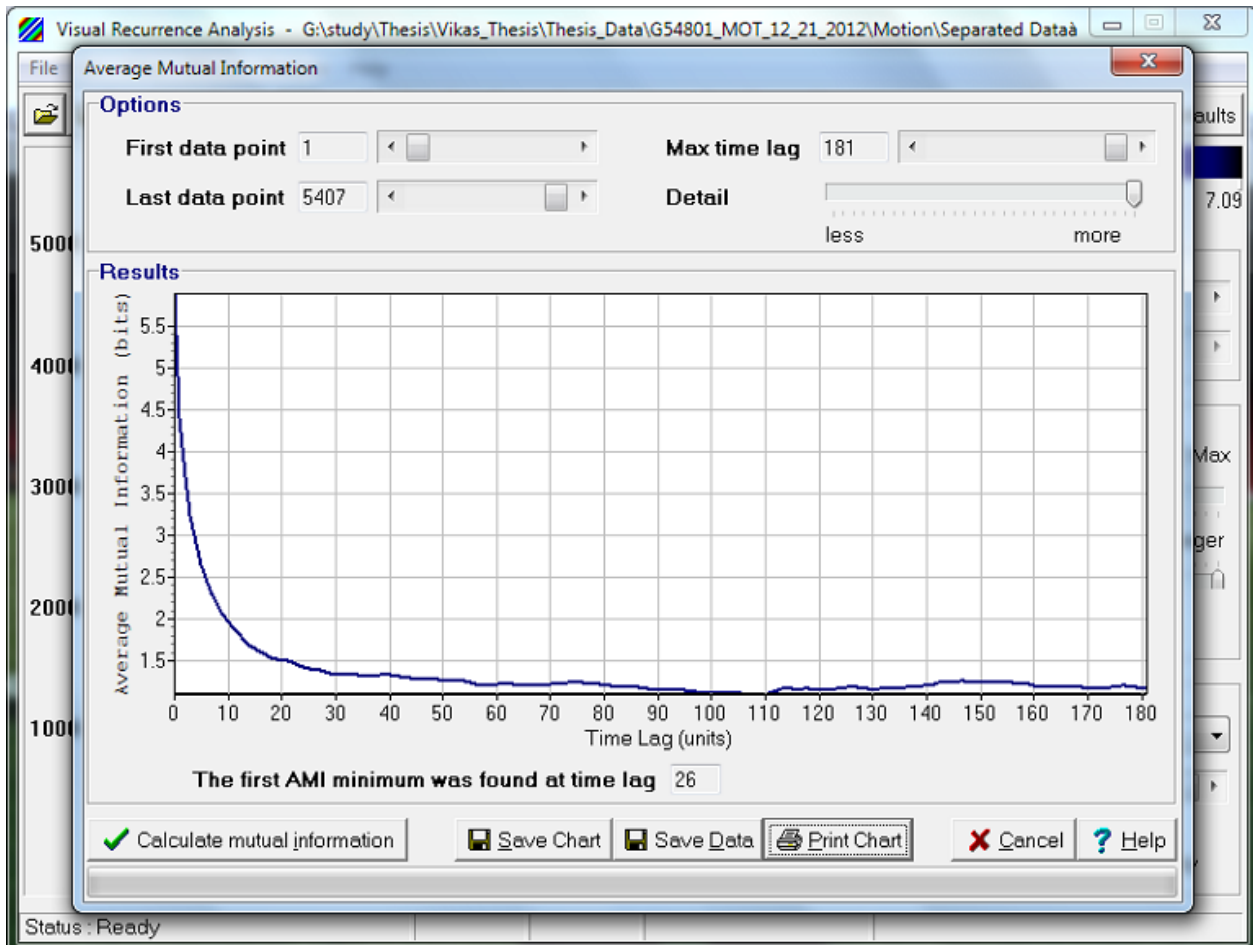


Figure 18: Time lag during walking with load = 0, Lumbar LB, subject 4

3.5.1.3. Embedding Dimension

Knowing the time delay T , the embedding dimension d for the dynamic system can be computed. The embedding dimension is the minimum number of variables required to form a

valid state space from a given time series, i.e. the minimum number of variables required to define a given dynamic system. The embedding dimension was estimated using the “global false nearest neighbors” algorithm proposed by Kennel et al. (1992) and Abarbanel et.al. 1996. This algorithm is based on the idea that in the passage from dimension d to $d + 1$, it is possible to differentiate between points on the orbit that are true neighbors and those that are not. If the embedding dimension d is too small, then too many false nearest neighbors will arise when the point X_i is considered as a point in the d dimensional state space, while if the embedding dimension is too large, the point become so distant in the d dimension state space that again they are essentially random (Figure 19).

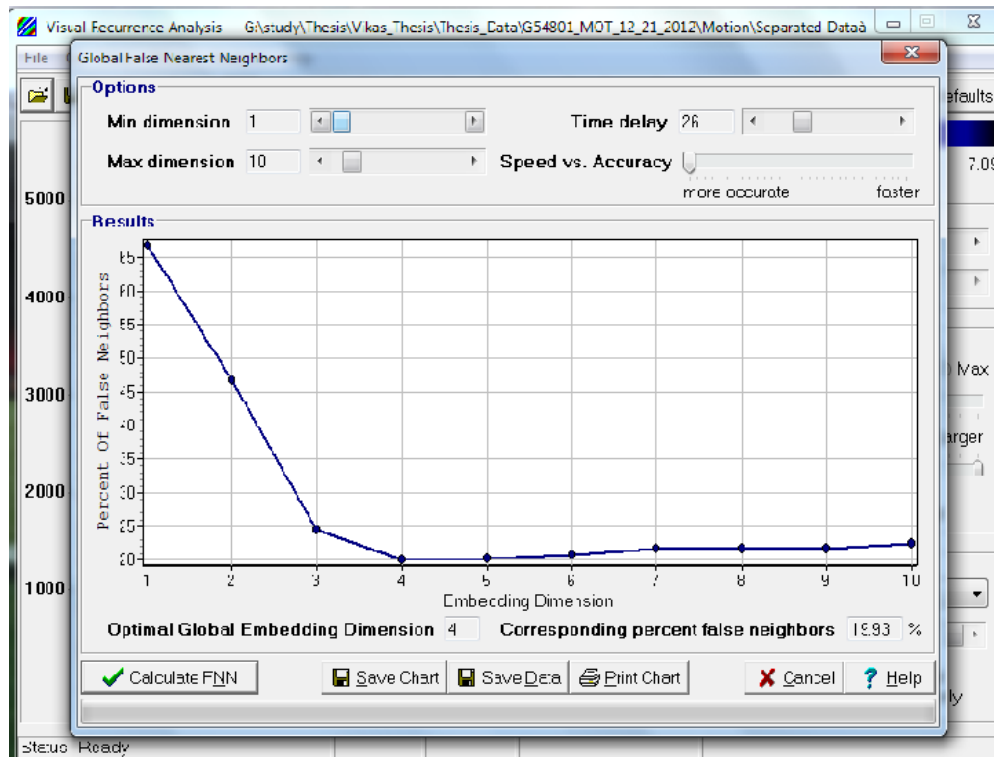


Figure 19: Embedding Dimension during walking without load = 0, Lumbar LB, subject 4

3.5.1.4. Correlation Dimension (CoD):

Once the time delay T and embedding dimension d have been calculated the time series can be classified using nonlinear tools such as Correlation Dimension. Correlation dimension approximates the fractal dimension of the region in state space occupied by the dynamic system [17, Theiler, 1986]. In chaos theory, the correlation dimension is a measure of the dimensionality of the space occupied by a set of random points. The most popular measure of dimension, it can be used to evaluate how the data points in a time series from a dynamic system are organized within the state space (Sprott and Rowland, 1992). Compared to other methods of measuring dimension (e.g. the box-counting dimension, and the information dimension), correlation dimension is straightforward and quickly calculated, less noisy when only a small number of points is available, and is often in agreement with other calculations of dimension [14]. The information dimension is usually based on spreading a grid of uniformly sized compartments over the trajectory like a quilt, which is akin to moving a measuring device over the object by equal, incremental lengths. Analysis for the correlation dimension could also take that approach, but instead the usual technique is to center a compartment on each successive data point in turn, regardless of how many points a region has and how far apart the points may be.

Many types of exponent dimension are essentially impossible to compute in practice, either because they apply to some unattainable limit (such as $\varepsilon \rightarrow 0$) or they are computationally very inefficient. The correlation dimension avoids those problems. Also, for a given dataset, it probes the attractor to a much finer scale than, say, the box-counting dimension. Two data points that plot close together in phase space are highly correlated spatially and one value is a close estimate of the other. However, depending on the trajectory's route between them, those same two points can be totally unrelated with regard to time, as the time associated with one point may be vastly and unpredictably different from the time of the other. The correlation dimension only

tests points for their spatial interrelations and ignores time, which is also true of the information dimension

Before moving on to the measuring procedure for CoD, both the Time Delay and Embedding Dimension must be determined. Visual Recurrence Analysis software can be used to compute the correlation dimensions as well as the Time lag or delay and the embedding dimension (Figure 20).

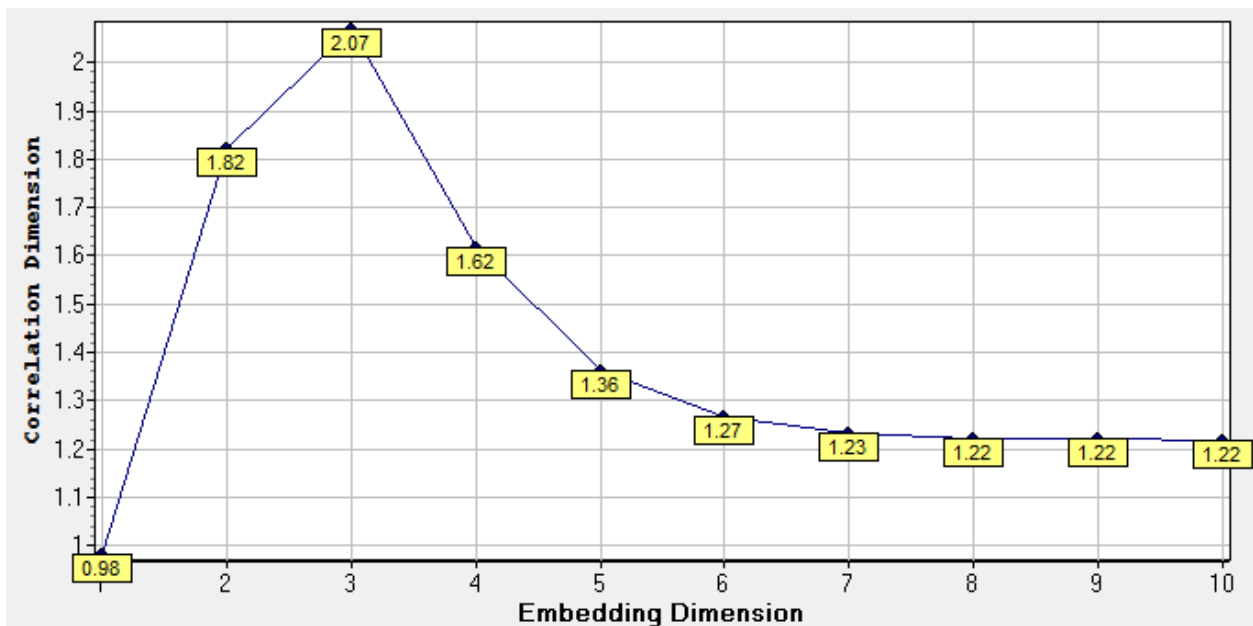


Figure 20: CoD during walking without load for Thoracic LB for subject 4

3.5.1.5. Quantify Correlation Dimension –

Once the lag is specified, the procedure usually begins with an embedding dimension of two (two-dimensional pseudo phase space) and proceeds as follows. First, situate the measuring cell such that its center is a datum point in the pseudo phase space. Next, count the number of data points in the cell. After that, center the cell on the reconstructed trajectory's next point (in the ideal approach) and make a new count. Keep repeating that same procedure, systematically moving the cell's center to each successive point on the trajectory. Consider an example with five

data points. First center the circle on point 1 (Figure 21). Within the circle, points 2 and 3 qualify. (The reference point is not included in the count.) Keeping that same radius and systematically centering the circle on each point, in turn, count the qualifying points within each circle. Once through the entire dataset with the *same* radius, add up the total number of qualifying points for that radius. Once through the entire dataset with the *same* radius, add up the total number of qualifying points for that radius.

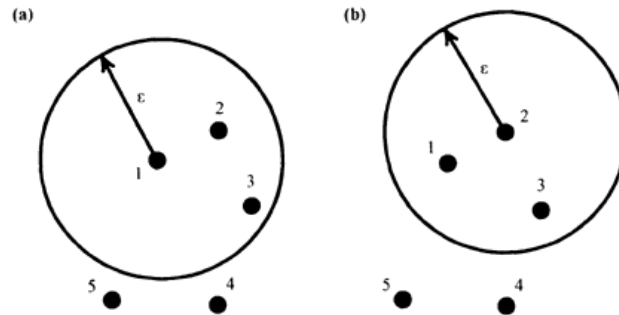


Figure 21: Identifying qualifying neighbors from (a) point 1 and (b) point 2

For example, Figure 21 has a total of eight points for the radius indicated: two points when the circle is centered at point 1, two more when it is on point 2, two again at point 3, and one point each for centering on points 4 and 5. Having obtained the total for the radius chosen, work only with that total rather than with the numbers pertaining to any particular point, referred to as the "total number of points within radius ϵ " or the "total number of qualifying points."

The total number of points defining the trajectory (i.e., the size of the basic-dataset) obviously influences the total count for a given radius. For instance, the count of qualifying points for a given radius is much smaller for a trajectory made up of ten points than for a trajectory of 10,000 points. For comparison purposes, therefore, normalize each count of qualifying points to account for the total number of points available on the trajectory by dividing

each total of qualifying points by some maximum reference constant. Here, this is the maximum number of total points obtainable by applying the circling-and-counting procedure to each point throughout the dataset, for a given radius. The normalized result is the correlation integral or correlation sum, C_ε , for the particular radius:

$$C_\varepsilon = \frac{\text{Total number of points within radius } \varepsilon}{\text{Largest number of mathematically possible points}} = \frac{\text{Total number of points within radius } \varepsilon}{N(N-1)} \quad (3)$$

in which N is the total number of points in the dataset (i.e., on the trajectory).

In the technical literature, Equation 24.2 often appears in an imposing symbol form, as follows:

$$C_\varepsilon = \lim_{n \rightarrow \infty} \frac{1}{N \cdot N} \sum_{i=1}^N \sum_{j=1}^N G(\varepsilon - |x_i - x_j|) \quad (4)$$

Here, x_i refers to the center of the measuring circle and x_j is each of the other points on the trajectory. For each center point, the absolute distance between x_i and x_j is $|x_i - x_j|$. The distance formula gives that absolute distance. Subtracting that distance from the radius ε by computing $\varepsilon - |x_i - x_j|$, if the answer is negative then the measured distance $|x_i - x_j|$ is greater than ε and point x_j is beyond the circle of radius ε and therefore will not qualify for inclusion. If $\varepsilon - |x_i - x_j|$ is positive, then $|x_i - x_j|$ is smaller than ε , and the point x_j is within the circle.

G is used to label each qualifying point — that is, each point for which $\varepsilon - |x_i - x_j|$ is positive (>0). If $\varepsilon - |x_i - x_j|$ is positive, the point x_j has to be counted and for all those cases the computer program assigns a value of 1 to the entire expression $G(\varepsilon - |x_i - x_j|)$. If, instead, $\varepsilon - |x_i - x_j|$ is negative, the point x_j is beyond the radius of the measuring device and the computer program assigns a value of 0 to $G(\varepsilon - |x_i - x_j|)$.

Equation 4 also normalizes the data by dividing the total number of qualifying points by the total number of available points. Strictly, the total number of available points is $N(N-1)$ so the counted total should be multiplied by $1/[N(N-1)]$.

Having determined the correlation sum for the first radius, the radius is increased and the process repeated for the new radius. Enlarging the radius includes more points than the smaller radius, and thus a larger total number of qualifying points (the numerator in Equation 3). The normalization constant N^2 depends only on the size of the basic dataset and so is constant regardless of the radius ϵ . Hence, the larger ϵ yields a larger correlation sum.

The procedure is repeated using larger and larger radii, with each new radius producing a larger and larger total of qualifying points and a larger correlation sum to generate a dataset of successively larger radii and their associated correlation sums. Those radii and correlation sums apply *only* to the two-dimensional pseudo phase space and it is necessary to move on to a three-dimensional pseudo phase space (an embedding dimension of three) and compute a similar dataset. All computed distances with the distance formula now involve three coordinates instead of two. Once the radii and associated correlation sums for three-dimensional pseudo phase space are assembled, this is extended four embedding dimensions, then five, and so on. A typical analysis involves computing a dataset for embedding dimensions of up to ten, depending on the plot of the data obtained.

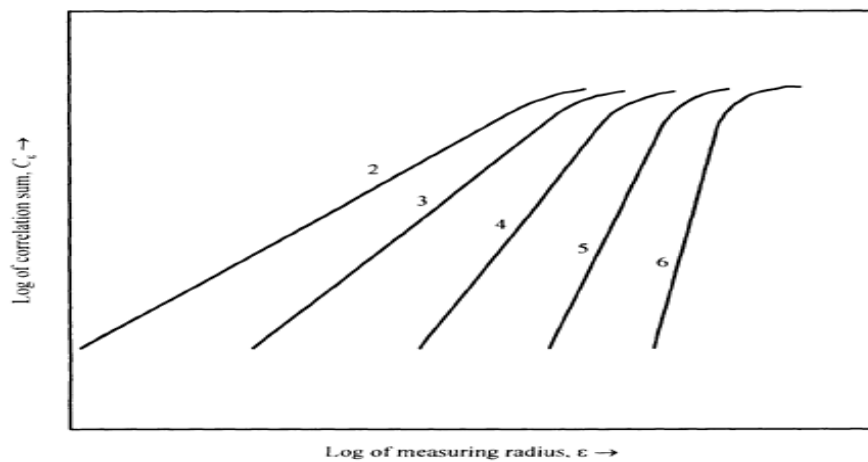


Figure 22: Idealized plot of Correlation Sum vs. Radius for increasing Embedding Dimension

The slope of the scaling region gives us the value of the CoD for that particular embedding dimension. Figure 22 shows the plots of correlation sum vs. measuring radius for successive embedding dimensions and illustrates how, the slopes of the scaling regions for the successive embedding dimensions tend to saturate to one particular value. This value of the slope is the CoD for the given time series.

Deterministic and Random Correlation Dimensions:

The correlation dimension or exponent for a given embedding dimension is represented by the slope of the straight line for that dimension in Figure 22. The steeper the slope, the greater the correlation dimension. Therefore, correlation dimension increases with increasing embedding dimension.

However, for highly deterministic or chaotic data, although the correlation dimension initially increases with increasing embedding dimension, eventually it becomes constant. The lower curve in Figure 23 shows an idealized relation, where the line for chaotic data flattens and becomes approximately horizontal at some final correlation dimension. If the correlation dimension is 2.68, for example, three variables might be enough to model the system.

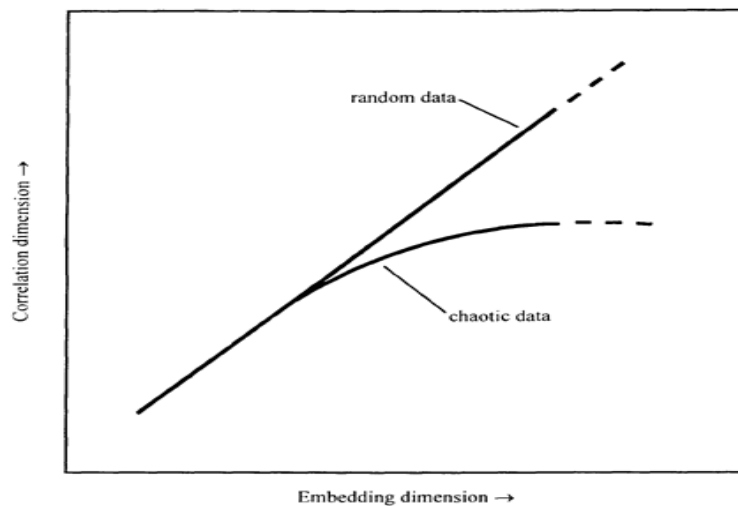


Figure 23: Hypothetical behavior (on arithmetic scales) of correlation dimension with increase in embedding dimension, for chaotic as compared to random data.

Random data, in contrast, continually fills the allotted space as the embedding dimension increases, at least for an infinite number of observations. Consequently, the slope (correlation dimension) continues to increase without any indication of becoming asymptotic, as shown in the upper curve in Figure 23 (Garnett P. Williams, 1997. Chaos Theory Tamed).

3.5.1.6. Approximate Entropy (ApEn)

Entropy is a statistical concept first introduced by Shanon and Weaver in 1963 as a measure of uncertainty or variability. The Approximate Entropy (ApEn) technique is used to quantify the amount of regularity and the unpredictability of fluctuations over time-series data.

Accurate entropy calculations require vast amounts of data and the results will be greatly influenced by system noise, making it impractical to apply these methods to experimental data. ApEn was developed by Pincus [68, 69] to handle these limitations by modifying an exact regularity statistic, Kolmogorov-Sinai entropy. ApEn was initially developed to analyze medical data but was later extended to areas such as finance, psychology, and human factors engineering [15]. Pincus defined ApEn as a specific method to determine complexity that can quantify the regularity or predictability of a time series. Approximate Entropy measures the logarithmic probability that a series of data points a certain distance apart will exhibit similar relative characteristics on the next incremental comparison within the state space [68,69]. If a time series has repetitive patterns of fluctuation, it renders that time series more predictable than a time series in which such patterns are absent. ApEn provides a direct measurement of feedback and connection. A low ApEn value often indicates predictability and high regularity of time series data, whereas a high ApEn value indicates unpredictability and random variation. ApEn values typically range between 0 and 2, with values close to 2 indicating greater complexity and those close to 0 indicating more predictability [22, 82]. Data points that exhibit greater possibilities of

remaining the same distance apart upon comparison will result in lower ApEn values, while those with large differences in distance between them will result in higher ApEn values.

3.5.1.7. Calculation of ApEn:

Calculating ApEn requires the selection of two parameters: m , the number of observation windows to be compared, and r , the tolerance factor. ApEn is defined mathematically according to the following procedure:

Step –1: Form a time series of data $u(1), u(2) \dots \dots \dots u(N)$. These are N raw data values from measurements taken at equally spaced points in time.

Step 2: Fix input parameters m , as an integer, and r , as a positive real number. The input parameter m represents the length of compared runs, and r represents the tolerance that specifies a filtering level.

Step 3: Form a sequence of vectors $x(1), x(2) \dots \dots \dots x(N - m + 1)$ in R^m , real m -dimensional space, defined by $x(i) = [u(i) \dots \dots u(i + m - 1)]$.

Step 4: Use the sequence $x(1), x(2) \dots \dots \dots x(N - m + 1)$ to construct for each $I, 1 \leq i \leq N - m + 1$.

$$C_i^m(r) = (\text{number of } x(j) \text{ such that } d[x(i), x(j)] \leq r) / (N - m + 1).$$

It is first necessary to define $d[x(i), x(j)]$ for vectors $x(i)$ and $x(j)$.

$$d[x, x^*] = \max_a |u(a) - u^*(a)|$$

where the $u(a)$ are the m scalar components of x . d represents the distance between the vectors $x(i)$ and $x(j)$, given by the maximum difference in their respective scalar components.

Step 5: Define

$$\Phi^m(r) = (N - m + 1)^{-1} \sum_{i=1}^{N-m+1} \ln C_i^m(r),$$

where \ln is the natural logarithm.

Step 6: Define Approximate Entropy (ApEn) as:

$$\text{ApEn}(m, r, N) = \Phi^m(r) - \Phi^{m+1}(r)$$

In order to compare the results, these parameters, along with the data length, must be kept the same for all calculations [22, 68, 69, and 82].

Typically $m = 2$ or 3 ; r depends on the application. The choice of m is made to ensure that the conditional probabilities, defined in the equation below for fixed m and r , are reasonably estimated from the N input data points. Theoretical calculations indicate that reasonable estimates of these probabilities, for fixed m and r chosen as discussed below, are achieved with between 10^m and 30^m points, analogous to the findings reported by Pincus [68, 69].

ApEn can be computed for any time series, chaotic or otherwise. The number of input points for ApEn computations typically ranges from 50 to 5,000 points. Using fewer than 50 data points yields less meaningful results, especially for $m = 2$ or 3 , while using more than 5,000 points will result in unacceptably long computational times. For noiseless, theoretically described systems such as Henon maps and logistic maps it has been shown that if entropy (A) \leq entropy (B), then $\text{ApEn}(m, r)(A) \leq \text{ApEn}(m, r)(B)$ and vice versa. Moreover, for both theoretical and experimental systems, if $\text{ApEn}(m_1, r_1)(A) \leq \text{ApEn}(m_1, r_1)(B)$, then $\text{ApEn}(m_2, r_2)(A) \leq \text{ApEn}(m_2, r_2)(B)$ and vice versa. This ability of ApEn to preserve the order is a relative property and is an important utility of ApEn [17, 18]. As a result, one should not conclude that for the same systems $\text{ApEn}(m_1, r_1)(A) \leq \text{ApEn}(m_2, r_2)(B)$, as ApEn values differ with different m and r values. The strength of ApEn is its ability to compare systems.

To calculate ApEn, two critical parameters (m and r) must be set in order to achieve reasonable results. Different m and r values would result in different results: $\text{ApEn}(2, 0.1, N)$ may be different from $\text{ApEn}(3, 0.01, N)$. ' r ' is effectively a filter level and in order to eliminate the effect of noise in the ApEn calculation, ' r ' must be chosen such that its value is above most

of the noise. In order to achieve reasonable results the magnitude of noise should rarely reach ' r '. Another key factor in choosing the value of r is that it should be large enough to achieve numerically stable conditional probability estimates. If the ' r ' value is small, unstable conditional probability estimates are obtained, while larger ' r ' values result in detailed system information being lost due to filter coarseness. In the current study a value of 2 was used for m and r was 0.2 [22, 68, 69, and 82].

3.5.2. EMG Data Analysis –

3.5.2.1. Identifying muscle activation pattern–

For this study, EMG data were obtained from 12 low back and abdomen muscles (Erector Spinae Left and Right, Multifidus Left and Right, Latissimus Dorsi Left and Right, Internal Obliques Left and Right, External Obliques Left and Right, and Rectus Abdominis Left and Right) using 12 channels of DELSYS sEMG sensors. EMG sensors measured the electrical activity of the muscles during walking. The EMG data was recorded using a DELSYS Bagnoli - 12 Channel EMG System at 1200 samples per second. The EMG signals were amplified 1000 times and band passed between 20 Hz and 500 Hz [27, 88]. EMG signal analysis identified the muscle activation pattern from recruited low back and abdomen muscles during gait while carrying a unilateral load. A time series was created from EMG signals and then analyzed. If a muscle was not recruited, then the spike in muscle activity was absent throughout the motion, indicating that that muscle was not involved in that motion.

3.5.2.2. Fast Fourier Analysis

Time series analyses are generally divided into two classes: frequency-domain methods and time-domain methods. Frequency domain analysis treats the data as a function of frequency and time domain analysis as a function of time [12, 77]. Frequency domain analysis is a powerful

data analysis tool employed by variety of disciplines, including mathematics, optics, genetics, and physics. The frequency domain transform most commonly used in biomechanics is the Fast Fourier Transform. In human movement, most data is collected in the time domain, but this is not the only way to examine the data. The data can be described as a sum of simple sinusoids each having specific frequency using Fourier transformations. A frequency domain representation can also include information on the phase shift that must be applied to each trace in order to recombine the frequency components and thus recover the original time signal. The Fourier transform decomposes a function into the sum of a (potentially infinite) number of sine wave frequency components. The 'spectrum' of frequency components is the frequency domain representation of the signal. This study will apply non-linear methods to calculate the chaos in a dynamic system, but it is first necessary to ensure that the system is indeed chaotic, as noted earlier. There are several ways this can be done, including Fast Fourier Transformation (FFT) and Phase Plane plots [57]. A **fast Fourier transform (FFT)** is an efficient algorithm to compute the discrete Fourier transforms (DFT) and it's inverse.

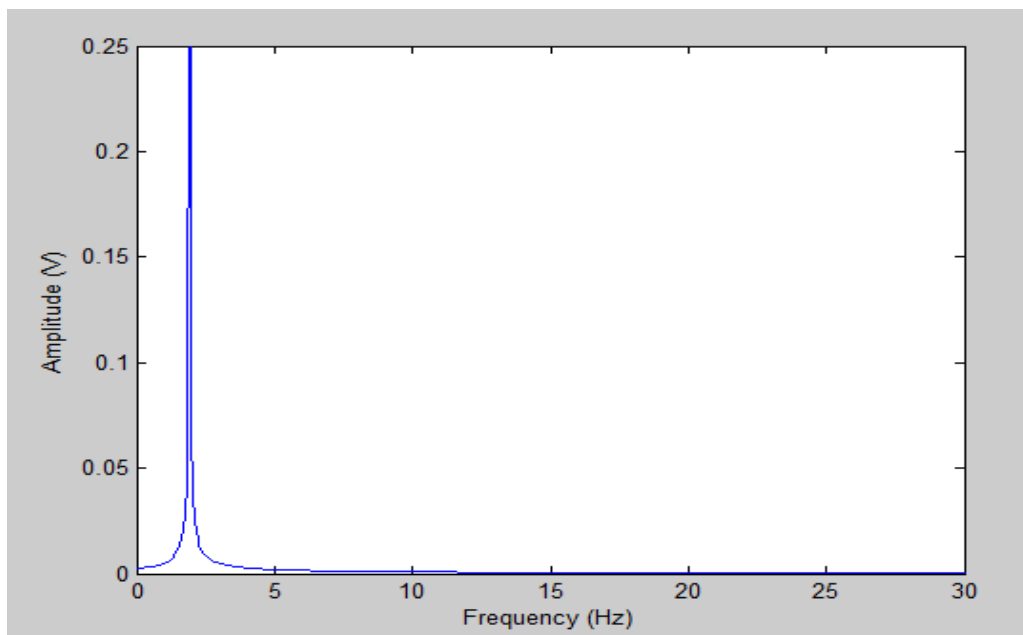


Figure 24: FFT of a periodic sine curve

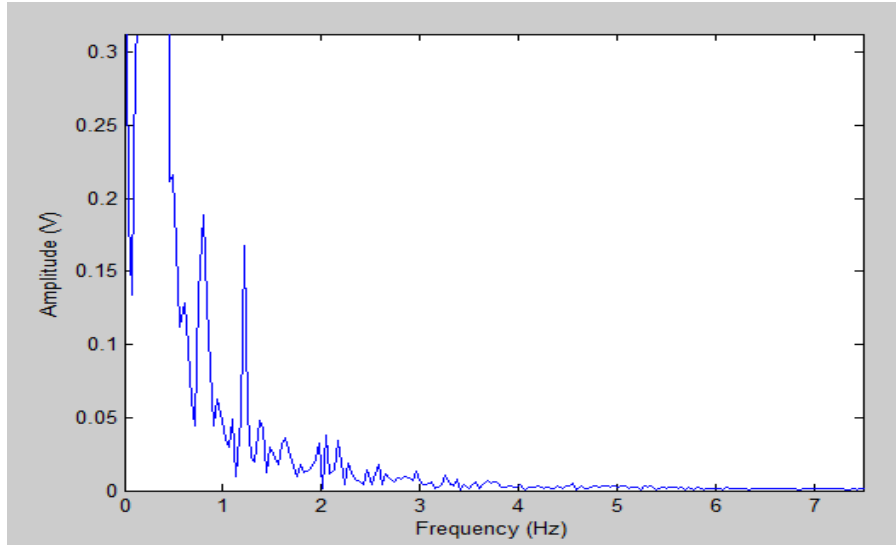


Figure 25: FFT of experimental motion data

Let x_0, \dots, x_{N-1} be complex numbers. The DFT are defined by the formula

$$X_k = \sum_{n=0}^{N-1} x_n e^{-i2\pi k \frac{n}{N}} \quad k = 0, \dots, N - 1.$$

The FFT plots in Figures 26 and 27 show that the experimental data contain continuous spectra over a limited range, as opposed to an FFT of a simple sine wave, which returns a single frequency. This is an indication that the experimental data might be chaotic. The next step is therefore to estimate the Power Spectral Density.

3.5.2.3. Power Spectral Density

Another way to examine the contribution of frequencies to the signal is by calculating the power spectral Density (PSD) of the signal (Thomson, 1982; Welch, 1967). The power spectrum of a given signal is unique and represents the square of the magnitude of the signal's Fourier transform. The Power Spectrum and PSD of the kinematics data and kinetic data have a high power at lower frequencies and vice-versa (winter et al.1974). In the case of the EMG data, this

represents a random process that makes the power spectrum noisy (Figure 26) as opposed to the estimated PSD, which represents a relatively smooth, process. Generally, PSD are used in the analysis of EMG signals, especially during fatigue protocols. It has been observed (DeAngelis et.al.1990; DeLuca et al. 1984; Linsseen et al. 1993) that the firing rate of muscles becomes slower with the onset of fatigue.

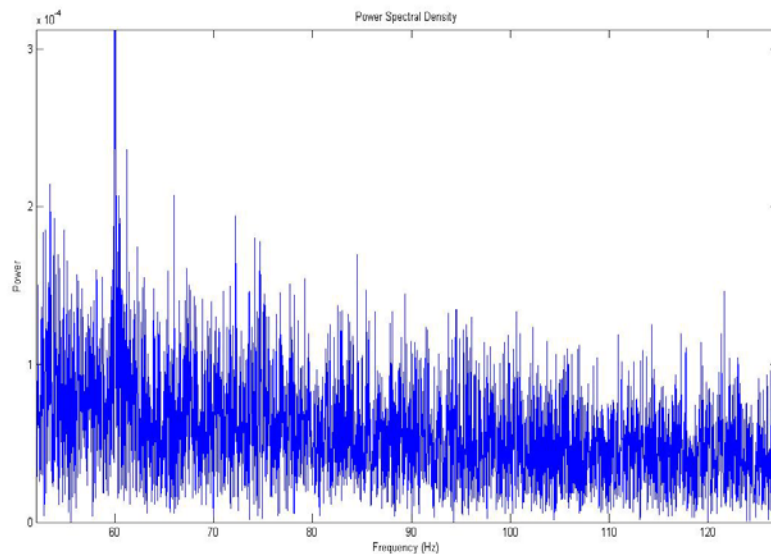


Figure 26: PSD for ES Left during walking with 10 lbs for participants 7.

3.5.2.4. Sampling Frequency

To ensure the data have been collected at the right sampling frequency, Shannon's sampling theorem (Hamill et al. 1997) must be applied. This states that a band limited at the frequency of f (Nyquist Frequency) signal should be recorded at a rate of at least $2f$. If a frequency lower than the Nyquist Frequency is utilized, vital information will be hidden. For example, consider the human eye. If it samples at approximately 14 pictures per seconds (14Hz), when a bicycle moves slowly we can easily see its wheels rotating forward, but when the wheel

rotates with higher velocity, the wheel appears to rotate backward. This is because the eye does not sample fast enough to capture the fast movement of the wheel. This has implications for data storage, however, as a higher sampling frequency requires more space to store the resulting data. In this study, for the Kinetic data and Kinematics Data a 120 Hz sampling frequency was selected and for the EMG data a 1200 Hz sampling frequency [46, 51, 77].

3.5.2.5. Mean and Median Frequency of sEMG signals –

The next step was to calculate the mean and median frequencies of the recorded sEMG signals from the calculated PSD. The median frequency is the frequency at which 50% of the total power of signal is reached. Mean frequency is the frequency at which the average power of signal is reached (BIOPAC Systems Inc., Application notes). Previous research has shown that the mean and median frequencies decrease with fatigue induced in muscles (Bilodeau et. al., 2003; Mannion et. al., 1997). It would therefore be interesting to see how the mean and median frequencies in the different muscles behave during walking with increasing loads. Here, mean and median frequencies were extracted using Power Spectral Density (Fourier analysis) using customized MATLAB programs in the Biomechanics et. al. Toolbox (BEAT) created by Ian Kremenec and Ali Sheikhzadeh from the Nicholas Institute of Sports Medicine and Athletic Trauma. The mean was calculated as the ratio of sum of product of signal amplitude and frequency to sum of amplitudes, whereas the median frequency was calculated as the frequency which divides the spectrum into two equal parts and has been demonstrated to be a valid measure of frequency shift or compression associated with fatigue [49] (Joseph K-F et al. 1997; Stulen and DeLuca, 1981; Medved, 2001). Several factors may affect the EMG frequencies, including changes in the motor unit firing rate, number of active motor units, age, load and decreases in movement velocity. Here, mean and median frequencies are used to define muscle fatigue. From

a neurophysiological perspective, neuromuscular fatigue is manifested as a reduction of the frequency content constituting the power density spectrum of the propagating myoelectric signal (Komi and Tesch, 1979; Viitasalo and Komi, 1977). Muscular fatigue, however, is observed biomechanically as a reduced capacity of the muscle to maintain a specified force output [54].

3.5.3. Ground Reactions Forces (GRF)

The ground reaction force (GRF) is the force exerted by the ground on a body in contact with it. The ground reaction force is equal in magnitude and opposite in direction to the force that the body exerts on the supporting surface through the foot. For example, a person standing motionless on the ground exerts a contact force on it equal to the person's weight, and at the same time an equal and opposite ground reaction force is exerted by the ground on the person. The use of the word reaction derives from Newton's third law, which essentially states that if a force, or action, acts upon a body, then an equal and opposite force, the reaction, must act upon another body. The component of the GRF parallel to the surface is the frictional force. When slippage occurs, the ratio of the magnitude of the frictional force to the normal force yields the coefficient of static friction [19].

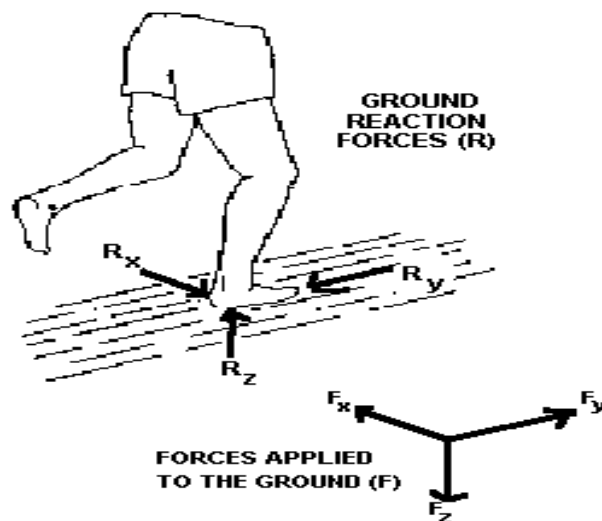


Figure 27: Ground Reaction Force

Figure 27 shows the three components (F_x , F_y , and F_z) of GRF. GRF data were collected during the stance phase using a force plate at 120 samples per second while participants walked back and forth on a wooden platform carrying increasing loads. The Force Plate (BERTEC 4060-NC) was embedded into the wooden platform. Whenever participants stepped on the force plate, it recorded the GRF. The data collection was then exported for further analysis. Force plates measure the ground reaction forces generated by a body standing on or moving across them to quantify balance, gait and other parameters of biomechanics [20]. For this analysis, only vertical ground reaction force (vGRF) was used. To quantify the vGRF pattern, the mean and standard deviation of the magnitude and time of occurrence of the vGRF were extracted from the force plate data using custom programs written in MATLAB R2010a. All steps recorded during the treadmill measurement were used for analysis to determine how increasing loads affect GRF.

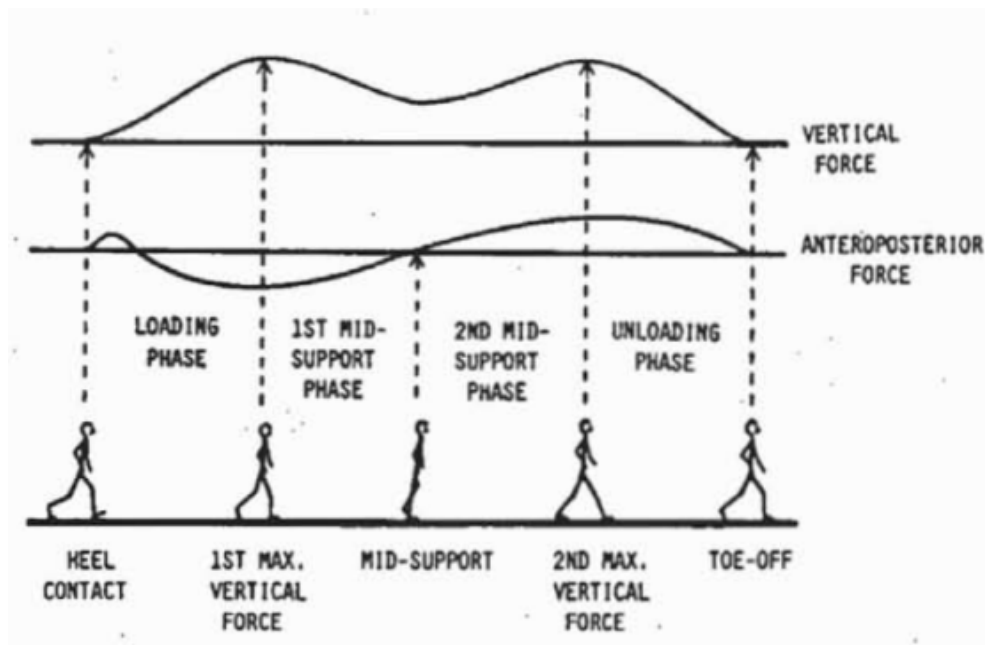


Figure 28: Identification of the four functional phases of gait

Figure 28 shows an example of a typical vGRF profile during walking (stance phase). The stance phase is from heel contact to toe off. During gait, the stance phase can be divided into

the Early Stance or Loading Phase (from heel contact to foot flat); Mid-Stance (from foot flat to heel off); and Late Stance or Terminal Phase (from heel off to toe off).

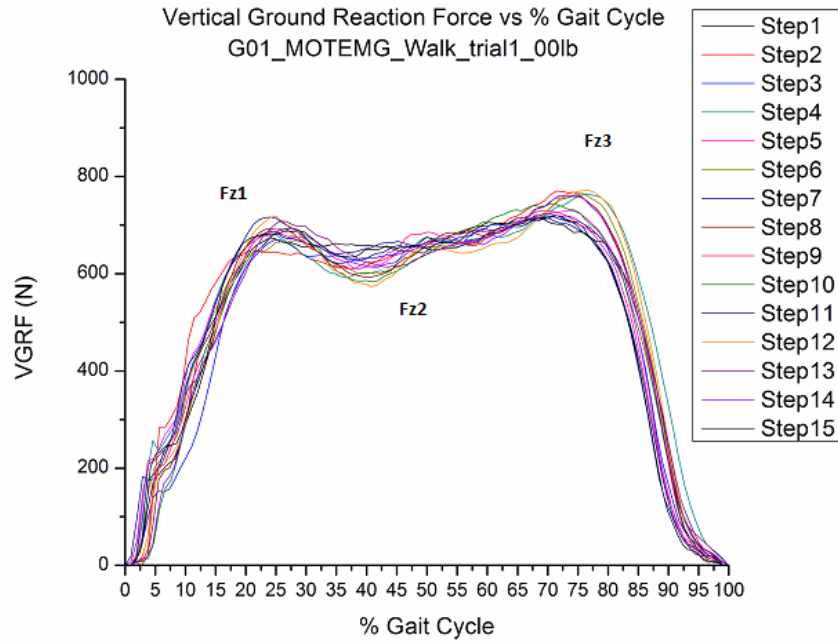


Figure 29: vGRF profile during walking

Figure 29 shows how the vertical ground reaction force consists of three component forces: Fz1, Fz2 and Fz3. Fz1 is the first peak on the vGRF profile, also known as the loading force, Fz3 is the peak force on the vGRF profile, also known as the unloading or propulsive force, and Fz2 is the minimum force between the first peak force and the 3rd peak force, known as the mid stance force.

Normalization is used to adjust values measured on different scales to a notionally common scale, often prior to averaging. The vGRF for each participant was normalized to their body weight for data analysis.

$$\text{Normalized vGRF} = \text{vGRF in Newtons} / \text{Body weight}$$

CHAPTER 4

RESULTS

4.1. Ground Reaction Forces

The one of the objective of the study was to assess the effects of increased load on vertical ground reaction forces during walking. Ground Reaction Force data were recorded using embedded force plate (BERTEC 4060-NC) in walkway at 120 samples per second while participants walked on wooden platform back and forth with carrying increasing loads. To quantify the vGRF pattern, the magnitude and time of occurrence of the vGRF were extracted from the force plate data. Mean and standard deviation were calculated for vGRF and its magnitude normalized to each participant's body weight.

Tables 3 and 4 show the magnitude (mean and SD) of the 1st peak (Fz1), 2nd peak (Fz3) and Fz2 of the Vertical Ground Reaction Forces (in Newtons) and normalized vGRF during walking with increasing loads for all 9 participants. In Table 3, the magnitude (Fz1, Fz3 and Fz2) shown is the mean for all 9 participants. In Table 4, the forces are normalized to each participant's body weight.

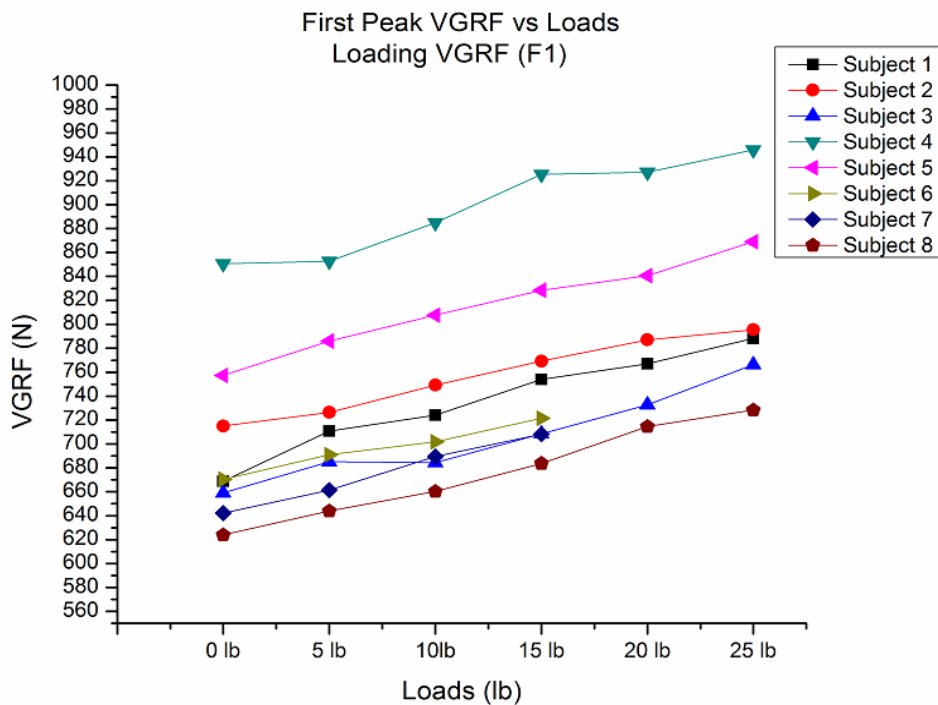
As the data in the tables 3 & 4 demonstrates, both vGRF (N) and normalized vGRF increased as the load increased from 0 lb to 25 lbs during walking. All three of the forces (Fz1, Fz2, and Fz3) increased with increasing load, which is consistent with the normalized vGRF data. Interestingly, the Propulsive or Unloading Force (Fz3) was always greater than the Loading Force (Fz1) for participants walking with increasing loads.

Table 3: Vertical Ground Reaction Forces (N) during walking carrying different loads

vGRF	0 lb	5 lb	10 lb	15 lb	20 lb	25 lb
Fz1	698.4 (74.5)	719.7 (69.1)	737.7 (74.9)	762.4 (79.9)	794.9 (78.4)	815.5 (78.7)
Fz2	662.3 (77.7)	680.9 (75.7)	703.2 (72.9)	723.9 (74.1)	766.4 (78.0)	788.7 (77.7)
Fz3	712.2 (89.4)	737.1 (89)	758.8 (89.5)	783.6 (87.8)	821.8 (88.9)	836.9 (91.1)

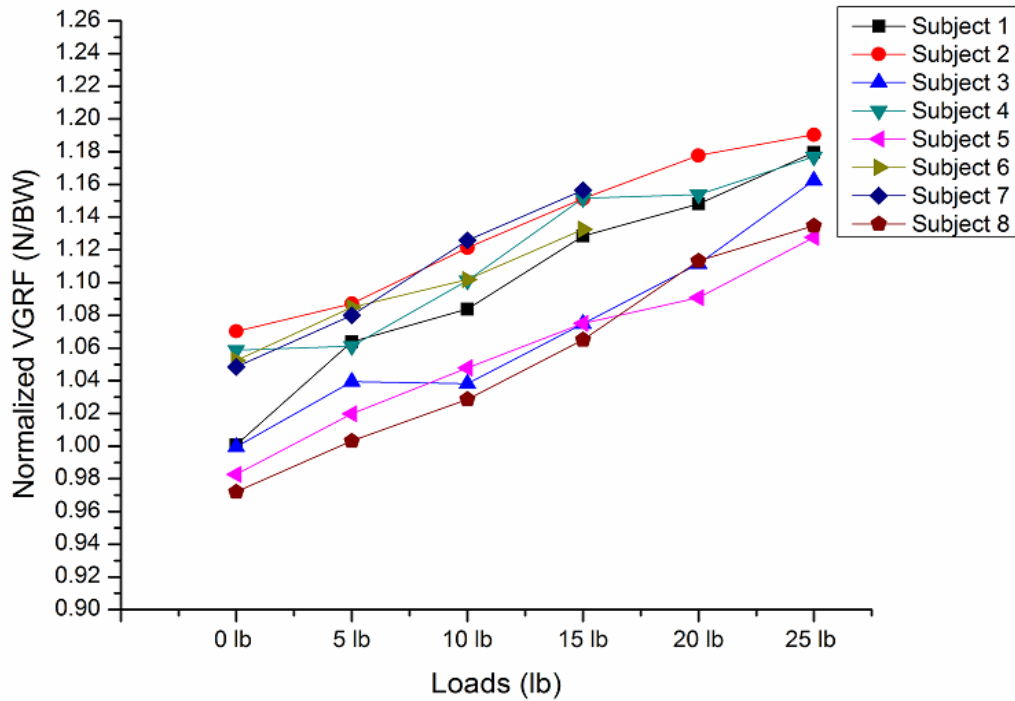
Table 4: Normalized vGRF during walking carrying different loads

vGRF (BW)	0 lb	5 lb	10 lb	15 lb	20 lb	25 lb
Fz1	1.02 (.04)	1.05 (.03)	1.08 (.04)	1.11 (.04)	1.13 (.03)	1.16 (.03)
Fz2	0.97 (.02)	0.99 (.02)	1.03 (.02)	1.06 (.02)	1.09 (.02)	1.12 (.02)
Fz3	1.04 (.05)	1.08 (.04)	1.11 (.04)	1.15 (.05)	1.17 (.05)	1.19 (.05)



(a)

First Peak VGRF(Normalized to Body weight) vs Loads



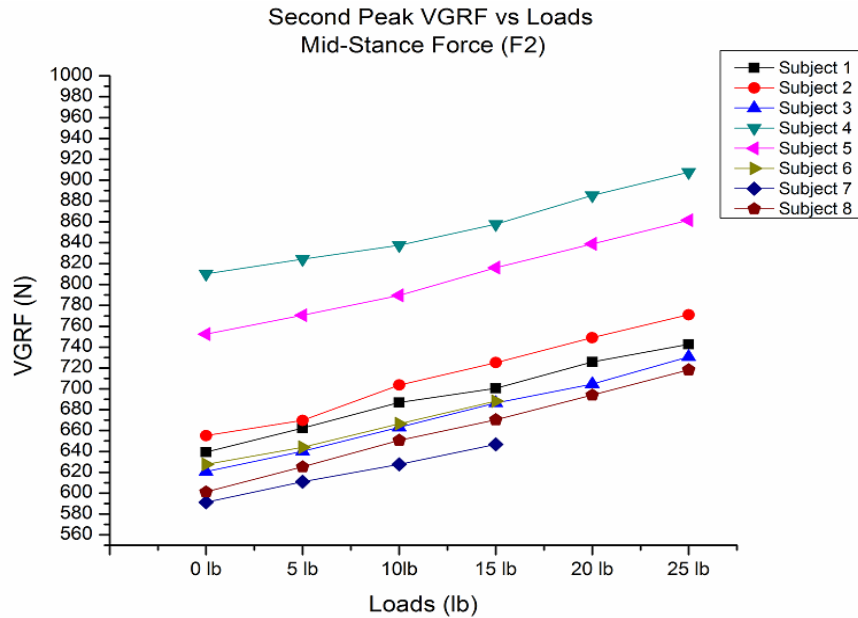
(b)

Figure 30: First peak Force a) vGRF (N) and b) Normalized vGRF during walking carrying varying loads

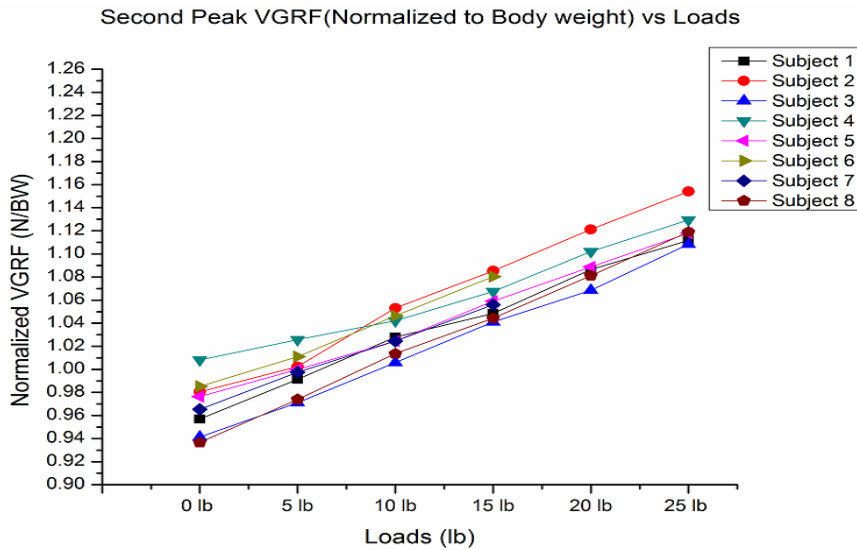
Figure 30 shows the 1st peak loading force for eight of the participants. In the averaged data, both vGRF (N) and normalized vGRF increased during walking as the loads increased from 0 lb to 25 lbs and the same pattern is visible in the data for the individual participants. As load increased, both vGRF (N) and normalized vGRF for each individual also increased.

Figure 31 shows the Fz2 (Mid-Stance Force) data for eight of the individual participants and the same pattern is again visible. As the load increased, both vGRF (N) and normalized vGRF for each individual also increased.

Figure 32 shows the 2nd peak force (Fz3, Unloading or propulsive Force) for eight individual participants, which once again display the same pattern as in the previous graphs. As the load increased, both vGRF (N) and normalized vGRF for each individual also increased.



(a)



(b)

Figure 31: 2nd peak Force a) vGRF (N) and b) Normalized vGRF during walking carrying varying loads

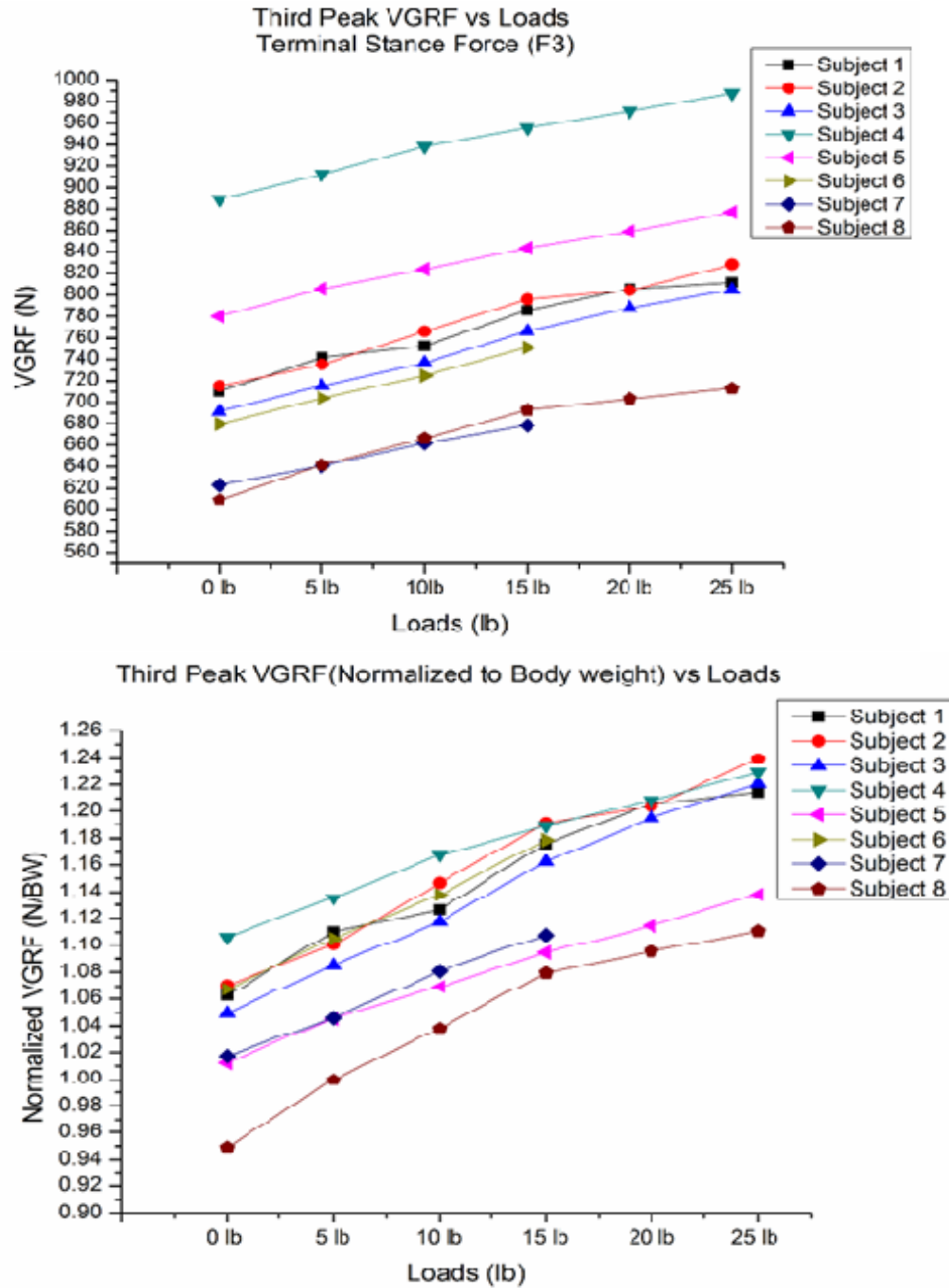
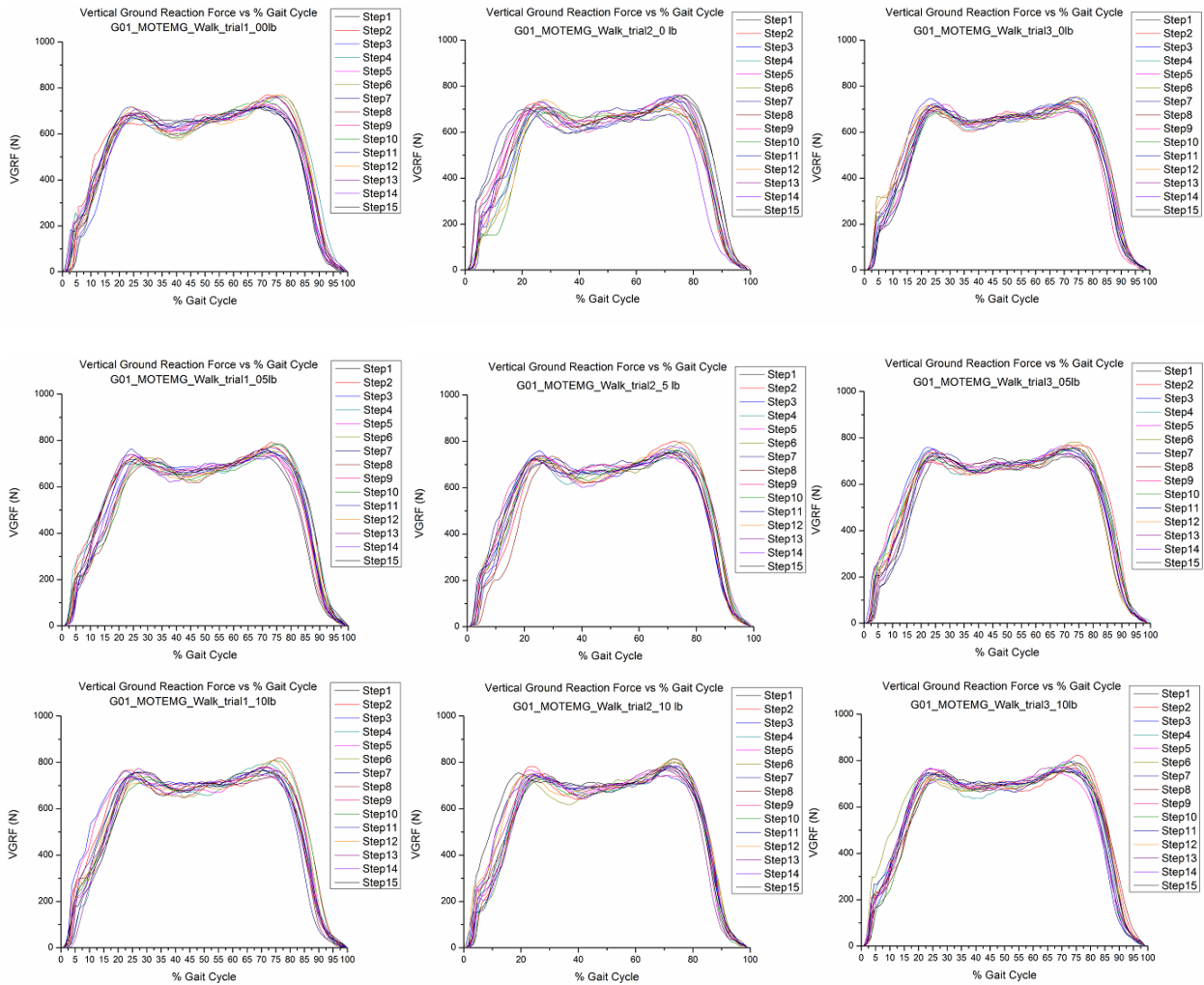


Figure 32: 3rd peak Force a) vGRF (N) and b) Normalized vGRF during walking carrying varying loads

Table (5) shows the time of occurrence of different gait events with increasing loads.

Table 5: Average time during different phases of gait

Time (s)	0 lb	5 lb	10 lb	15 lb	20 lb	25 lb
Loading	0.29 (.05)	0.28 (.06)	0.30 (.09)	0.41 (.03)	0.32 (.09)	0.32 (.10)
Mid-stance	0.17 (.03)	0.17 (.03)	0.19 (.04)	0.19 (.04)	0.19 (.02)	0.19 (.02)
	0.27 (.03)	0.26 (.05)	0.40 (.05)	0.22 (.05)	0.23 (.03)	0.23 (.05)
Unloading	0.33 (.06)	0.28 (.03)	0.32 (.05)	0.31 (.06)	0.30 (.04)	0.32 (.05)



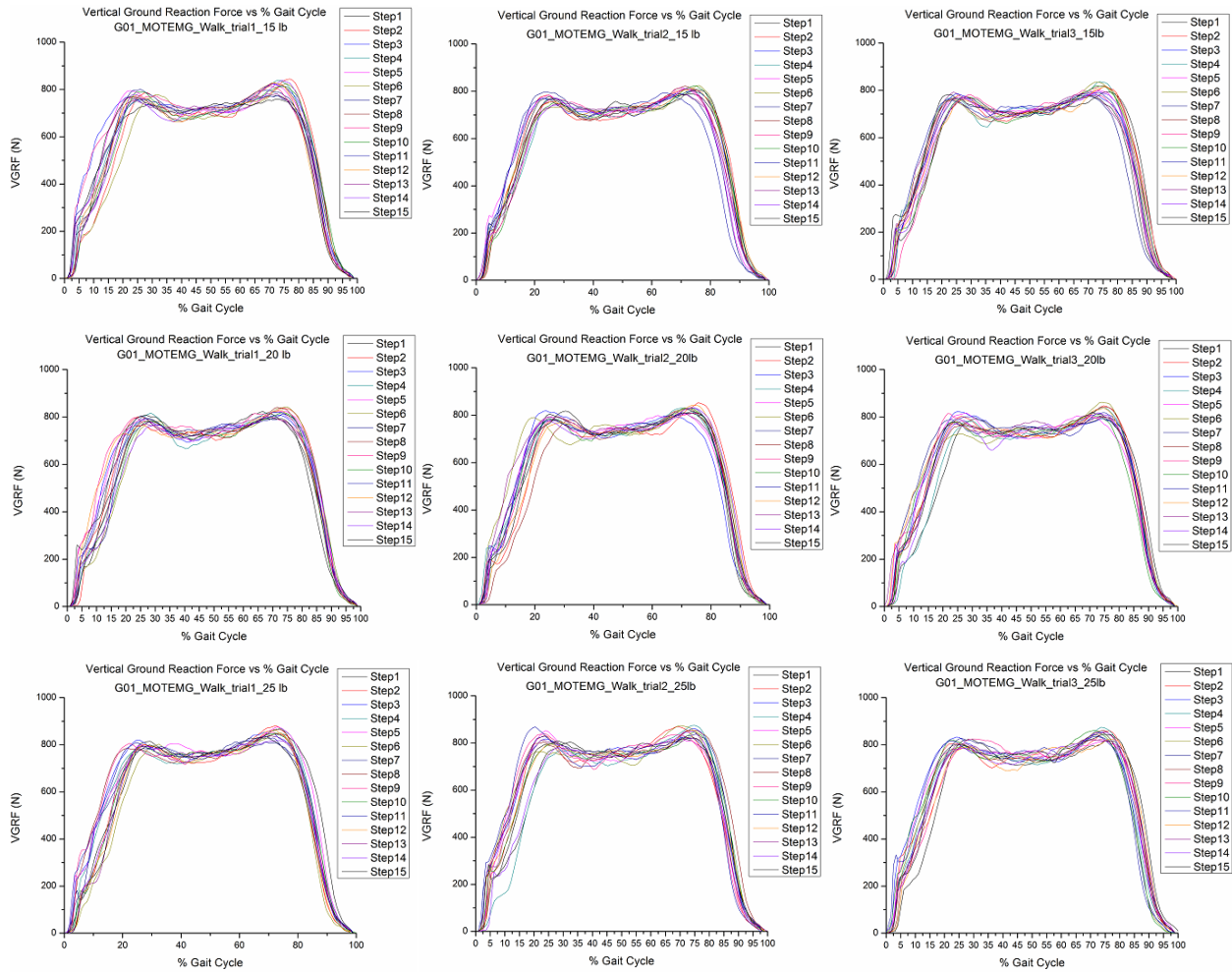


Figure33: vGRF (N) vs. % Gait Cycle during walking carrying varying loads

Figure 33 shows the vertical ground reaction force profile during walking with increasing loads. According to the experimental protocol, participants stepped on the force plate 15 times. The above graphs represent the vertical ground reaction force profile for 15 steps. There was considerable consistency in all 15 of the steps monitored when walking with increasing loads, with very little time differences during different gait events even with increasing loads. This indicates that loading force ($Fz1$), Mid-Stance force ($Fz2$) and Unloading force ($Fz3$) occur at around the same time in spite of the increasing loads (0 lb – 25lb).

One-way ANOVA revealed significance differences ($p < 0.05$) in the forces themselves, namely Fz1, Fz2, and Fz3, during walking with increased loads even though the timing was unaffected.

4.2. EMG:

Data were collected from 12 muscles (Erector Spinae Left and Right, Multifidus Left and Right, Latissimus Dorsi Left and Right, Internal Obliques Left and Right, External Obliques Left and Right, and Rectus Abdominis Left and Right) using the DELSYS system. Data were recorded at a sampling frequency of 1200 Hz and the raw EMG data were then filtered and processed using a custom Matlab program. EMG data were analysed in 2 ways: first, to identify the muscle recruitment during walking with varying loads for each participant and then to calculate the mean and median frequency using Fast Fourier Transformation during walking with varying loads.

Identify the muscles recruitment during gait for each participant:

Interestingly, the participants recruited different numbers of muscles when walking with varying loads. Here, the root mean square values (RMS) during walking were compared with the MVC RMS values. Table 6 shows details regarding which muscle was recruited and by how many participants during walking with varying loads. The muscle activation was categorized in 4 phases: Active (above 60% MVC), Moderately Active (30-60% MVC), Low Activity (10-30% MVC) and Not Active (less than 10% MVC).

As the table 6 shows, for ES Left, 8 participants recruited that muscle for loads from 0 lb to 15 lb and all the participants recruited it for loads of 20 lb to 25 lb, while ES Right all participants recruited that muscles from 0 lb to 25 lb.

**Table 6: Muscles recruitment during Walking by number of participants.
Where A: Active, MA: Moderate Active, LA: Low Active**

Muscle	No. of participants who used that muscle during walking varying loads																	
	0 lb			5 lb			10 lb			15 lb			20 lb			25 lb		
	A	M	L	A	M	L	A	M	L	A	M	L	A	M	L	A	M	L
ES Left	6	2		7	1		7	1		7	1		7			7		
ES Right	7	2		7	2		7	2		7	2		5	2		5	2	
RA Left	4	2	3	4	2	3	4	3	2	4	3	2	3	3	1	3	3	1
RA Right	5	1	2	5	1	2	5	1	2	5	1	2	3	1	2	3	2	2
EO Left	2	4	2	3	4	1	3	5	1	3	5	1	4	2	1	4	2	1
EO Right	2	4	1	2	3	2	2	4	1	2	5		1	3	2	1	3	2
IO Left	2	4	3	3	4	2	2	6	1	3	5	1	4	2	1	4	2	1
IO Right	3	4	2	3	4	2	2	5	2	2	5	2	2	3	2	2	3	2
LD Left	6	3		6	2		6	3		7	2		5	2		5	2	
LD Right	8	1		8	1		9			9			7	1		7	1	
MF Left	8	1		8	1		9			9			7			7		
MF Right	8	1		8	1		8	1		8	1		6	1		6	1	

For RA Left, all the participants recruited the muscle for loads from 0 lb to 25 lb, while for RA Right, 8 participants recruited that muscle for loads from 0 lb to 15 lb and 6 participants recruited it for loads from 20 lb to 25 lb. For EO Left, 8 participants recruited the muscle for loads from 0 lb to 15 lb and all the participants recruited it for loads from 20 lb to 25 lb, while for EO Right 7 participants recruited the muscle for loads from 0 lb to 15 lb and 6 participants recruited it for loads from 20 lb to 25 lb. For all the remaining muscles, namely IO Left, IO Right, LD Left, LD Right, MF Left and MF Right, all the participants recruited these muscles for all the loads carried.

Mean and Median Frequency during Walking with varying loads –

The figures 34 below show the results of the mean and median frequency calculations for the data obtained from all muscles during walking with varying loads. The range of the mean frequency during walking with varying loads was between 80-210 Hz and the range of the median frequency during walking with varying loads was between 55-180 Hz.

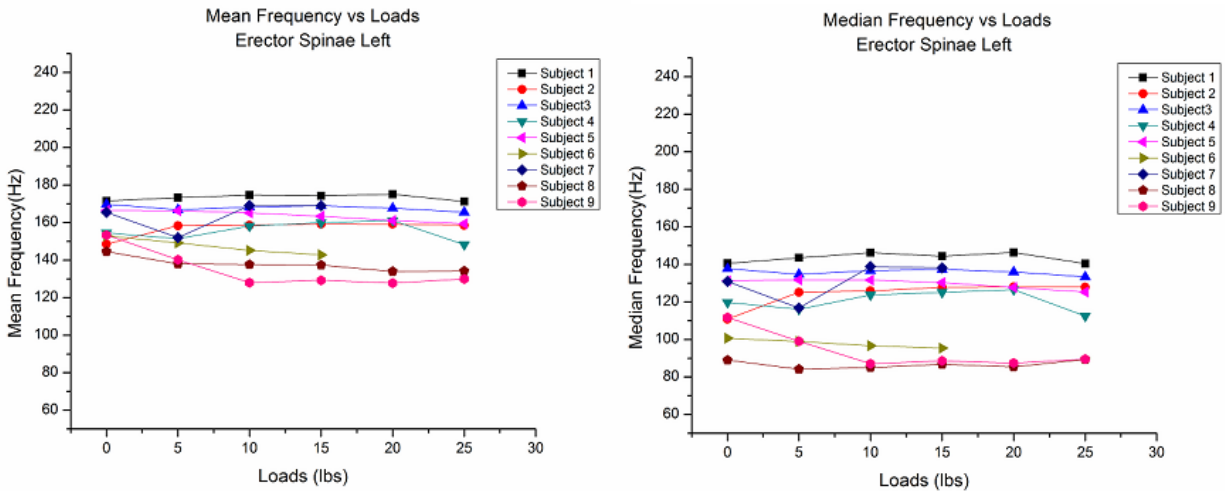


Figure 34: ES Left – Mean Frequencies and Median Frequencies during walking with varying loads

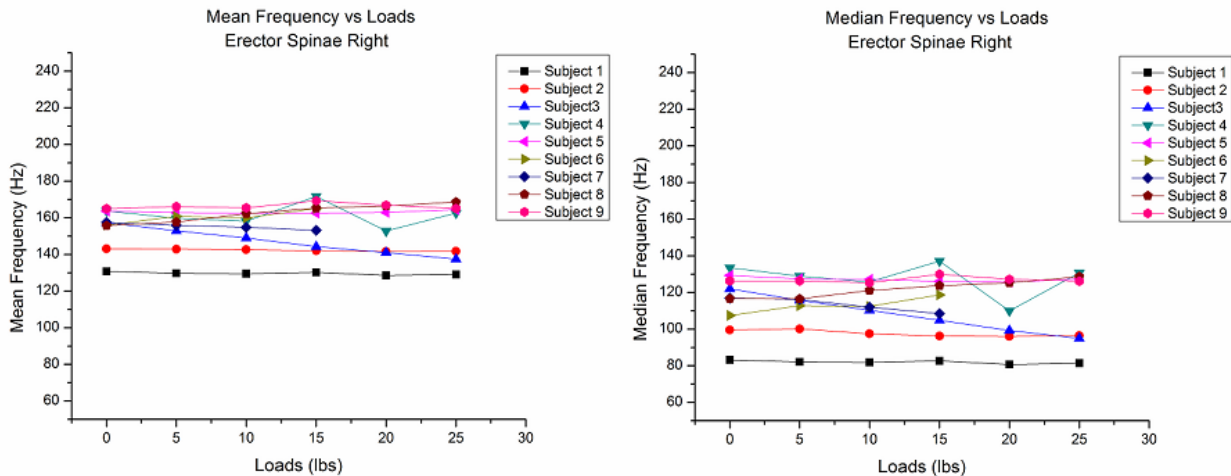


Figure 35: ES Right - Mean Frequencies and Median Frequencies during walking with varying loads

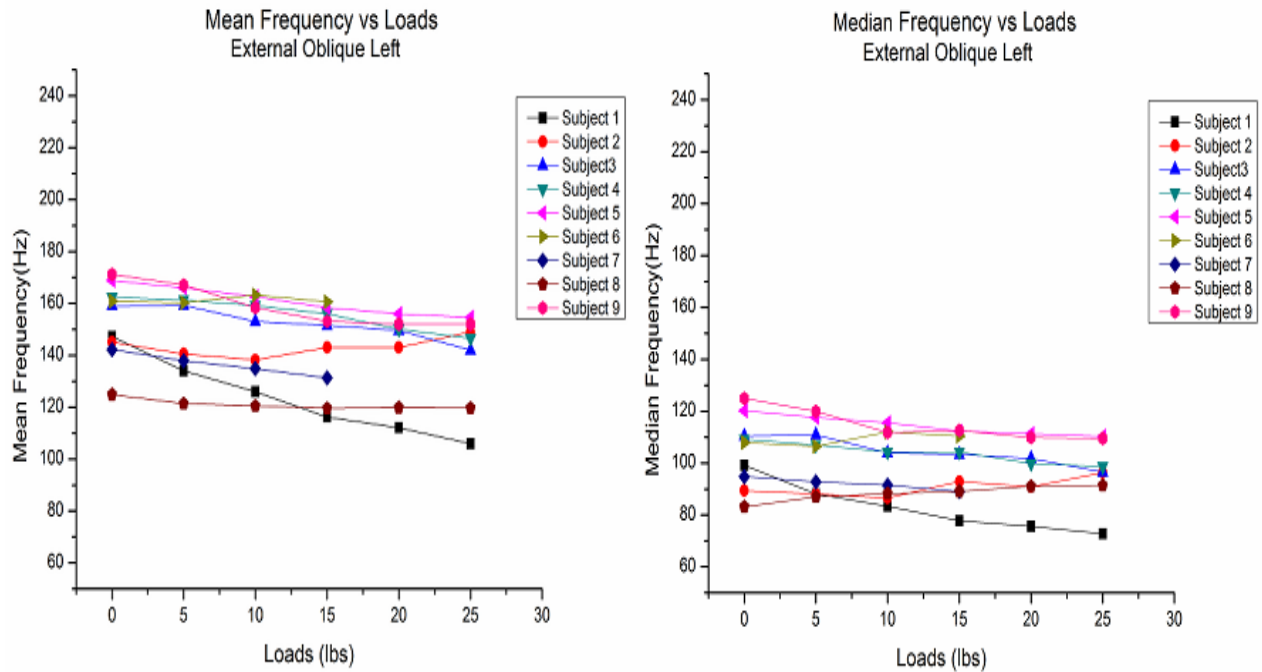


Figure 36: EO Left - Mean Frequencies and Median Frequencies during walking with varying loads

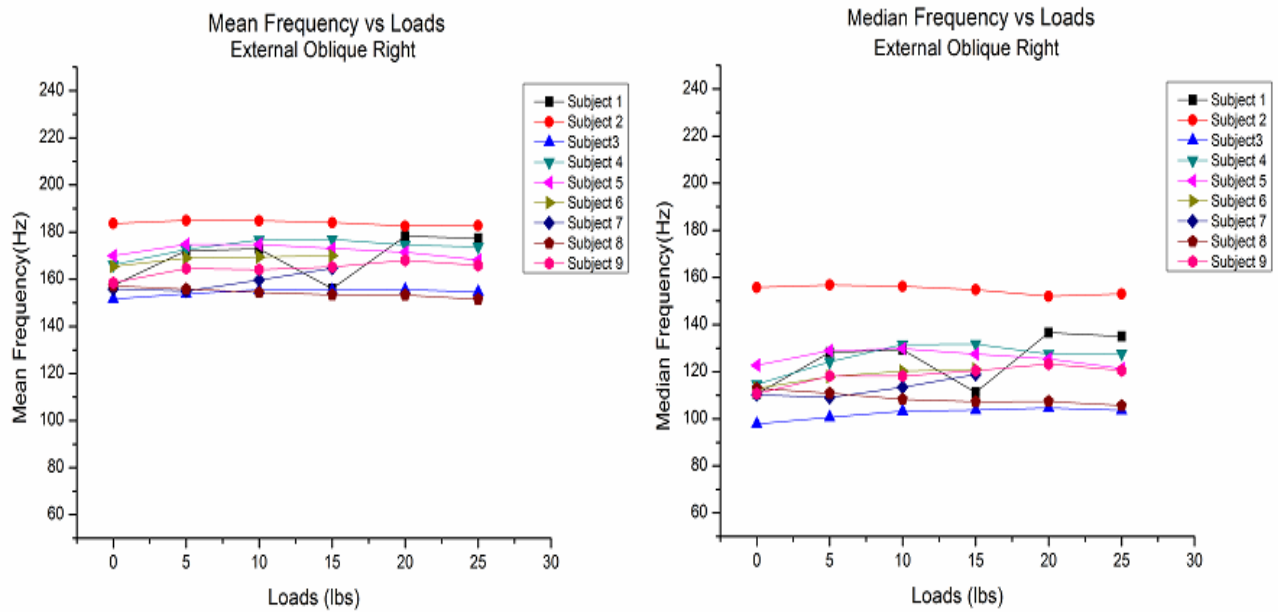


Figure 37: EO Right - Mean Frequencies and Median Frequencies during walking with varying loads

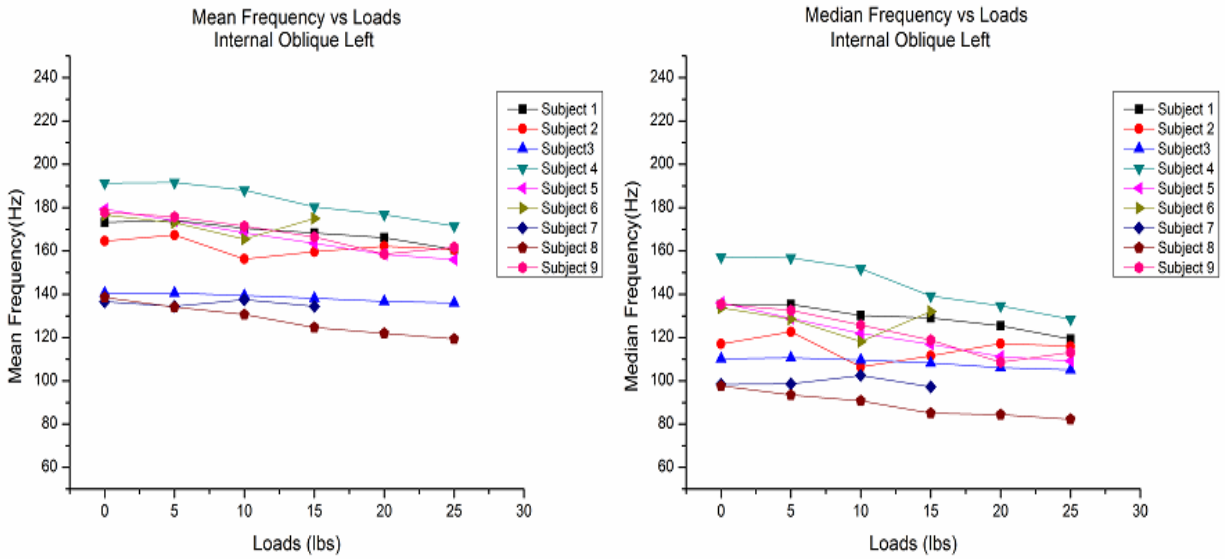


Figure 38: IO Left - Mean Frequencies and Median Frequencies during walking with varying loads

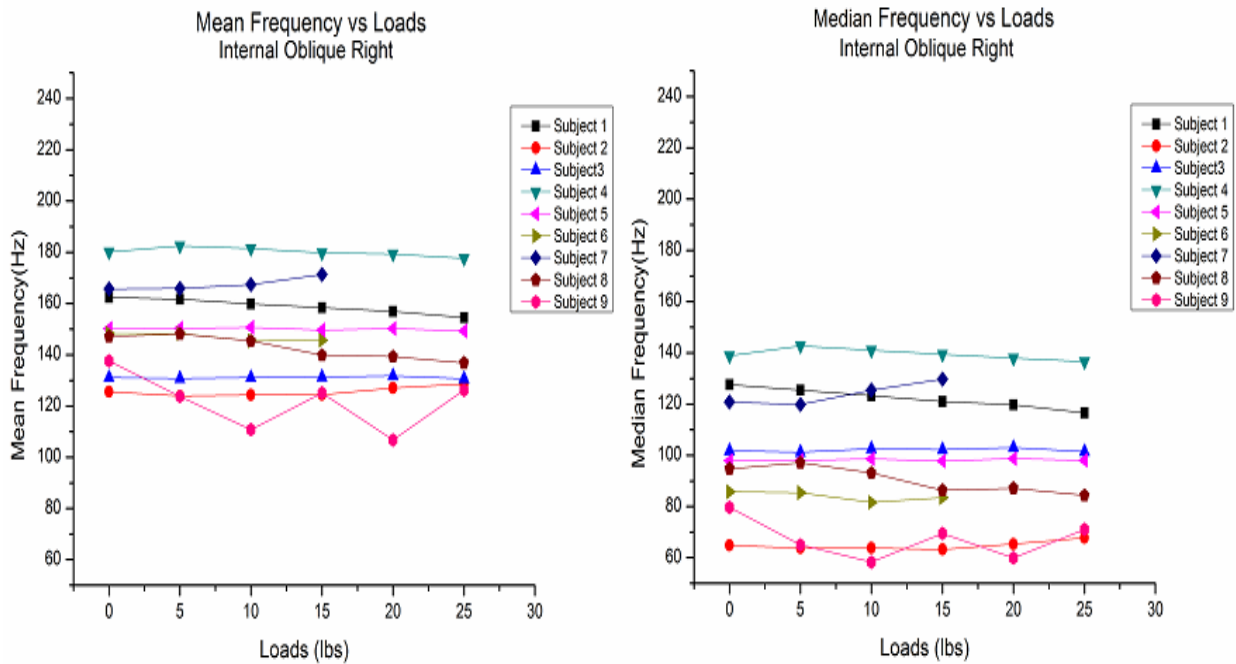


Figure 39: IO Right - Mean Frequencies and Median Frequencies during walking with varying loads

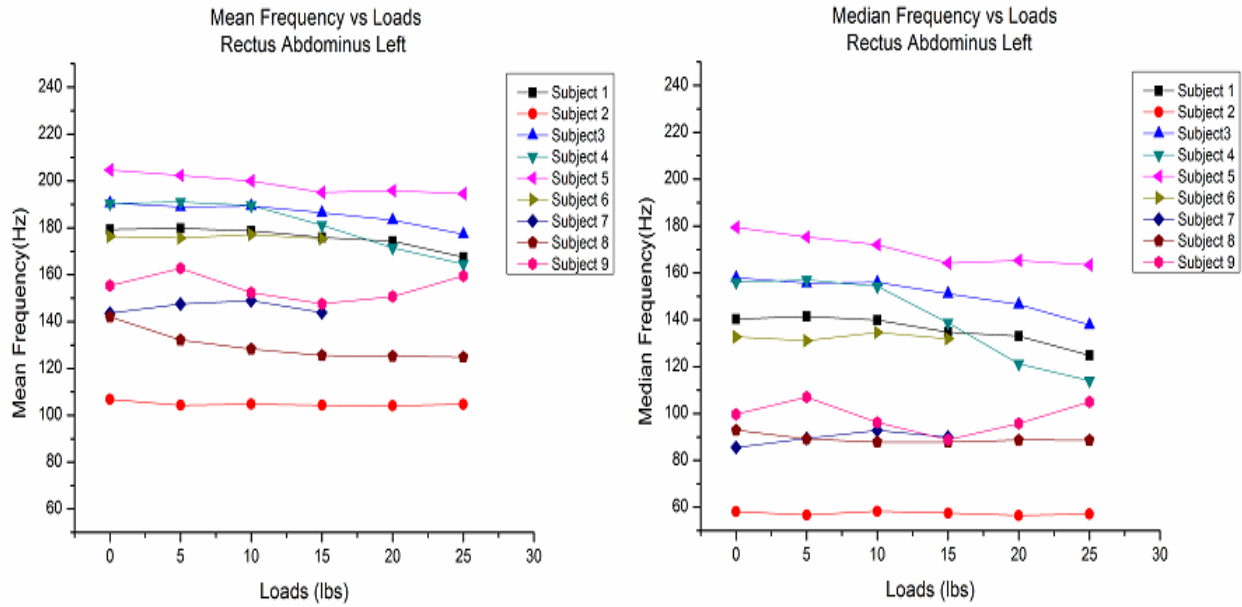


Figure 40: RA Left - Mean Frequencies and Median Frequencies during walking with varying loads

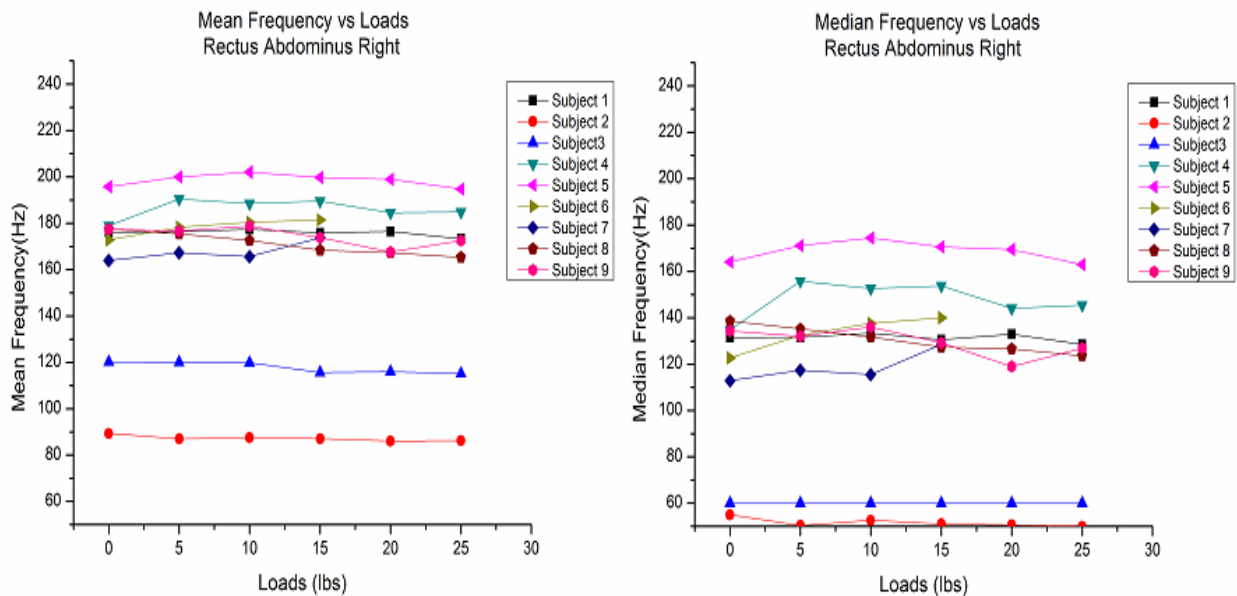


Figure 41: RA Right - Mean Frequencies and Median Frequencies during walking with varying loads

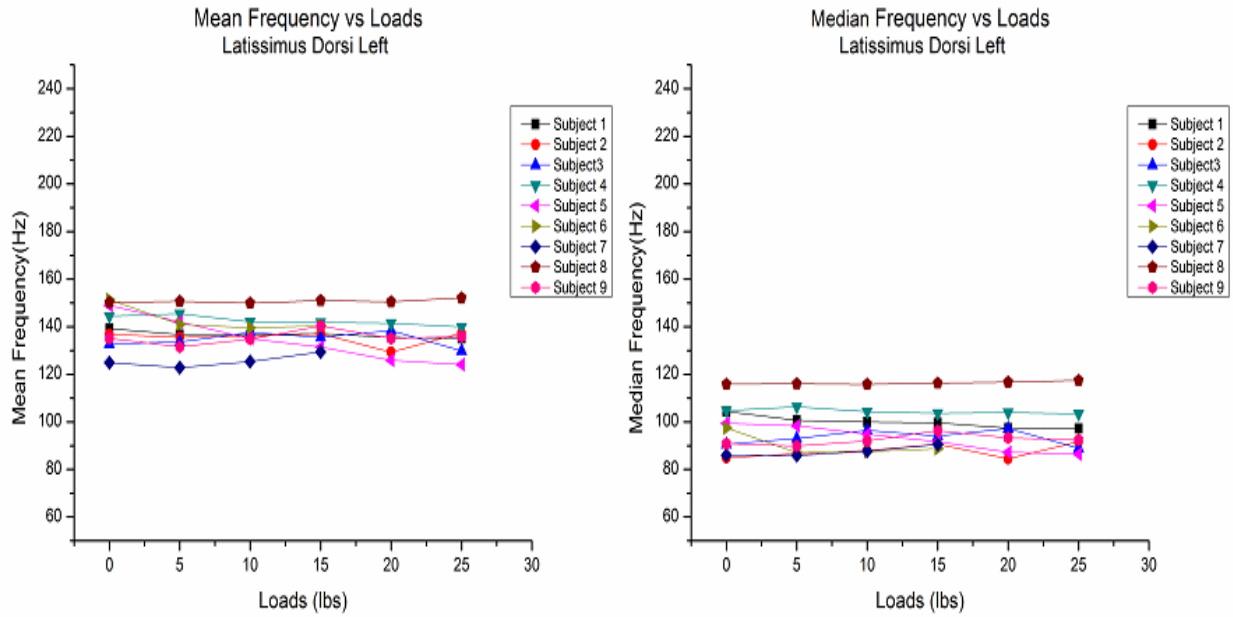


Figure 42: LD Left - Mean Frequencies and Median Frequencies during walking with varying loads

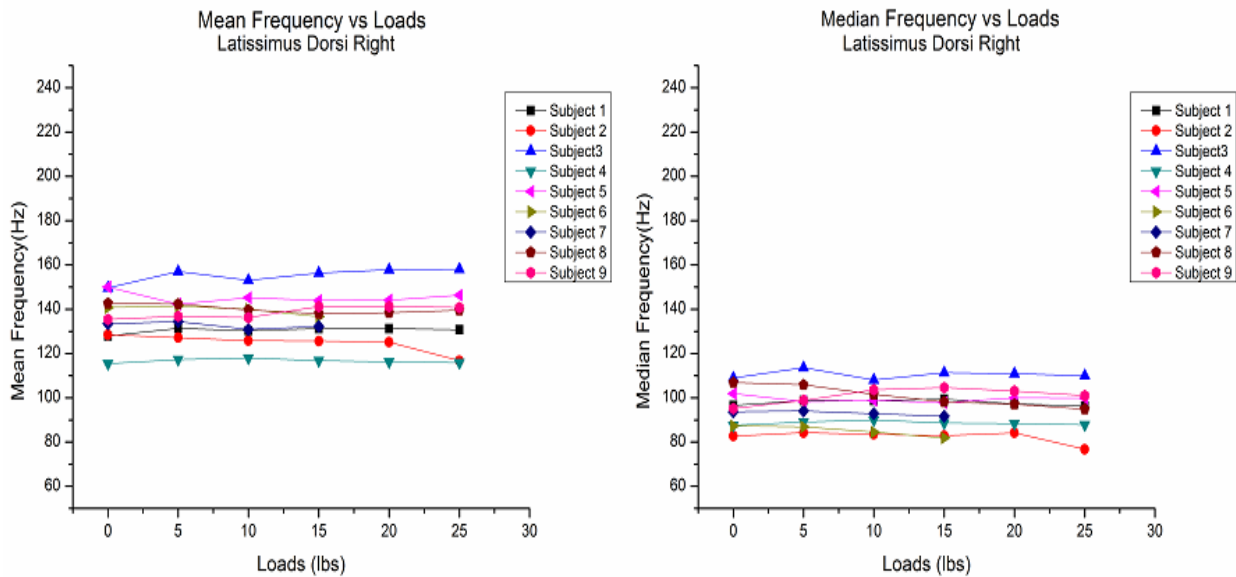


Figure 43: LD Right - Mean Frequencies and Median Frequencies during walking with varying loads

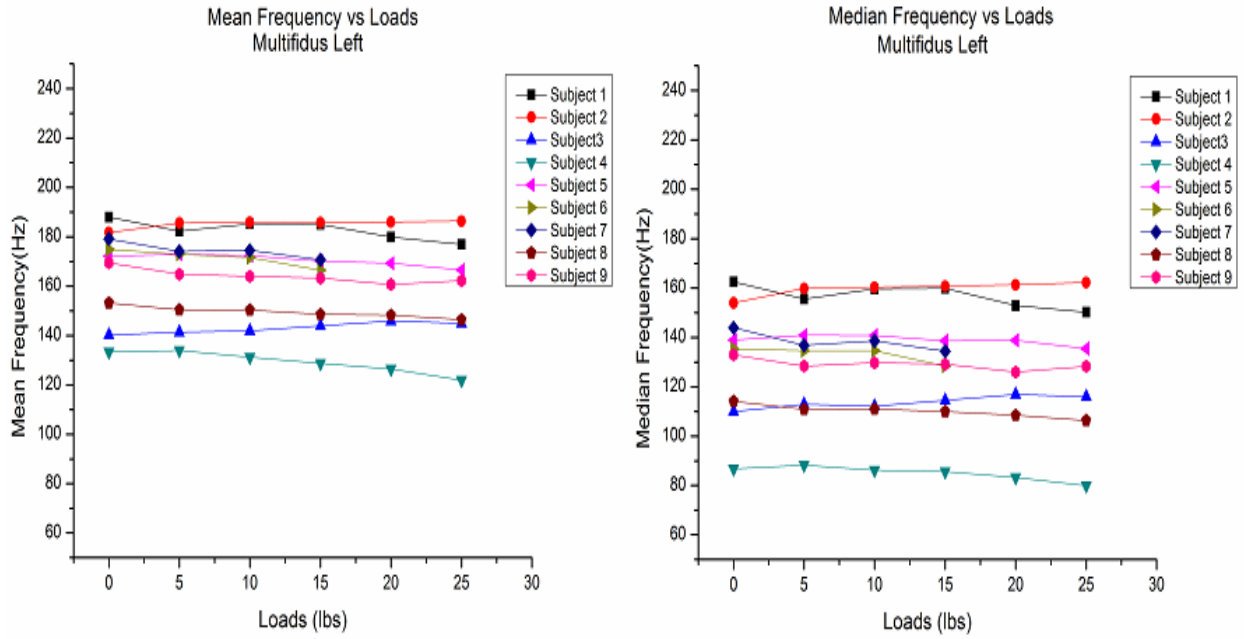


Figure 44: MF Left - Mean Frequencies and Median Frequencies during walking with varying loads

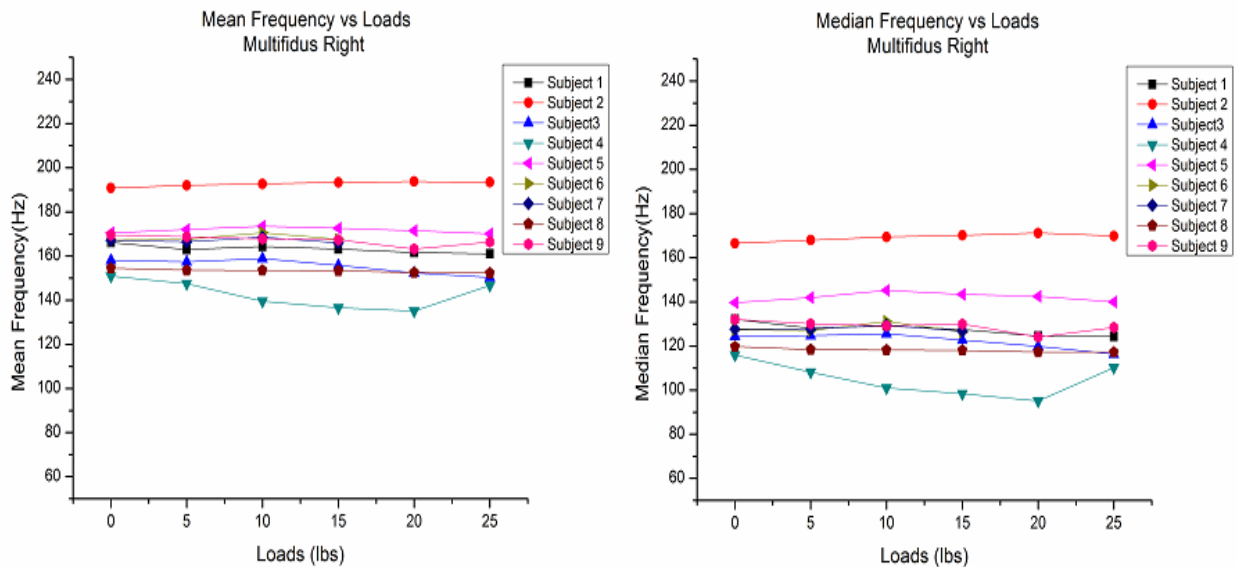


Figure 45: MF Right - Mean Frequencies and Median Frequencies during walking with varying loads

Table 7: Mean (SD) values of Mean Frequencies during walking with increasing loads.

Muscle	Mean (SD) value of Mean Frequencies in Hz					
	0 lb	5 lb	10 lb	15 lb	20 lb	25 lb
ES Left	158.56 (9.8)	155.1 (12.1)	156.1 (15.8)	156 (15.7)	155.1 (17.5)	152.5 (15.6)
ES Right	154.7 (11.1)	154.3 (11.4)	153.8 (11.6)	155.9 (14.3)	151.4 (14.8)	152.7 (16.1)
RA Left	165.4 (30.9)	164.9 (31.7)	163.2 (31.8)	159.4 (30.7)	157.8 (33)	156.1 (30.9)
RA Right	161.3 (33.9)	163.4 (36.2)	163.6 (36.4)	162.8 (36.8)	156.7 (40.4)	156 (39.8)
EO Left	153.5 (14.8)	149.8 (16.5)	146.2 (16.5)	143.3(16.9)	140.4 (17.2)	138.6 (18.5)
EO Right	162.8 (9.7)	166.9 (10.6)	167.9 (10.4)	166.5 (10.5)	169.1 (11.1)	167.7 (11.5)
IO Left	164.2 (20.5)	162.7 (20.9)	158.6 (19.1)	156.7 (19.5)	154.4 (18.7)	152.3 (18.1)
IO Right	149.8 (17.4)	148.4 (19.9)	146.3 (21.9)	147.3 (19.6)	141.6 (23.3)	143.4 (18.5)
LD Left	140.4 (8.9)	137.7 (8.2)	137.4 (6.5)	138.2 (6.3)	136.6 (8.1)	136.3 (8.7)
LD Right	135.9 (11.2)	136.7	135.4 (10.5)	135.8 (11.3)	136.3 (13.6)	135.4 (15.4)
MF Left	165.8 (19.1)	164.2 (18.2)	164.1 (19.1)	162.5 (18.9)	159.5 (20.9)	157.9 (21.8)
MF Right	166.1 (11.6)	165.3 (12.7)	165.5 (14.6)	163.9 (15.4)	161.4 (18.3)	162.8 (15.9)

Above table (7) shows mean and standard deviation values of mean frequencies during walking with increasing loads from 0 lb to 25 lb from all participants. From Above Table, for ES Left, ES Right, RA Left, EO Left, IO Left, IO Right, LD Left, MF left, and MF Right, mean frequency is decreasing with increasing loads from 0 lb to 25 lb.

Table 8 p-values for mean frequency

Mean Frequency	
Muscles	p-value
ES Left	0.980
ES Right	0.989
RA Left	0.987
RA Right	0.997
EO Left	0.464
EO Right	0.877
IO Left	0.804

IO Right	0.968
LD Left	0.917
LD Right	1.000
MF Left	0.966
MF Right	0.989

The results of the one-way ANOVA test (Table 8) revealed no significant difference ($p>0.05$) in the mean frequency values for all muscles during walking as the load increased from 0 lb to 25 lb.

Table 9: Mean (SD) values of Median Frequencies during walking with increasing loads.

Muscle	Mean (SD) value of Median Frequencies in Hz (S.D.)					
	0 lb	5 lb	10 lb	15 lb	20 lb	25 lb
ES Left	119.2 (17.5)	116.7 (19.5)	119.1 (23.3)	119.3 (22.7)	119.6 (23.7)	116.9 (20.6)
ES Right	114.9 (15.9)	114.1 (14.9)	112.6 (15)	114.2 (17.5)	109.2 (17.9)	112.3 (20.5)
RA Left	122.5 (40.2)	122.5 (39.2)	121.3 (38.6)	116.1 (35.8)	115.3 (37.4)	112.9 (34.4)
RA Right	117.1 (36.5)	120.7 (40.3)	121.5 (40.4)	121.2 (39.9)	114.7 (43.7)	113.9 (42.5)
EO Left	104.4 (13.9)	101.9 (13.2)	99.7 (12.4)	99.1 (12.4)	97.2 (12.5)	96.5 (12.6)
EO Right	116.5 (16.1)	121.7 (16.1)	123.4 (15.7)	121.8 (15.3)	125.2 (16.3)	123.8 (17.1)
IO Left	124.5 (19.9)	123.0 (19.6)	117.5 (17.8)	115.4 (17.2)	112.5 (15.9)	110.5 (14.5)
IO Right	101.3 (23.9)	99.8 (26.5)	98.6 (28.1)	99.2 (26.5)	95.9 (27.9)	96.5 (24.7)
LD Left	97.1 (10.1)	95.9 (10.3)	96.3 (9.3)	96.8 (8.7)	97.2 (10.8)	96.8 (10.7)
LD Right	95.6 (8.9)	96.6 (9.4)	95.7 (8.6)	95.1 (9.8)	97.2 (8.9)	95.2 (10.6)
MF Left	130.9 (23.6)	129.8 (22.7)	130.3 (24)	129.0 (23.8)	126.8 (26.9)	125.5 (27.7)
MF Right	131.7 (14.8)	130.5 (16.7)	130.9 (18.6)	129.3 (19.4)	127.8 (23.7)	129.5 (20.3)

Table 9 shows the mean and standard deviation values of the median frequencies during walking with increasing loads from 0 lb to 25 lb for all the participants. As the data in the table shows, median frequency decreased with increasing load from 0 lb to 25 lb for RA Left, EO Left, IO Left, IO Right, LD Right and MF left, but the remaining muscles showed no definitive pattern.

Table 10: p-values for median Frequency

Median Frequency	
Muscles	p-value
ES Left	1.000
ES Right	0.988
RA Left	0.992
RA Right	0.998
EO Left	0.826
EO Right	0.909
IO Left	0.551
IO Right	0.999
LD Left	1.000
LD Right	0.997
MF Left	0.998
MF Right	0.999

The one-way ANOVA test (Table 10) revealed no significant differences ($p > 0.05$) for median frequency values for any of the muscles during walking as the load increased from 0 lb to 25 lb.

4.3. Approximate Entropy (ApEn)

ApEn provides a direct measurement of feedback and connection, and a low ApEn value often indicates predictability and high regularity of time series data, whereas a high ApEn value indicates unpredictability and random variation. ApEn values typically range between 0 and 2, with values closer to 2 indicating greater complexity and those closer to 0 indicating more

predictability [22, 82]. The results for ApEn of Lumbar Flexion/Extension(FE), Lateral bending(LB) and Rotation (ROT) and Thoracic Flexion/Extension, Lateral bending and Rotation data recorded during walking carrying increased loads from 0 lb to 25 lb are given in turn below.

Lumbar segment:

Table 11 shows the results for the ApEn values for lumbar FE, LB and ROT recorded during walking with increased loads. All the ApEn values recorded were in the range between 0 and 2, as expected based on the literature review.

Table 11: ApEn values for Lumbar FE, LB, and ROT

	0 lb	5 lb	10 lb	15 lb	20 lb	25 lb
FE	0.27 (0.12)	0.28 (0.13)	0.28 (0.12)	0.28 (0.13)	0.26 (0.19)	0.25 (0.19)
LB	0.22 (0.07)	0.23 (0.07)	0.23 (0.07)	0.24 (0.08)	0.22 (0.08)	0.22 (0.09)
ROT	0.37 (0.09)	0.39 (0.09)	0.38 (0.08)	0.37 (0.08)	0.38 (0.09)	0.37 (0.09)

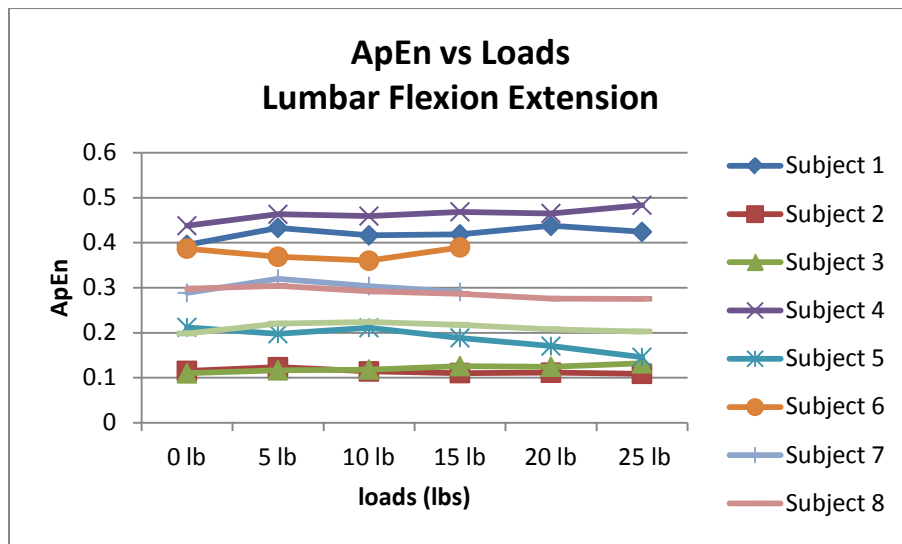


Figure 46: ApEn results for Lumbar Flexion Extension during increasing loads

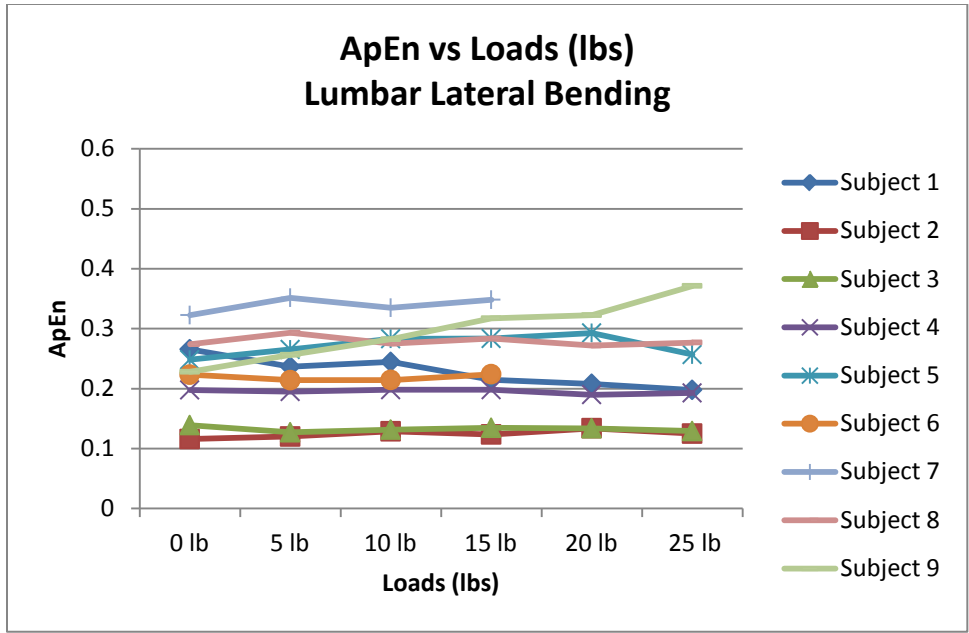


Figure 47: ApEn results for Lumbar Lateral Bending during increasing loads

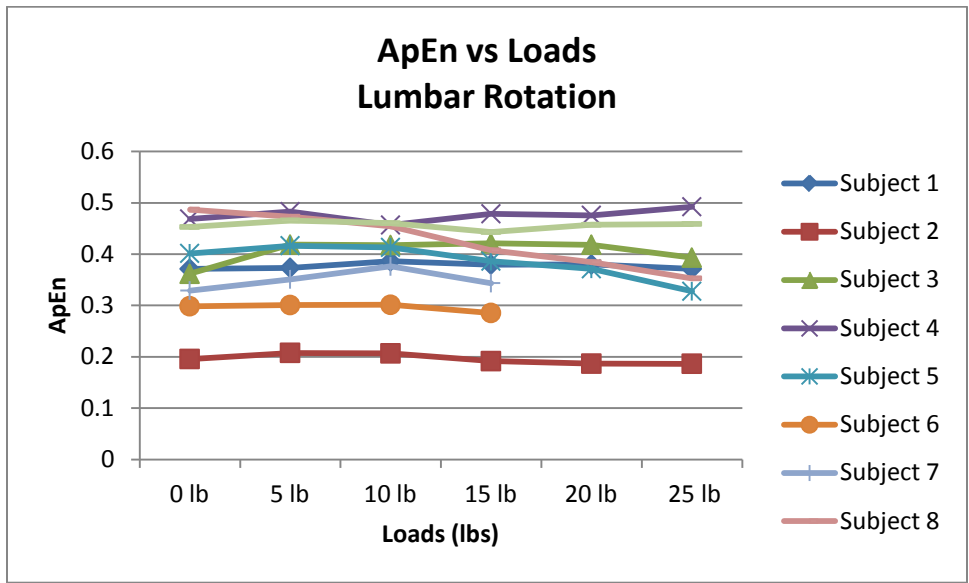


Figure 48: ApEn results for Lumbar Rotation during increasing loads

Table 12: one-way ANOVA test for ApEn values for Lumbar FE, LB & ROT vs loads

One-way ANOVA: Lumbar FE versus Loads (lb)					
<i>Source</i>	<i>DF</i>	<i>SS</i>	<i>MS</i>	<i>F</i>	<i>P-value</i>
Loads	5	0.0059	0.0012	0.07	0.997
Error	44	0.7548	0.0172		
Total	49	0.7606			
One-way ANOVA: Lumbar LB versus Loads (lb)					
<i>Source</i>	<i>DF</i>	<i>SS</i>	<i>MS</i>	<i>F</i>	<i>P-value</i>
Loads	5	0.00156	0.0031	0.06	0.998
Error	44	0.24820	0.00564		
Total	49	0.24977			
One-way ANOVA: Lumbar ROT versus Loads (lb)					
<i>Source</i>	<i>DF</i>	<i>SS</i>	<i>MS</i>	<i>F</i>	<i>P-value</i>
Loads	5	0.00269	0.0054	0.06	0.997
Error	44	0.36489	0.0829		
Total	49	0.36758			

The one-way ANOVA test (Table 12) revealed no significant differences ($p > 0.05$) in the ApEn values for lumbar FE, LB and ROT during walking as the load increased from 0 lb to 25 lb.

Thoracic segment:

Table 13 shows the results for the ApEn values for Thoracic FE, LB and ROT during walking with increased loads. Once again, all values were between 0 and 2.

Table 13: ApEn values for Thoracic FE, LB, and ROT

	0 lb	5 lb	10 lb	15 lb	20 lb	25 lb
FE	0.33 (0.08)	0.33 (0.09)	0.33 (0.09)	0.33 (0.1)	0.32 (0.1)	0.32 (0.11)
LB	0.43 (0.06)	0.42 (0.06)	0.42 (0.05)	0.42 (0.05)	0.41 (0.06)	0.41 (0.07)
ROT	0.39 (0.07)	0.39 (0.07)	0.38 (0.07)	0.38 (0.07)	0.39 (0.07)	0.38 (0.08)

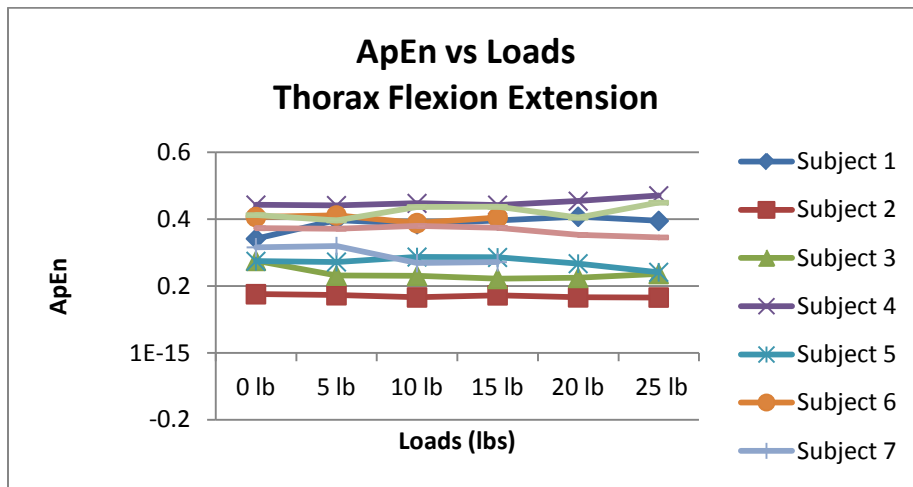


Figure 49: ApEn results for Thoracic FE

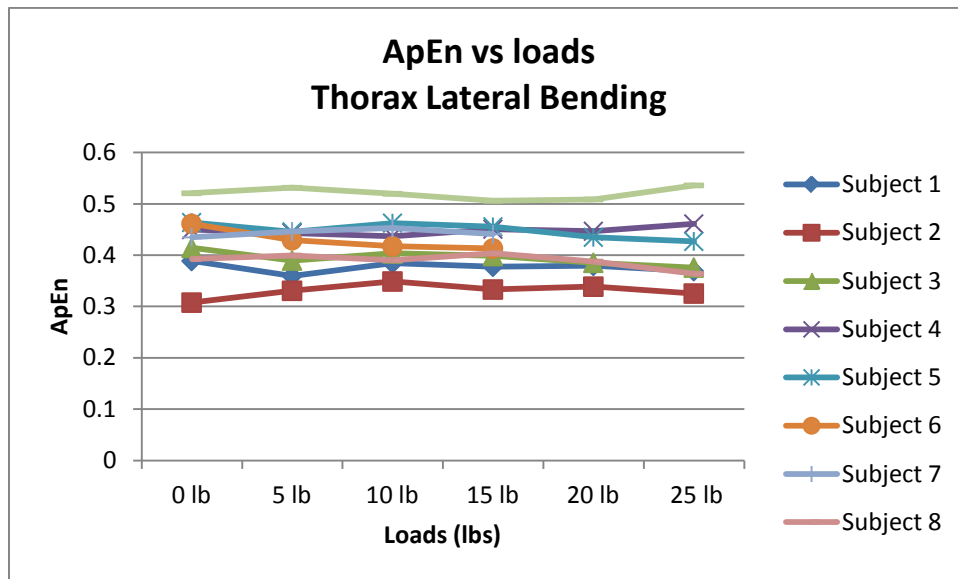


Figure 50: ApEn results for Thoracic LB

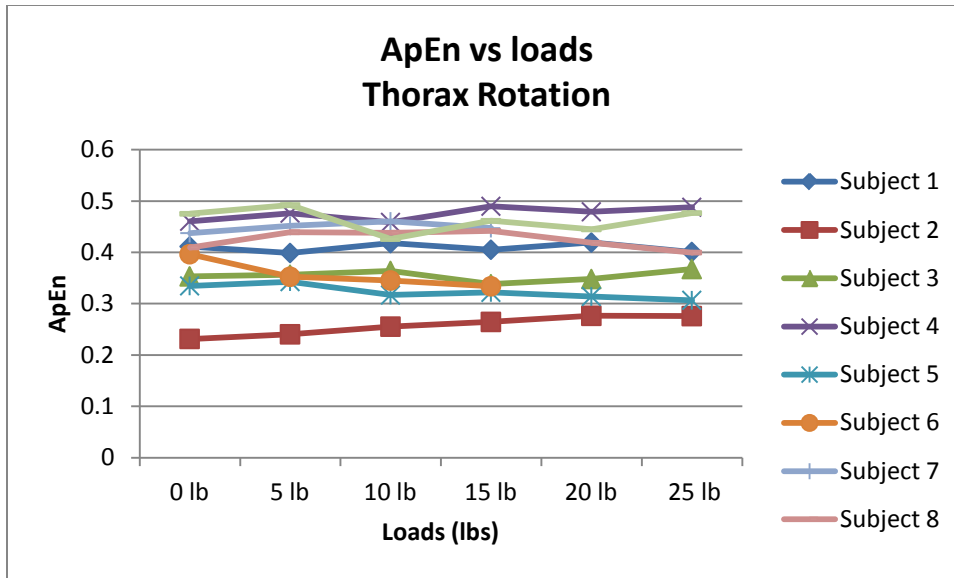


Figure 51: ApEn results for ROT

Table 14 one-way ANOVA test for ApEn values for Thoracic FE, LB & ROT vs loads

One-way ANOVA: Thoracic FE versus Loads (lb)					
<i>Source</i>	<i>DF</i>	<i>SS</i>	<i>MS</i>	<i>F</i>	<i>P-value</i>
Loads	5	0.0058	0.0012	0.01	1.000
Error	44	0.43007	0.0977		
Total	49	0.43065			
One-way ANOVA: Thoracic LB versus Loads (lb)					
<i>Source</i>	<i>DF</i>	<i>SS</i>	<i>MS</i>	<i>F</i>	<i>P-value</i>
Loads	5	0.00185	0.0037	0.11	0.989
Error	44	0.14676	0.00334		
Total	49	0.14861			
One-way ANOVA: Thoracic ROT versus Loads (lb)					
<i>Source</i>	<i>DF</i>	<i>SS</i>	<i>MS</i>	<i>F</i>	<i>P-value</i>
Loads	5	0.00040	0.00008	0.01	1.000
Error	44	0.25448	0.00578		
Total	49	0.25488			

The one-way ANOVA test (Table 14) revealed no significant difference ($p > 0.05$) in the ApEn values for Thoracic FE, LB and ROT during walking as the load increased from 0 lb to 25 lb.

4.4. Correlation Dimension

The correlation dimension is a measure of the dimensionality of the space occupied by a set of random points. Correlation Dimension (CoD) for the motion data during walking with increasing loads was calculated using an algorithm developed by Grassberger and Procaccia [17]). The CoD for Lumbar LB and Thoracic LB were calculated for participants walking with different loads. Below are the results for the CoD of experimental data recorded during walking against 0 lb, 5 lb, 10 lb, 15 lb, 20 lb and 25 lb resistance.

Table 15: mean (SD) of CoD for lumbar LB and Thoracic LB during walking with increased loads from all subjects

	0 lb	5 lb	10 lb	15 lb	20 lb	25 lb
Lumbar LB	1.32 (0.04)	1.33 (0.03)	1.28 (0.05)	1.29 (0.04)	1.28 (0.03)	1.27 (0.04)
Thoracic LB	1.25 (0.03)	1.24 (0.04)	1.25 (0.02)	1.26 (0.02)	1.26 (0.03)	1.26 (0.03)

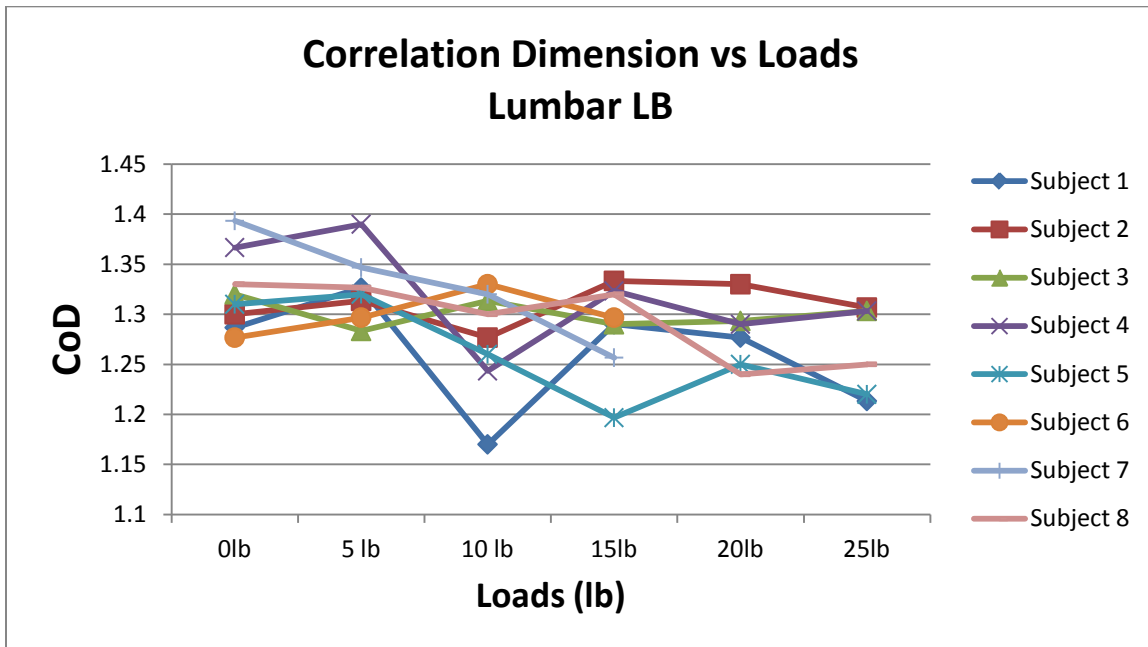


Figure 52: CoD results for Lumbar LB

Table 16: one-way ANOVA test for CoD values for Lumbar LB vs increasing loads

One-way ANOVA: lumbar LB versus Loads (lb)					
<i>Source</i>	<i>DF</i>	<i>SS</i>	<i>MS</i>	<i>F</i>	<i>P-value</i>
Loads	5	0.02304	0.00461	2.63	0.039
Error	38	0.06646	0.00175		
Total	43	0.08950			

The one-way ANOVA test (Table 16) revealed a significant difference ($p < 0.05$) for the CoD values for Lumbar Lateral Bending during walking as the load increased from 0 lb to 25 lb.

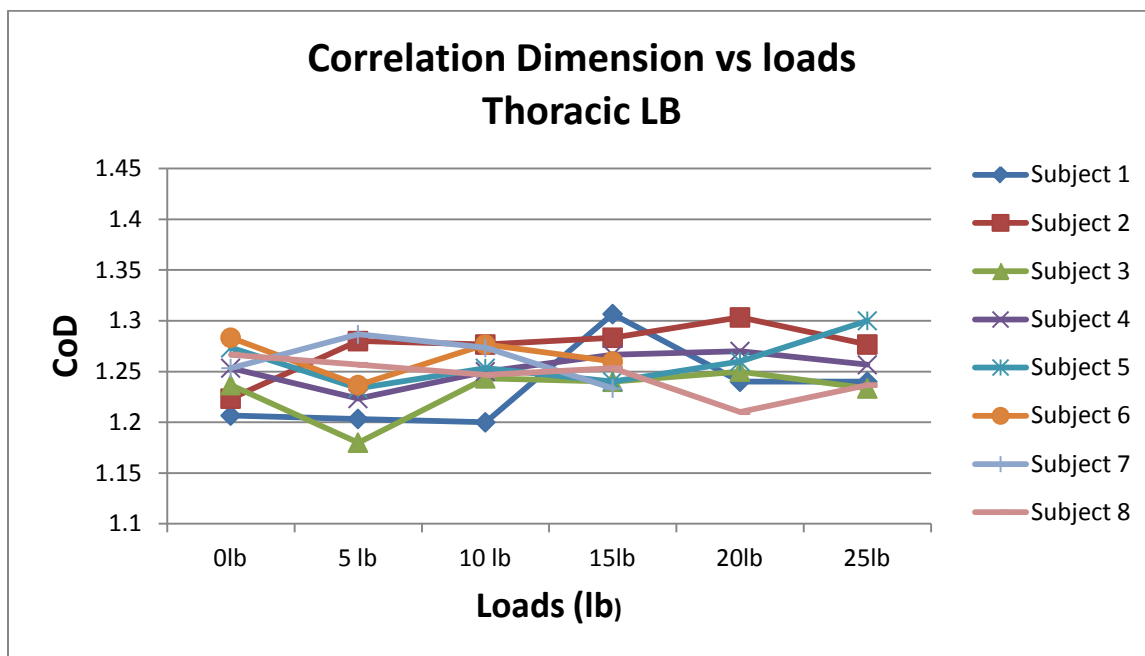


Figure 53: CoD results for Thoracic LB

Table 17: one-way ANOVA test for CoD values for Thoracic LB vs increasing loads

One-way ANOVA: Thoracic LB versus Loads (lb)					
<i>Source</i>	<i>DF</i>	<i>SS</i>	<i>MS</i>	<i>F</i>	<i>P-value</i>
Loads	5	0.002534	0.000507	0.62	0.687
Error	38	0.031166	0.000820		
Total	43	0.033700			

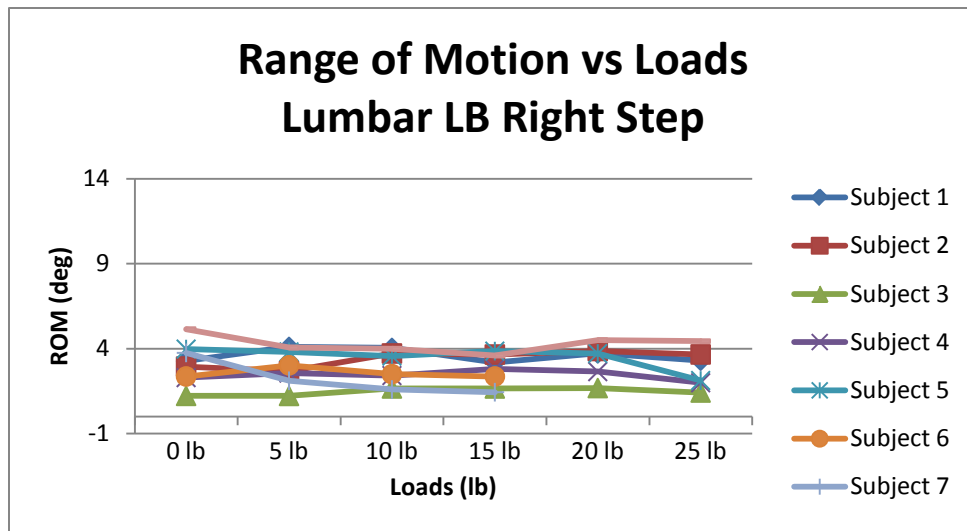
The one-way ANOVA test (Table 17) revealed no significant difference ($p>0.05$) for CoD values for Thoracic Lateral Bending during walking as the load increased from 0 lb to 25 lb.

4.5. ROM Results

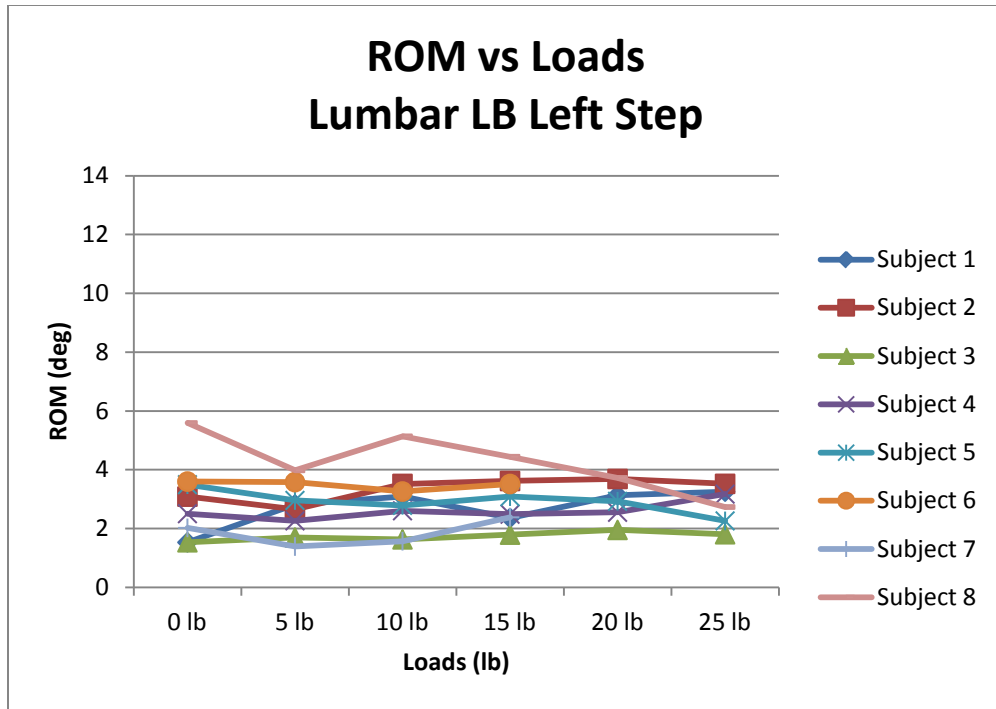
Table 18 shows the results for range of motion (ROM) for Lumbar Lateral Bending and Thoracic Lateral bending during walking with increased load.

Table 18: mean (SD) values for ROM for Lumbar LB and Thoracic LB during walking with increased loads

	0 lb	5 lb	10 lb	15 lb	20 lb	25 lb
Lumbar LB Right Step	3.13 (1.20)	2.95(1.01)	2.94 (1.02)	2.82 (0.92)	3.36 (1.01)	2.82 (1.16)
Lumbar LB Left Step	2.92 (1.35)	2.67 (0.88)	2.95 (1.13)	2.96 (0.86)	2.99 (0.68)	2.79 (0.65)
Thoracic LB Right Step	6.70 (2.86)	7.84 (2.26)	7.69 (1.88)	7.27 (1.99)	7.08 (1.50)	6.74 (1.50)
Thoracic LB Left Step	7.65 (3.02)	8.15 (2.06)	8.01 (2.08)	7.60 (1.99)	8.63 (2.35)	8.01 (2.06)

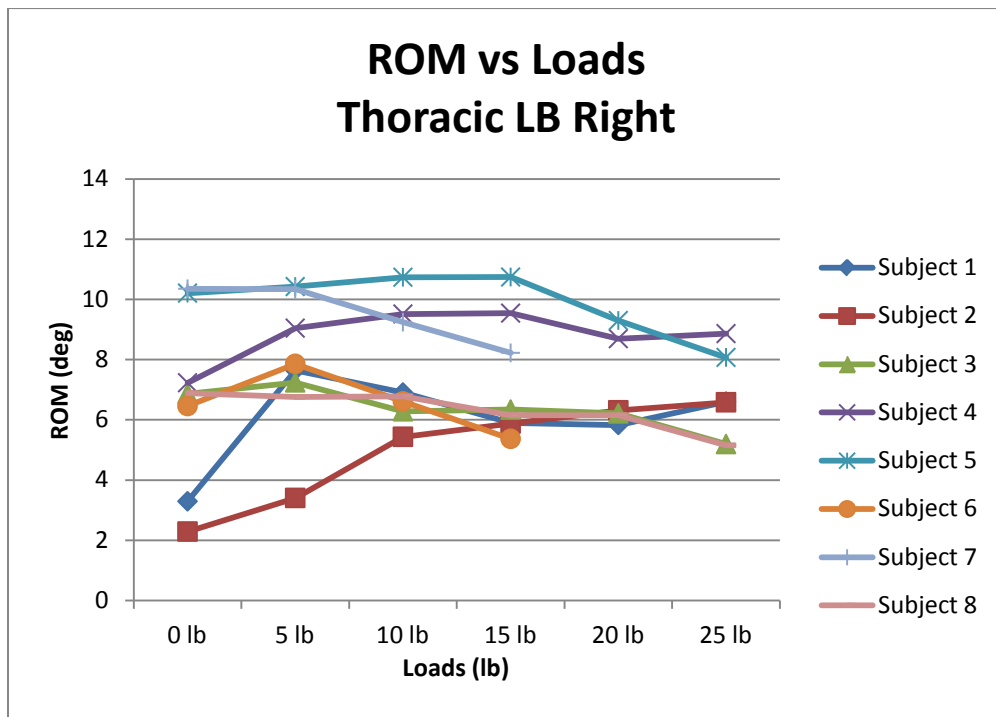


(a)

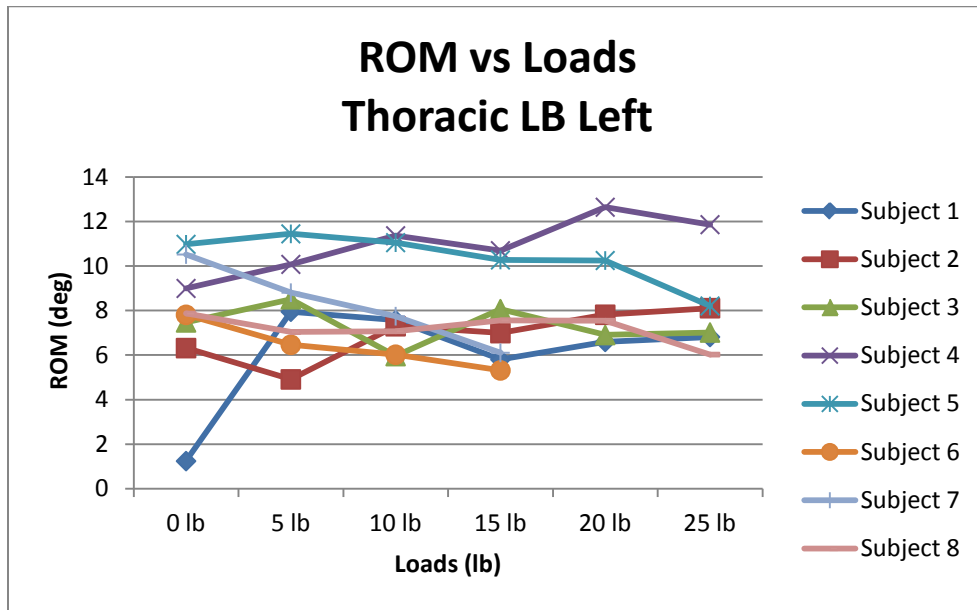


(b)

Figure 54: ROM vs. Loads a) Lumbar LB Right Step b) Lumbar LB Left Step



(a)



(b)

Figure 55: ROM vs. Loads a) Thoracic LB Right Step b) Thoracic LB Left Step

As Table 18 and Figures 54 and 55 shows, the ROM values for Lumbar LB are much smaller than the ROM values for Thoracic LB.

Table 19: p-values for ROM

ROM	
Motion	p-value
Lumbar LB Right Step	0.938
Lumbar LB Left Step	0.987
Thoracic LB Right Step	0.857
Thoracic LB Left Step	0.968

The one-way ANOVA test revealed that the ROM for Lumbar LB and Thoracic LB did not change significantly ($p > 0.05$) as the load increased from 0 lb to 25 lb during walking.

CHAPTER 5

DISCUSSION

The objective of this study was to develop a test procedure to study the effect of carrying a unilateral load or laptop bag or briefcase on posture and trunk biomechanics during walking (Gait) using Non-Linear methods. Kinematics, kinetic and EMG data were collected from 9 healthy participants. Linear (Mean, Standard Deviation & Range) methods and Non-Linear (ApEn and CoD) methods were used for kinematics (motion) data analysis, kinetic data (force plate data) analysis was performed using linear methods, and EMG data analysis was done using mean frequency and median frequency calculations.

Kinematics, kinetics and EMG data were recorded from study participants using the protocols approved by the Institutional Review Boards of Auburn University and Palmer College of Chiropractic, IA. Data from one of the subjects could not be used due to problems with the data acquisition. Following data collection, data were exported and reduced for further analysis. Motion data was analysed using ROM, ApEn and CoD calculations.

Range of motion (ROM) is the difference between the largest and smallest observations during motion. ROM for lumbar LB and thoracic LB were calculated during walking with increasing loads, with rotation about the y-axis described as lateral bending in for the purposes of this study. In the lumbar and thoracic regions, the displacement was towards the load bearing side. Lumbar LB and thoracic LB both demonstrated consistent pattern within steps and between participants. As the data presented in Table 18 demonstrate, ROM decreased as the

load increased from 0 lb (ROM=3.13 (1.20)) to 15 lb (ROM=2.82 (0.92)), increased from 15 lb to 20 lb (ROM=3.36 (1.01)), and then finally decreased for lumbar LB during a right step on the force plate. This pattern was not repeated in lumbar LB for a left step on the force plate, where instead ROM increased as the load increased from 0 lb (ROM=6.70 (2.86)) to 5 lb (ROM=7.84 (2.26)), decreased from 5 lb to 25 lb (ROM=6.74 (1.50)), and then decreased again for Thoracic LB.

The data in Table 18 and the accompanying graphs (Figures 54 and 55) indicating that the ROM for lateral bending in the lumbar region exhibited less displacement than ROM for thoracic LB is consistent with the findings of previous research. The values for ROM for Lumbar LB obtained in the present study are smaller than those in earlier reports but similar to those observed for thoracic LB. For example, Crosbie et al. 1997 reported ROM values of 9.0 (3.0) for lumbar LB during walking and 7.0(3.5) for thoracic LB and Dalichau et al. 1998 reported a ROM value of 6.5 for lumbar LB during gait, which is also higher than that found in the present investigation. The findings of other studies have been closer to the results reported here: Rowe and White [72] reported ROM of 4.0 for lumbar LB during gait, and Callaghan [45] investigation of three dimensional low back loads, spinal motions and trunk muscular activity found that ROM for lumbar LB varied from 1.12° to 7.13°. The current study found similar patterns in the lumbar LB and thoracic LB profiles during walking, and increasing load did not appear to affect the lateral bending during walking significantly.

A one-way ANOVA test revealed that the ROM for lumbar LB and thoracic LB did not change significantly ($p > 0.05$) as the load increased from 0lb to 25 lb during walking. No significant change in the variability was observed.

The ROM does not explain the effect of increasing load on either lumbar LB or thoracic LB during walking, so nonlinear methods were applied to the data to better understand the dynamics of low back motion. Traditional linear tools can mask the true structure of variability in the gait pattern, since a few strides are averaged to generate a “mean” picture of the subject’s gait, but in the course of this averaging procedure, any temporal variations of the gait pattern are lost. Instead, nonlinear techniques focus on understanding how gait pattern changes over time. From a statistical point of view, the use of traditional linear tools to study variability assumes that variations between strides during gait are random and independent, but recent studies have shown that such variations may actually be deterministic in origin [34, 80]. Traditional linear tools also give different answers to nonlinear tools regarding stability and complexity [34 77, 82] as traditional linear tools does not describe the effect of increasing resistance on motion. Nonlinear tools readily describe deterministic dynamics and hence are better suited to helping us understand the dynamics of gait [77]

Entropy is a widely accepted measure of uncertainty or variability; Approximate Entropy (ApEn) is often used to quantify the amount of regularity and the unpredictability of fluctuations over time-series data, especially to quantify the regularity or predictability of a time series [68, 69]. If a time series is composed of repetitive patterns of fluctuation, it renders that time series more predictable than a time series in which such patterns are absent. ApEn thus provides a direct measurement of feedback and connection; a low ApEn value often indicates predictability and high regularity of time series data, whereas a high ApEn value indicates unpredictability and random variation. ApEn values typically range between 0 and 2, with values closer to 2 indicating greater complexity and those closer to 0 indicating more predictability [22, 23, 51, 68, 69, and 82]

As the data presented in Table 13 show, the ApEn values for both lumbar motion (FE, LB and ROT) and thoracic motion (FE, LB and ROT) did not vary significantly. There was no consistent pattern for either lumbar motion (FE, LB and ROT) or thoracic motion (FE, LB and ROT) observed during walking with increased loads.

For lumbar FE, and LB, ApEn values increased for loads of 0 lb to 5 lb, remained constant from 5 lb to 15 lb, then decreased for 20 lb to 25 lb. There was no similar pattern for lumbar ROT. The results of a one-way ANOVA test revealed no significant difference ($p>0.05$) for ApEn values for lumbar FE, LB and ROT during walking as the load increased from 0 lb to 25 lb. ApEn values for lumbar FE, LB and ROT reported by previous researchers ranged between 0.20 and 0.40 [22, 82]

For thoracic FE, ApEn values were constant for 0 lb to 15 lb, and then decreased for 20 lb to 25 lb. For LB, ApEn values decreased over the whole range from 0 lb to 25 lb. There was no similar pattern for ROT. A one-way ANOVA test revealed no significant difference ($p>0.05$) for ApEn values for thoracic FE, LB and ROT during walking as the load increased from 0 lb to 25 lb. The thoracic FE, LB and ROT ApEn values all lay between 0.30 and 0.50, with little change in variability in the walking pattern with increasing load.

The literature review does not support the above finding. Many studies have been done on the effect of increased speed or other factors during human gait using nonlinear methods, but little research has focused on human gait with different forms of loads using nonlinear tools. Kavanagh and Anastasios [23, 51] found that ApEn values increased with increasing speed, with values ranging from 0.1 to 0.95. Buzzi & Ulrich [81] studied the dynamic stability of gait cycles in children with and without Downs Syndrome and found ApEn values differed significantly ($p<0.05$), with children with Downs Syndrome exhibiting increasing ApEn value during walking

in all segments, signifying a reduction in mean dynamic stability. Arif et al. 2004 found variability in walking pattern also increased with age, again revealing a reduction in stability.

The findings of the current study did not reveal a consistent change in walking pattern with increased load in healthy young participants, although the range of ApEn values obtained were similar to the results reported in other studies conducted on healthy participants to study variability [22, 23, 68, 69, 82]. Here, the ApEn values for lumbar motion and thoracic motion were close to zero, which indicates predictability and high regularity of time series data so the data is more predictable and not random. ApEn values for lumbar motion (0.20 to 0.40) and thoracic motion (0.30 to 0.50) all lay between 0 to 2, as expected, but were noticeably smaller for lumbar motion as compared to thoracic motion. This indicates that lumbar motion is more predictable and regular than thoracic motion. The analysis revealed little change in variability in walking pattern with increasing load in healthy young participants.

Correlation dimension approximates the fractal dimension of the region in state space occupied by a dynamic system (Grassberger and Procaccia, 1983b; Theiler, 1986). . In chaos theory, the correlation dimension is a measure of the dimensionality of the space occupied by a set of random points. The Correlation Dimension (CoD) for the motion data obtained during walking with increasing loads was calculated using an algorithm developed by Grassberger and Procaccia [17].

As the data in Table 15 and Figures 52 and 53 reveal, there was no consistent pattern in CoD values for either lumbar LB or thoracic LB during walking with increasing loads for healthy participants. This finding for lumbar LB supports previous findings, but this is not the case for the thoracic LB. For lumbar LB, a one-way ANOVA test revealed a significant difference ($p < 0.05$) for CoD values during walking as the load increased from 0 lb (1.32) to 25 lb

(1.27). Buzzi and Stergiou [77, 80] studied the effect of aging on variability during gait using nonlinear methods and found that CoD values for variation in knee angle for young people were 2.3° compared to 2.7° for old people. In particular, they found significantly increased dimensionality in the elderly (CoD values above 3) when compared to young adults (CoD values below 2) during treadmill walking. Dingwell and Cusumano [34] also found differences between controls and patients with peripheral neuropathy during over ground walking. However, no such consistent pattern during walking was observed in the current study.

A one-way ANOVA test revealed no significant difference ($p > 0.05$) in CoD values for Thoracic Lateral Bending during walking as the load increased from 0 lb (1.25) to 25 lb (1.26).

The values of the CoD results reported here were similar to results obtained in several other studies conducted on healthy participants to study variability. The CoD values for lumbar LB and thoracic LB fell between 1.2 and 1.4 during walking as loads increased in a healthy population. The correlation dimension was found to be larger for lumbar LB than for thoracic LB. Buzzi [80] reported CoD values for a periodic time series of 1.167, for a chaotic time series of 1.941, and for a random time series of 4.723. Our results suggest that lumbar LB and thoracic LB time series data are not random; the data in Table 15 and Figures 52 and 53 reveal little change in variability during walking as the loads increased.

Overall, the results for both ApEn and CoD indicate little change in variability as the loads increased during walking.

It must be noted that the aim of this exercise was to develop a test procedure to study the effect of carrying a unilateral load such as a laptop bag or briefcase on an individual's posture and trunk biomechanics during walking (Gait) using Non-Linear methods. The sample size used

for this initial study was relatively small and the results of the statistical analysis may not be sufficiently rigorous to generalize the results over the entire healthy population. This procedure needs to be fine tuned in future before a larger pilot study is conducted. Statistical analysis of a much larger population will give a better estimate of variability during walking with increasing loads.

Electromyography is widely used in gait analysis to describe the muscular activity in the body's lower extremities. However, few researchers have focused specifically on the lower back muscles and abdomen muscles during gait. In the current study EMG data were recorded from 9 healthy participants from 12 muscles (Erector Spinae Left and Right, Multifidus Left and Right, Latissimus Dorsi Left and Right, Internal Obliques Left and Right, External Obliques Left and Right, and Rectus Abdominis Left and Right) at 1200 Hz. Data were exported and reduced for further analysis. Mean and median frequencies were extracted from a power spectral density estimation of EMG data and PSD estimation was done via Fast Fourier Transformation. Mean frequency and median frequency from recorded EMG signals were calculated to examine how increasing loads affect different muscles during walking. The literature review revealed evidence to suggest that muscle fatigue typically decreases both the mean and median frequencies and increases the RMS amplitude values. Several factors may result in this decreased EMG mean and median frequency, such as decreased motor unit firing rate, decreased number of active motor units, age, loads, and increase in movement velocity [50, 56, 58, 63, 66, and 74]. Joseph [49] found that the increase in amplitude observed during a fatiguing task may be attributed to the recruitment of additional motor units and an increased firing frequency of motor units in order to maintain force output. He stated that the change in EMG amplitude is especially

pronounced near the mechanical failure point, whereas the MF decrease is more evident at the beginning of a sustained contraction.

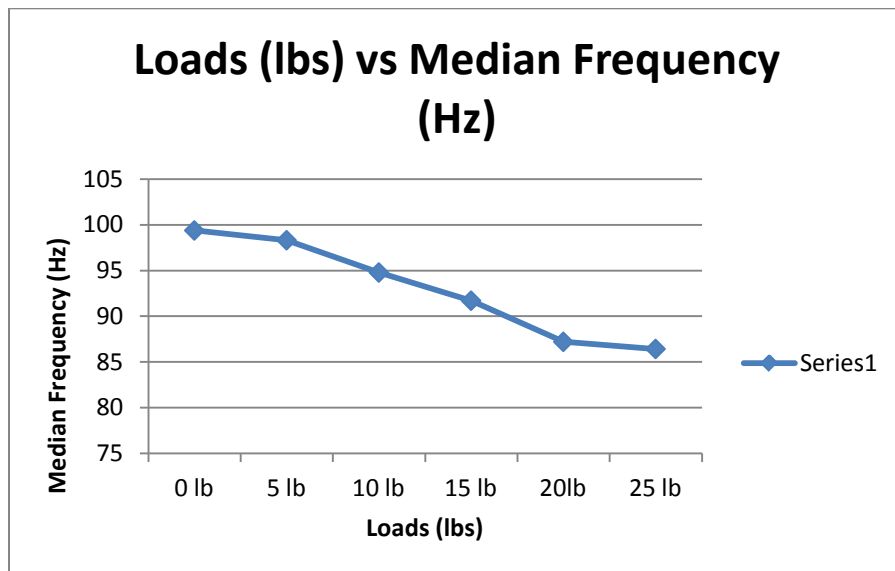
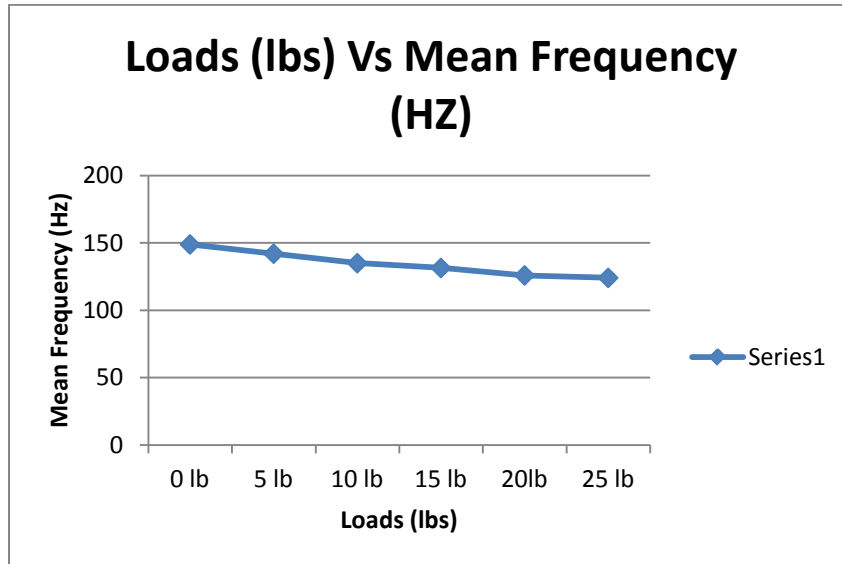


Figure 56: Mean and Median Frequency results for LD Left muscle for participant 5 during walking with increasing load

Figure 56 shows how both the mean and median frequencies for participant 5's Latissimus Dorsi Left decrease as the load during walking increases. This indicates that fatigue is being induced in these muscles as the load increases. This is not consistent for all muscles.

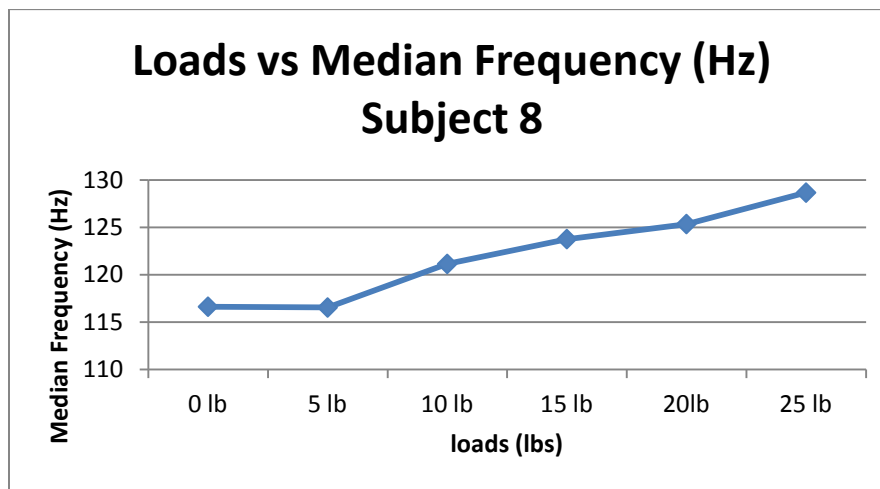
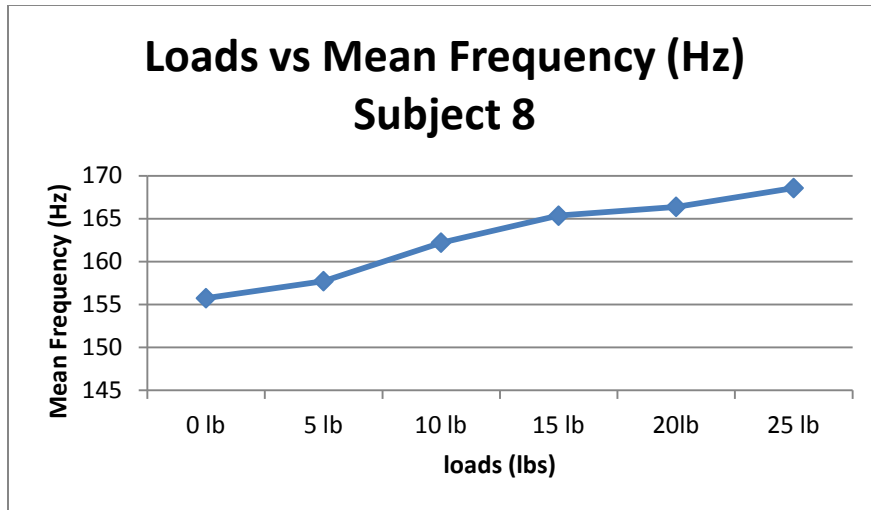


Figure 57: Mean and Median Frequency results for ES Right muscle for participant 8 during walking with increasing load

Figure 57 shows the mean and median frequency results for the ES Right muscle of participant 8 during walking with increasing loads. Here, the mean and median frequencies increased as the load increased during walking. There are several reasons this may happen, including an increased motor unit firing rate, younger age, and/or an increased number of active motor units. [58]

In previous research, Hong [87] reported median frequency decreased with increases in walk speed. Olson [64] reported median frequencies of the power density spectrum of the EMG

signal from individuals were compressed during fatigue conditions, indicating neuromuscular signs of fatigue. They reported that the frequency content of the Lumbar Paraspinal (LP) muscle group decreased significantly over time from 80 ± 15 to 61.9 ± 15 Hz in the 50% condition. Both the LP (73 ± 15 to 61.9 ± 30.7 Hz) and Biceps Femoris (BF) (88 ± 12 to 74.4 ± 11.4 Hz) muscles showed signs of neuromuscular fatigue in the 70% condition. However, their study excluded data for the RA and EO muscles since there was no significant change in the median frequency of the power density spectrum for these muscle groups.

We examined muscle activation in human subjects during walking with increasing loads. The overall effects of increasing loads during walking were consistent with those reported by previous researchers [50, 56, 58, 63, 66, and 74]. From Table 7, for ES Left, ES Right, RA Left, EO Left, IO Left, IO Right, LD Left, MF left, and MF Right, the mean frequency decreased with increasing load from 0 lb to 25 lb, but this is not consistent for the other muscles. Similarly, the data in Table 9 reveal that for RA Left, EO Left, IO Left, IO Right, LD Right and MF left, the median frequency decreased with increasing load from 0 lb to 25 lb, while once again the pattern in the remaining muscles is not consistent. This confirms that as expected, muscle fatigue was induced in the participants during walking due to increasing loads.

Tables 8 and 10 reveal that overall there was no significance change ($p > 0.05$) in mean and median frequencies during walking with increase in loads and no muscle fatigue was induced in the participants during walking due to the increasing loads. The overall results (Tables 7-10) show that mean and median frequencies either remained constant or decreased slightly as the loads carried when walking increased.

Reports in the literature suggest that the range for mean and median frequency generally falls between 60-140 Hz for different functional activities [50, 56, 58, 63, 66, and 74]. Our results were broadly in agreement, with a range of mean frequency and median frequency during walking with varying loads of between 55-210 Hz.

One of the main objectives of this study was to assess the effects of increased load on vertical ground reaction forces during walking. Ground reaction force has three force components (Fx, Fy, and Fz), but here only the vertical ground reaction force (vGRF; Fz) was used. To quantify the vGRF pattern, the magnitude and time of occurrence of the vGRF was extracted from the force plate data (Tables 3, 4 and 5). Vertical ground reaction force consists of three components: Fz1, Fz2 and Fz3. Fz1 is the first peak on the vGRF profile which is also known as the loading force, Fz3 is the peak force on the vGRF profile known as the unloading or propulsive force, and Fz2 is the minimum force between the first peak force and the third peak force. Mean and standard deviation were calculated for vGRF and the magnitude of vGRF was also normalized to individual participants' body weights.

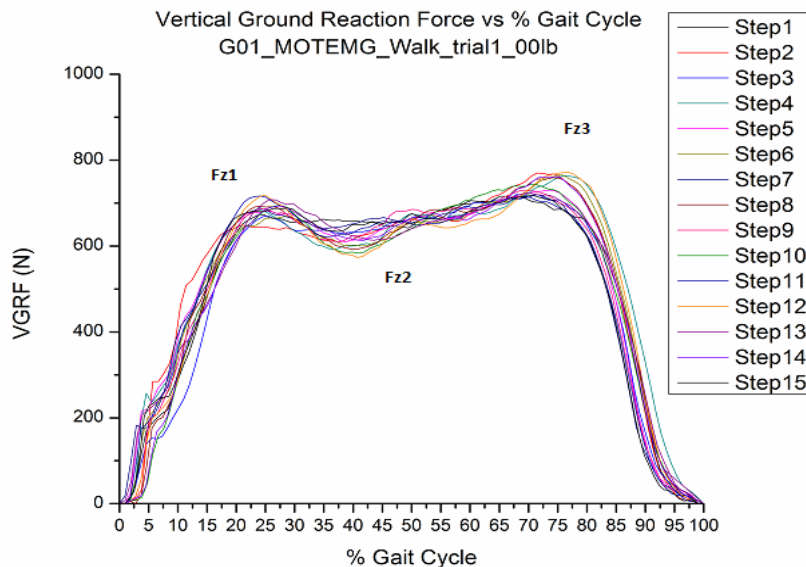


Figure 58: Typical vGRF profile

The vGRF patterns were similar to those identified in the literature review, as shown in Figure 58. The data in Tables 3 and 4 show that both vGRF (N) and Normalized vGRF (BW) increase as the load increases from 0 lb to 25 lbs during walking. Fz1, Fz2 and Fz3 all increased as the load increased from 0 lb to 25 lb. This is also consistent with the results for the Normalized vGRF, which increased from 1.02 at 0 lb to 1.16 at 25 lb for Fz1. The same pattern was observed for Fz2 and Fz3, with normalized Fz2 increasing from 0.97 at 0 lb to 1.12 at 25 lb and normalized Fz3 increasing from 1.04 at 0 lb to 1.19 at 25 lb. Figures 32-34 reveal that as load increases, both vGRF (N) and normalized vGRF for each individual also increase.

This finding supports those of previous studies [43, 44, 48, 54, 65, 76, 78, 84] which found that vGRF (N) and normalized vGRF (BW) (Fz1, Fz2, and Fz3) during gait increased with increasing loads. Birrell [78] found that both vertical and anterior-posterior ground reaction forces (GRF) produced during gait increased when a load was applied to a body. They found that the maximum propulsive force (BW) increased from 0.222 to 0.321 during different loads conditions. Our finding also supported by Wang [43], who reported that under different loading conditions, normalized vertical ground reaction force increased from 1.27 to 1.99. They also found that walking in a fatigued state was accompanied by increased vertical ground reaction force. Zhang [84] found that vGRF (body weight) increased from 1.6 at 0% BW to 2.5 at 20% BW. McCrory [48] reported that both the first and second vertical force peaks were lower on the affected leg of arthroplasty subjects than in either their unaffected leg or the control group, noting that the 1st peak force (BW) in the control was 1.05, an affected limb 1.02, and an unaffected limb 1.06. The 2nd peak force (BW) in the control was 1.02, an affected limb 1.0 and an unaffected limb 1.02. However, there was little difference in the time profile of different events in these subjects. Damavandi and Hsiang [65, 76] both reported that adding weight to the

body increase the overall vertical ground reaction forces (GRFs) the body is subjected to. It is also likely that an increase in walking speed will cause an increase in GRFs as the overall momentum of the body increases. The results for vertical ground reaction forces reported here are therefore in agreement with previous reports in the literature. Another interesting finding of the current study is that the magnitude of the Propulsive Force or Unloading Force ($Fz3$) is always greater than that of the Loading Force ($Fz1$) during walking with increasing loads.

However, the main objective of this study was the development of a test protocol for the analysis of trunk biomechanics during gait. The test procedure developed here needs further fine tuning before it can be applied to a larger population. Future studies need to consider developing a set of recommendations for obtaining more meaningful data based on healthy subjects. In further analyses, the calculation of a Lyapunov Exponent could be usefully deployed to obtain more accurate results. Wireless EMG electrodes and motion sensor could also be used to avoid noise problems during the data capture phase caused by the wires swaying during walking. Also, once the protocol is perfected, further testing needs to be carried out on a larger sample size in order to generalize the results.

CHAPTER 6

CONCLUSIONS

The aim of the study was to develop a test procedure with which to study the effect of unilateral loads on the posture and trunk biomechanics of walkers using traditional and nonlinear methods. Spinal motions, Force Plate Data and muscle activity in the lower back and abdomen muscles were investigated during walking with increasing loads. The results of spinal motion (Lumbar LB and Thoracic LB) analysis during walking revealed that variability in the lumbar LB and thoracic LB does not change with increasing loads. Kinematics analysis was performed using both traditional methods (means and standard deviation values) and nonlinear methods (ApEn and CoD). The result of motion analysis using the traditional method was supported by the non-linear methods (ApEn and CoD) to study the effect of increased loads on spinal motions. Force plate data were analyzed using traditional methods (means and standard deviation). The findings revealed that there is a significance difference ($p < 0.05$) in vGRF (Fz1, Fz2, and Fz3) during walking with increasing loads, with vGRF increasing as the load increased. Mean and median frequencies were computed to analyze the muscle activity in the lower back and abdomen muscles. The range of the mean frequency during walking with varying loads fell between 80-210 Hz and the range of the median frequency during walking with varying loads was between 55-180 Hz. This study revealed no significant difference ($p > 0.05$) for mean frequency values and median frequency for any of the muscles during walking as the load increased from 0 lb to 25 lb. This indicates that the increased loads during walking did not

induce serious fatigue in the muscles of the study's participants, which may have helped the participants to provide the required neuromuscular response to increasing loads.

The population used in this study was small and the results of the statistical analysis were therefore not adequate to generalize the results over the entire healthy population. Statistical analyses for a much larger population is needed to provide a better estimate of the effect of increasing loads on variability during walking. In future, this study will form the basis for a more detailed and in-depth study to assess the trunk biomechanics during gait, but before this is possible more testing needs to be done to provide a solid database of the characteristic values for healthy subjects.

Both traditional and non-linear methods gave similar results, which confirm the findings of previous studies. Therefore, both methods are equally promising to serve as a useful way to assess variability during gait in future research in this area.

REFERENCES

1. Read more: [Back Problems Caused by Heavy Book Bags | eHow.com](http://www.ehow.com/about_5044276_back-caused-heavy-book-bags.html#ixzz1mwJUAOVA)
http://www.ehow.com/about_5044276_back-caused-heavy-book-bags.html#ixzz1mwJUAOVA
2. http://en.wikipedia.org/wiki/Low_back_pain
3. http://en.wikipedia.org/wiki/Vertebral_column
4. http://en.wikipedia.org/wiki/Human_vertebral_column
5. http://en.wikipedia.org/wiki/Thoracic_vertebrae
6. http://en.wikipedia.org/wiki/Lumbar_vertebrae
7. http://en.wikipedia.org/wiki/Sacral_vertebrae
8. http://en.wikipedia.org/wiki/Erector_spinae_muscles
9. <http://en.wikipedia.org/wiki/Electromyography>
10. <http://en.wikipedia.org/wiki/Electromyography#References>
11. http://en.wikipedia.org/wiki/Time_series
12. http://en.wikipedia.org/wiki/Fast_Fourier_Transform
13. http://en.wikipedia.org/wiki/Chaos_theory
14. http://en.wikipedia.org/wiki/Correlation_dimension
15. http://en.wikipedia.org/wiki/Approximate_entropy
16. <http://mathworld.wolfram.com/CorrelationDimension.html>
17. http://www.scholarpedia.org/article/Grassberger-Procaccia_algorithm

18. <http://www.codeforge.com/s/0/correlation-dimension-matlab-code>
19. https://en.wikipedia.org/wiki/Ground_reaction_force
20. http://en.wikipedia.org/wiki/Force_platform
21. Abarbanel, H.D.I., (1996). Analysis of Observed Chaotic Data. *Springer-Verlag, New York*.
22. Ahsan H Khandoker, Marimuthu Palaniswami and Rezaul K Begg (2008). A comparative study on approximate entropy measure and poincaré plot indexes of minimum foot clearance variability in the elderly during walking. *Journal of NeuroEngineering and Rehabilitation*, 5:4.
23. Anastasios D. Georgoulis, Constantina Moraiti, Nicholas stergiou. (2006). A novel approach to measure variability in the anterior cruciate ligament deficient knee during walking: the use of the Approximate Entropy in Orthopaedics. *Journal of ClinicalMonitoring and computing* 20:11-18.
24. Baker, G. L. and Gollub, J. B, (1996). Chaotic Dynamics: An Introduction, 2nd ed. Cambridge, England: Cambridge University Press.
25. Birrell S.A. (2008). The influence of rifle carriage on the kinetics of human gait. *Ergonomics* , 816-826.
26. Cara M. Wall- Scheffler (2010). EMG activity across gait and incline: The impact of muscular activity on human morphology. *Am J Phys Anthropol.* 2010 December; 143(4): 601–611.
27. Christoph Anders, HeikoWagner, ChristianPuta, RolandGrassme, Alexander Petrovitch, Hans-Christoph Scholle, (2007). Trunk muscle activation patterns during walking at different speeds. *Journal of Electromyography and Kinesiology* 17, 245–252.
28. Chuansi GAO (2008). Gait muscle activity during walking on an inclined icy surface. *Ind Health.*; 46(1):15-22.
29. Rubin DI, (2007). Epidemiology and risk factors for spine pain. *Neurol Clin.*; 25(2): 353-371.
30. CHRISTA DEVROEY, ILSE JONKERS, AN DE BECKER, GERLINDE LENAERTS and ARTHUR SPAEPEN, (2007). Evaluation of the effect of backpack load and position during standing and walking using biomechanical, physiological and subjective measures. *Ergonomics Vol. 50, No. 5, 728–742.*
31. Crosbie Jack, Vachalathiti Roongtiwa, Smith Richard, (1995). Age, gender and speed effects on spinal kinematics during walking. *Gait & Posture* 5 13–20.

32. Crosbie Jack, Vachalathiti Roongtiwa, Smith Richard, (1997). Patterns of spinal motion during walking. *Gait & Posture* 5, 6–12
33. Deepti Majumdar, Madhu Sudan Pal and Dhurjati Majumdar, (2010). Effects of military load carriage on kinematics of gait. *Ergonomics Vol. 53, No. 6, June 2010, 782–791.*
34. Dingwell, J.B., Cusumano, J.P., Cavanagh, P.R., & Sternad, D. (2001). “Local dynamic stability versus kinematic variability of continuous overground and treadmill walking.” *Journal of Biomechanical Engineering, 123:27-32.*
35. Donald A Neumann, Thomas M Cook, Rhonda L Sholty, Dennis C Sobush, (1992). An Electromyography Analysis of Hip Abductor Muscle Activity When Subjects Are Carrying Loads in One or Both Hands. *Phys Ther.; 72(3):207-17.*
36. Duk-Hyun An, (2010). Comparisons of the gait parameters of young Korean women carrying a single strap bag. *Nursing and Health Science 2010,12,87-93*
37. Edwin Y Hanada, (2011). A comparison of trunk muscle activation amplitudes during gait in older adults with and without chronic low back pain. *PM R.; 3(10):920-8.*
38. Fowler N. E., Rdacki A.L.F., (2006). Changes in stature and spine kinematics during a loaded walking task. *Gait & Posture* 23; 133–141.
39. Frigo C., Carabalona R., Dalla M., Negrini S., (2003). The upper body segmental movements during walking by young females. *Clinical Biomechanics* 18; 419–425.
40. Garnett P. Williams, (1997). Chaos Theory Tamed.
41. Gerdle B, Karisson S, (1994) The mean frequency of the EMG of the knee extensors is torque dependent both in the unfatigued and the fatigued states. *ClinPhysiol* 1994; 14: 419-432.
42. Giakas Giannis (1997). Time and frequency domain analysis of ground reaction forces during walking: an investigation of variability and symmetry. *Gait & Posture Vol. 5, Issue 3, 189-197.*
43. He Wang; Jeff Frame; Eiiicia Ozimek; Daniei Leib; Eric L Dugan, (2012).Influence of Fatigue and Load Carriage on Mechanical Loading During Walking. *Mil ed.;177(2):152-6.*
44. HIROShi KINOSHiTA, (1985). Effects of different loads and carrying systems on selected biomechanical parameters describing walking gait. *Ergonomics. ;28(9):1347-62.*
45. Jack P. Callaghan, Aftab E. Patla, Stuart M. McGill, (1999). Low back three-dimensional joint forces, kinematics, and kinetics during walking. *Clinical Biomechanics Volume 14, Issue 3, Pages 203–216.*

46. James T Cavanaugh, (2007). Approximate entropy detects the effect of a secondary cognitive task on postural control in healthy young adults: a methodological report. *Journal of NeuroEngineering and Rehabilitation* 2007.
47. Jason C. Gillette (2010). The effects of age and type of carrying task on lower extremity kinematics. *Ergonomics* 355-364.
48. Jean L. McCrory, (2001). Vertical Ground Reactions Forces: objectives measures of gait following hip arthroplasty. *Gait Posture.*; 14(2):104-9.
49. Joseph K-F Ng, Carolyn A Richardson, Jull A Gwendolen (1997). Electromyographic Amplitude and Frequency Changes in the Iliocostalis Lumborum and Multifidus Muscles during Trunk Holding Test. *Phys Ther.* ;77(9):954-61.
50. Joseph Mizrahi, Arkady Voloshin, Dalia Russek, Oleg Verbitsky and Eli Isakov ,(1997).The Influence of Fatigue on EMG and Impact Acceleration in Running.
51. Justin J Kavanagh. (2009). “Lower trunk motion and speed-dependence during walking.” *Journal of NeuroEngineering and Rehabilitation* 6: 9
52. Karmakar, C.K., Khandoker, A.H., Begg, R.K., Palaniswami, M., & Taylor, S, (2006). “Understanding ageing effects by approximate entropy analysis of gait variability.” *Conf Proc IEEE Eng Med Biol Soc. 2007:1965-1968.*
53. Katrina M. Simpson, (2012). Does load position affect gait and subjective responses of females during load carriage? *Applied Ergonomics* 43, 479-485.
54. KEI MASANI, Motoki Kouzaki and Tetsuo Fukunaga, (2002). Variability of ground reaction forces during treadmill walking. *J Appl Physiol* 92:1885-1890.
55. Kenji Masumoto, (2004). Electromyographic analysis of walking in water in healthy humans. *Journal of Physiological Anthropology and applied Human Science.*
56. Kunju Nissan, Kumar Neelesh, (2009). EMG signal Analysis for Identifying Walking patterns of Normal Healthy Individuals. *Indian Journal of Biomechanics: Special Issue.*
57. L. F. P. FRANCA (2001). Distinguishing Periodic and Chaotic Time Series Obtained from an Experimental Nonlinear Pendulum. *NonLinear Dynamics, Volume 26, Issue 3, pp 255-273.*
58. L. Van Gestel, H. Wambacq, E. Aertbelie'n , P. Meyns , H. Bruyninckx , L. Bar-On ,G. Molenaers, P. De Cock, K. Desloovere, (2011). To what extent is mean EMG frequency during gait a reflection of functional muscle strength in children with cerebral palsy? *Res Dev Disabil.*; 33(3):916-23.
59. Lenth, R.V. (2001). —Some practical guidelines for effective sample-size determination. *The American Statistician*, 55:187-193.

60. Luo, X., Pietrobon, R., Sun, S.X., Liu, G.G. & Hey, L. (2004). "Estimates and patterns of direct health care expenditures among individuals with back pain in the United States." *Spine*, 29 (1):79-86.
61. M.B.I. Raez, M.S. Hussain, F. Mohd-Yasin, (2006) 'Techniques of EMG signal analysis: detection, processing, classification and applications' *Biol Proced Online*. 8: 11–35
62. Malgorzata Syczewska, Tommy Oberg, Dan Karlsson, (1999). Segmental movements of the spine during treadmill walking with normal speed. *Clinical Biomechanics* 14, 384 – 388.
63. Mehrotra R, Sahay KB, (1994). A power spectral study of surface EMG of muscles subjected to non-repetitive task. *Electromyogr Clin Neurophysiol (EEN)* 34 (5): 265-274.
64. Michael W. Olson (2009). Trunk extensor fatigue influences trunk muscle activities during walking gait. *Electrophysiological Kinesiology (impact factor: 2)*. 05/2009; 20(1):17-24.
65. Mohsen Damavandi, Philippe C. Dixon, David J. Pearsall, (2012). Ground reaction force adaptations during cross-slope walking and running. *Hum Mov Sci.;31 (1):182-9* 21840076
66. Nagata S, Arsenault AB, Gagnon D, Smyth G, Mathieu P-A: EMG power spectrum as a measure of muscular fatigue at different levels of contraction (1990). *Med&BiolEng&Comput*, 28:374-378.
67. Papadakis, N.C., Christakis, D.G., Tzagarakis, G.N., Chlouverakis, G.I., Kampanis, N.A., Stergiopoulos, K.N., & Katonis, P.G. (2009). "Gait variability measurements in lumbar spinal stenosis patients: part A. Comparison with healthy subjects." *Physiological Measurement*, 30: 1171–1186.
68. Pincus SM. (1990). "Approximate entropy as a measure of system complexity." *Proc. Nati. Acad. Sci.* 88: 2297-2301
69. Pincus, S. & Golberger, A.L. (1994). "Physiological time-series analysis: What does regularity quantify?" *American Journal of Physiology*, 266(4):H1643-1656.
70. Prosser Laura A., Lee Samuel, VanSant Ann F., Lauer Richard T., (2010). Trunk and hip muscle activation patterns are different during Walking in Young Children with and without Cerebral Palsy. *Phys Ther.* 2010 July; 90(7): 986–997.
71. Rafael F Escamilla, Eric Babb, Ryan DeWitt, Patrick Jew, Peter Kelleher, Toni Burnham, Juliann Busch, Kristen D'Anna, Ryan Mowbray, Rodney T Imamura, (2006). 'Electromyographic Analysis of Traditional and Nontraditional Abdominal Exercises: Implications for Rehabilitation and Training' *Physical Therapy . Volume 86. Number 5*.

72. Rowe P.J., White M., (1996). Three dimensional spinal kinematics during gait, following mild musculoskeletal low back pain in nurses. *Gait & Posture* 4, 242–251.
73. Roy SH, De Luca CJ, Casavant DA, 1989. Lumbar muscle fatigue and chronic lower back pain. *Spine (Phila Pa 1976)*; 14(9):992-1001.
74. Sabut S.K., Kumar R., Lenka P.K., Mahadevappa M. (2010). Surface EMG Analysis of Tibialis Anterior Muscle in Walking with FES in Stroke Subjects. *Conf Proc IEEE Eng Med Biol Soc.*: 5839-42
75. Scott A. England, Kevin P. Granata (2007). The influence of gait speed on local dynamic stability of walking. *Gait & Posture* 25; 172–178.
76. Simon M Hsiang (2002). The effect of gait speed and load carrying on the reliability of ground reaction forces. *Safety Science, Volume 40* (7).
77. Stergiou, N. (2004). —Innovative Analysis of Human Movement. || Human Kinetics.
78. Stewart A. Birrell, (2007). The effect of military load carriage on ground reaction forces. *Gait & Posture* 26; 611–614.
79. Tomoyuki Matsuo, (2008). Asymmetric load carrying in young and elderly women: relationship with lower limb coordination. *Gait and posture* 28.
80. Ugo H. Buzzi, (2003). Nonlinear dynamics indicates aging affects variability during gait. *Clinical Biomechanics* 18. 435 - 443
81. Ugo H. Buzzi and Beverly D. Ulrich, (2004). Dynamic Stability of Gait Cycles as a Function of Speed and System Constraints. *Motor Control. July*; 8(3): 241–254.
82. Vaillancourt DE, Newell KM., (2000). The dynamics of resting postural tremor in Parkinson's disease. *Clinical Neurophysiology*; 111:2046–2056.
83. White, Steven, G.; Mcnair, Peter, J., (2002): Abdominal and erector spinae muscle activity during gait: The use of cluster analysis to identify patterns of activity. *Clinical Biomechanics* 17(3): 177-184
84. Xi A. Zhang, Ming Ye and Cheng T. Wang (2010). Effect of unilateral load carriage on postures and gait symmetry in ground reaction force during walking. *Computer Methods in Biomechanics and Biomedical Engineering Vol. 13, No. 3*, 339–344
85. Xingda Qu, (2011). Effects of load carriage and fatigue on gait characteristics. *Journal of Biomechanics* 44, 1259-1263.
86. Youlian Hong, Jing Xian Li, (2004). Influence of load and carrying methods on gait phase and ground reactions in children's stair walking. *Gait & Posture Volume 22, Issue 1*, pages 63-68.

87. Youlian Hong, Jing-Xian Li, Daniel Tik-Pui Fong (2007). Effect of prolonged walking with backpack loads on trunk muscle activity and fatigue in children. *Journal of Electromyography and Kinesiology (impact factor: 1.97); 18(6):990-6.*
88. Yu Okubo, Koji Kaneoka, Atsushi Imai, Itsuo Shiina, Masaki Tatsumura, Shigeki Izumi, Shumpei Miyakawa, (2010). 'Electromyographic Analysis of Transversus Abdominis and Lumbar Multifidus Using Wire Electrodes During Lumbar Stabilization Exercises' *journal of orthopaedic & sports physical therapy Volume 40, Number 11, 743-750.*

7. PROJECT ASSURANCES

PROJECT TITLE: Development of a test procedure to study the effect of carrying a unilateral load or laptop bag or briefcase on the posture and trunk biomechanics during walking (Gait) using Non-Linear methods.

A. PRINCIPAL INVESTIGATOR'S ASSURANCES

1. I certify that all information provided in this application is complete and correct.
2. I understand that, as Principal Investigator, I have ultimate responsibility for the conduct of this study, the ethical performance this project, the protection of the rights and welfare of human subjects, and strict adherence to any stipulations imposed by the Auburn University IRB.
3. I certify that all individuals involved with the conduct of this project are qualified to carry out their specified roles and responsibilities and are in compliance with Auburn University policies regarding the collection and analysis of the research data.
4. I agree to comply with all Auburn policies and procedures, as well as with all applicable federal, state, and local laws regarding the protection of human subjects, including, but not limited to the following:
 - a. Conducting the project by qualified personnel according to the approved protocol
 - b. Implementing no changes in the approved protocol or consent form without prior approval from the Office of Human Subjects Research
 - c. Obtaining the legally effective informed consent from each participant or their legally responsible representative prior to their participation in this project using only the currently approved, stamped consent form
 - d. Promptly reporting significant adverse events and/or effects to the Office of Human Subjects Research in writing within 5 working days of the occurrence.
5. If I will be unavailable to direct this research personally, I will arrange for a co-investigator to assume direct responsibility in my absence. This person has been named as co-investigator in this application, or I will advise OHSR, by letter, in advance of such arrangements.
6. I agree to conduct this study only during the period approved by the Auburn University IRB.
7. I will prepare and submit a renewal request and supply all supporting documents to the Office of Human Subjects Research before the approval period has expired if it is necessary to continue the research project beyond the time period approved by the Auburn University IRB.
8. I will prepare and submit a final report upon completion of this research project.

My signature indicates that I have read, understand and agree to conduct this research project in accordance with the assurances listed above.

P. K. Raju

Printed name of Principal Investigator

Principal Investigator's Signature
(SIGN IN BLUE INK ONLY)

July 24, 20
Date

B. FACULTY ADVISOR/SPONSOR'S ASSURANCES

1. By my signature as faculty advisor/sponsor on this research application, I certify that the student or guest investigator is knowledgeable about the regulations and policies governing research with human subjects and has sufficient training and experience to conduct this particular study in accord with the approved protocol.
2. I certify that the project will be performed by qualified personnel according to the approved protocol using conventional or experimental methodology.
3. I agree to meet with the investigator on a regular basis to monitor study progress.
4. Should problems arise during the course of the study, I agree to be available, personally, to supervise the investigator in solving them.
5. I assure that the investigator will promptly report significant adverse events and/or effects to the OHSR in writing within 5 working days of the occurrence.
6. If I will be unavailable, I will arrange for an alternate faculty sponsor to assume responsibility during my absence, and I will advise the OHSR by letter of such arrangements. If the investigator is unable to fulfill requirements for submission of renewals, modifications or the final report, I will assume that responsibility.
7. I have read the protocol submitted for this project for content, clarity, and methodology.

P.K. Raju

Printed name of Faculty Advisor / Sponsor

Signature (SIGN IN BLUE INK ONLY)

July 24, 20
Date

C. DEPARTMENT HEAD'S ASSURANCE

By my signature as department head, I certify that I will cooperate with the administration in the application and enforcement of all Auburn University policies and procedures, as well as all applicable federal, state, and local laws regarding the protection and ethical treatment of human participants by researchers in my department.

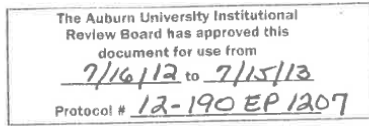
Jeffrey Suhling

Printed name of Department Head

Signature (SIGN IN BLUE INK ONLY)

7-24-12
Date

Participants Informed Consent Form:



PCC Study Number: 2012G144
Original Approval: 06-21-2012
Expiry Date: 06-21-2013

**Palmer Center for Chiropractic Research
741 Brady St
Davenport IA 52803**

Development of a test procedure to study the effect of carrying a unilateral load, laptop bag or briefcase on the posture and trunk biomechanics during walking (Gait) using Non-Linear methods

Informed Consent for Participants

You are invited to take part in a research project that will develop and refine methods that measure how the human body responds to this test procedure. The principal investigators for this study are Dr M.R. Gudavalli, Ph.D. and Dr. P. K. Raju, Ph.D. (Auburn University). This study is also part of a Master's student thesis at Auburn University.

PURPOSE OF THE RESEARCH PROJECT: The purpose of the proposed investigation is to develop a test procedure to study the effect of carrying a one-sided load, laptop bag or briefcase on the posture and body biomechanics during walking (Gait). Information obtained as a result of developing and testing these biomechanical procedures will help develop tests for future studies.

PROCEDURE:

Prior to enrolling as a participant, a licensed doctor of chiropractic will perform an examination to evaluate the safety of the testing procedures. The examination may last up to one hour. If determined eligible, study personnel will schedule a time to conduct this test.

What is experimental about this study?

The experimental part of this study involves measuring the posture of the spine and activity of your lower back muscles during walking while carrying loads on one side.

Who is eligible to take part in this study?

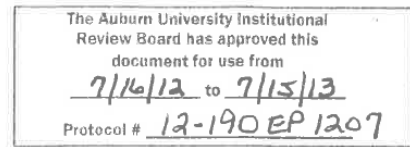
Participants between the ages of 18 and 65 will be eligible for this study. You will receive an examination by a licensed doctor of chiropractic for the purpose of evaluating your safety and to determine whether you are eligible for this study.

How many people will take part in the study?

We expect to enroll 10 people in this study.

How long will I be in this study?

You will be expected to participate in one baseline visit and one test visit. The estimated time for the baseline visit is approximately two hours, and the testing visit will be approximately 1 hour.



What will happen during this study?

During the study you will be asked to complete the following activities:

- 1 baseline visit, which includes an examination by a doctor of chiropractic.
- 1 test visit, in which biomechanical measurements will occur.

Baseline Visit

The baseline visit may last up to 2 hours. This will help the research team know if you are eligible for this study. The visit will include the following activities:

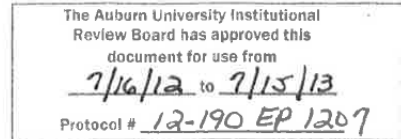
- Screening Questionnaires: you will be asked to answer questions about your past health, prior injuries, medications you take and other background information.
- Demographic data and vitals collection (i.e. height, weight, gender, and age)
- Exam: A doctor of chiropractic will complete a health history and conduct a physical examination to see if you are eligible for this study. We will collect health information about your neck, back, and other areas as well as your general health status.

Test Visit:

If you are eligible for this study, the following measurements will occur during your biomechanical testing. The test may be video recorded to allow investigators to collect information about the test procedure. You may choose not to have this session video recorded by marking the appropriate box on this Statement of Consent. This will not affect your eligibility for this study. Research personnel will be in the room to video record this session and to conduct this test.

Human Lumbar Spine Motion and muscle activation during walking carrying a one-sided load:

We will identify areas on your low back and spine for attaching surface electromyography (EMG) sensors and motion sensors. These sensors detect muscle activity and motion. Sensors will be placed on your low back, along your lower ribs on each side and on the abdomen. EMG electrode and motion sensor attachment sites will be prepared using an alcohol wipe and a mild abrasive pad to allow better contact with the skin. The areas where the electrodes are to be attached may be shaved using a disposable razors or sterilized electric razor if excessive hair is present, because hair may prevent quality recording of data. Shaving will be done entirely with your agreement and you may refuse this procedure. Surface EMG sensors and motion tracking sensors will be attached to muscles using double sided tape. You will wear a scrub top and short provided by the Palmer Research Clinic for the testing. Please wear comfortable pants or shorts, as well as socks. You will warm up by walking for 2-3 minutes in the biomechanics lab. You will be asked to walk back and forth on a wooden platform at a comfortable walking speed. This platform measures are 5' x 8'. You will be measured carrying varying loads (sand bags) of 0, 5, 10, 15, 20, and 25 pounds in one hand at intervals of 30 steps each. There will be several wires from the EMG sensors and motion tracking sensors. A member of research team will walk with you during these procedures to keep the wires out of your walking path. We will collect EMG data and motion data using a computer. You will be asked to walk 30 steps, three separate times, while carrying each load. Data will be collected each time you walk followed by a two minute break. The total estimated duration of this test is approximately 1hour. You will be tested only once for this study.



Information obtained as a result of the development and testing of these biomechanical procedures will help develop future studies, as well as provide information regarding efficient biomechanical testing procedures.

What are the risks of this study?

Rarely, participants develop a skin reaction to the double-sided tape, which appears as a rash or itching and is usually resolved within 48 hours. Some participants have sore muscles after the testing procedures. This soreness usually goes away within 48 hours. There is also a slight chance of participants experiencing a minor cut while shaving. If this occurs, electrode/sensors will not be attached to the affected site for the test. There is a possibility of participants falling due to imbalance while performing the task. However, it must be noted that these are the only known risks associated only with this biomechanical test. In this case, First Aid care is available from research clinicians who have First Aid and CPR certifications.

In the event that this research activity results in injury, First Aid treatment will be available from the Palmer Research Clinic. If additional care other than First Aid is necessary, Research Clinic staff will provide recommendations and assist, if possible, in finding appropriate care and treatment. It is important to note that Palmer cannot provide financial assistance or other coverage for any related costs for other treatment.

If you feel any discomfort or pain during any treatment or measurement procedure, tell us right away and we will modify or stop the procedure accordingly.

What protections are used to decrease my risk in this study?

We screen our participants carefully to make sure that only people who meet the study criteria are enrolled in this study. If our doctors determine that other tests are needed to diagnose a condition, to determine eligibility or render an opinion regarding your safety during testing, you will not be eligible for this study. In this case, we may refer you to another health care provider for evaluation.

What are the benefits of this study?

There may be no direct benefit to any individual from participating in this study. However, knowledge gained through these testing procedures will be useful for designing future studies.

Will it cost me anything to participate in this study?

During this study, there are no charges for the exam, or testing provided to you at the Palmer Research Clinic. You will spend time and effort to complete the study. You will also be responsible for the transportation to and from the Palmer Research Clinic.

Will I be paid for participating in this study?

No, you will not be paid for taking part in this study.

Is being in this study voluntary?

Yes, your participation in this study is entirely voluntary. You may refuse to take part in this study and you can quit at any time without penalty.

What are my alternatives to participating in this study?

There are no alternatives for this study, because we are developing a test procedure for future studies. Participation in this study is entirely voluntary.

What happens if I am injured during this study?

In the unlikely event that you are injured while in this study, we will provide first aid to you without cost. However, other treatment costs and/or financial compensation are not available from the Auburn University and Palmer College of Chiropractic. You and/or your insurance provider are responsible for any medical costs related to illness or injury.

It is important to tell us if you feel you have been injured as a result of taking part in this study. Let us know if you have any changes to your health that you think are related to this study. You may also contact the study's lead investigator (Dr. Ram Gudavalli) by telephone at 563-884-5260.

How is my personal information kept confidential?

The information that you share during this study is kept private. Only people performing this study may look at your health data.

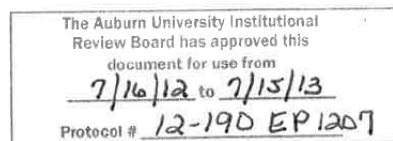
Your name will not be available to anyone other than those conducting this study. Your research records will be identified with an assigned number. If information is published or presented at scientific meetings, your name and personal information will not be used.

During the course of the study, all paper forms are stored in locked cabinets. Computer records can only be accessed by password and are stored on a network secured by Palmer College.

The Palmer Research Clinic keeps research records for seven years. Upon request, you may obtain reports summarizing your exam findings.

Who is funding this study?

This study is funded by Auburn University, Alabama & Palmer Center for Chiropractic Research, Davenport, Iowa.



Special Procedure Permissions

Voicemail Message Permission

We may call you to remind you of appointments or give you updates during this study. Sometimes, we may need to leave you a message on voicemail or answering machine. Please remember this when we ask for your best telephone contact number. We will leave a voicemail only if you give us permission. This decision will **not** affect your eligibility for this study.

- I give my permission for voicemail messages during this study.
- I do not give my permission for voicemail messages during this study.

Video and Audio Permission

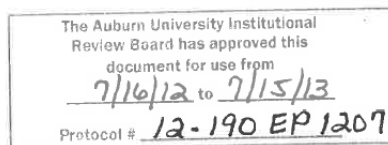
The biomechanical measurement visit will be video and audio recorded. If other parts of the study require recording, you will be notified. You may choose to not have your study visits video and audio recorded. This decision will not affect your eligibility for this study.

- I give my permission for video and/or audio recordings to be made during my participation in this study.
- I do not give my permission for video and/or audio recordings to be made during my participation in this study.

Release of Health Information Permission

Your health records and study data are kept private. However, we may identify health problems during this study that would require a referral to another healthcare provider. We will only send a referral letter containing protected health information with your permission. This decision will not affect your eligibility for this study.

- I give my permission to release a referral letter to my designated health care provider or other healthcare specialist.
- I do not give my permission to release information about my health to any other health care providers.



Statement of Consent

Participation in this study is entirely voluntary. I reserve the right to refuse to take part or withdraw at any time without the loss of benefits of any kind, or my education at Palmer, or jeopardizing any future request for services from the clinics of the Palmer College of Chiropractic.

I have reviewed the consent form and understand it. I understand all of the information provided and I agree to participate in the test procedures marked with an "x" in the Testing Procedures section of this Informed Consent Document. I have had a chance to read this Informed Consent Document and any questions have been answered to my satisfaction. I understand a copy of this signed document will be provided to me upon request.

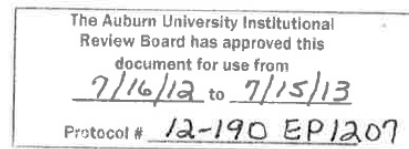
I also understand that I may contact Dr. Gudavalli, Principal Investigator, at (563) 884-5260, or Dr. Ronnie Firth, Chair of the Institutional Review Board at (563) 884-5843, and may also contact at office of Research Compliance, 115 Ramsay Hall, Auburn University, AL 36849, (334) 844-5966 if I have further questions.

Signature of participant Date

Name

Signature of Witness Date

Name



B. Palmer College Of Chiropractic IRB Approval Document:



June 21, 2012

M Ram Gudavalli, PhD
Palmer College of Chiropractic
Davenport Campus

Re: IRB Assurance # 2012G144

Dear Dr Gudavalli:

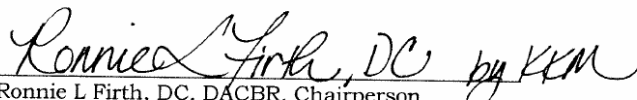
On June 21, 2012, the Institutional Review Board Chairperson reviewed the revisions to your Application for the study

**Development of a Test Procedure to Study the Effect of Carrying a
Unilateral Load or Laptop Bag or Briefcase on the Posture or
Trunk Biomechanics During Walking (Gait) Using Non-Linear Methods**

and approved it as a non-exempt study, based on the information contained in the revised IRB Application. This approval is valid for one year, after which time you are required to complete a Progress Report on an annual basis, or more often as necessary. The IRB will review these Progress Reports in order to authorize the continuation of your study.

The Board is fully aware of the regulations governing the Institutional Review Board (Title 45, Code of Federal Regulations, Part 46) and believes that its operations are in compliance with those regulations.

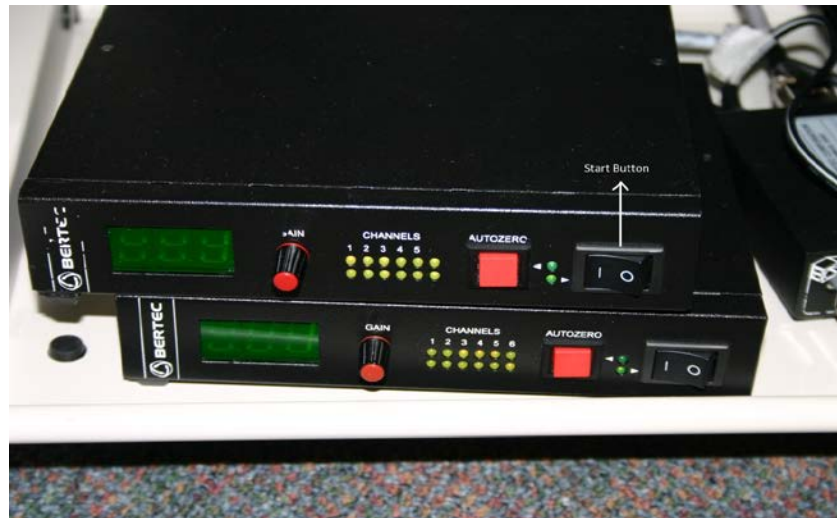
Sincerely,


Ronnie L Firth, DC, DACBR, Chairperson
Institutional Review Board
Palmer College of Chiropractic

C. Data Collection:

1. Switch on all the equipment:

- i. Turn on the computer, and A/D board.
- ii. Switch on Bertec Amplifier: Auto Zero by pressing Auto zero buttons and Gain should be 1 If it is not than set gain =1 by rotating Gain Switch.



- iii. Switch on EMG DELSYS system.



2. Log in Computer.
3. To Start The Motion Monitor Software:

i. Open Motion Monitor by click on Motion Monitor Icon on Desktop >>
Please select your ID: **TEST** >>ok.

ii. New window pop up >> Select data to collect:

1. Position/Orientation Sensor Data: Biomechanical Data

2. Data Acquisition board data:

a. Force Plate Data

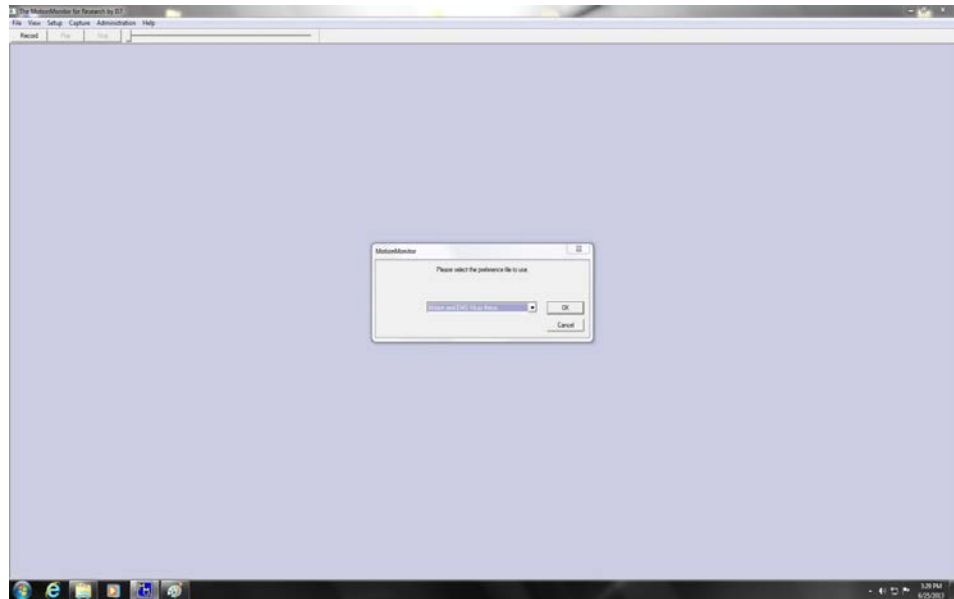
b. EMG Data

4. Load Preference File:

i. Go to File menu >> Load preference file >> Setup Analysis.

ii. New window will pop-up: **Preference File Option** >> Ok.

iii. Please Select the preference file: **Motion and EMG Vikas Thesis** >> Ok.



5. Activate Sensors:

i. Go to Setup>> Activate sensor>> Ok.

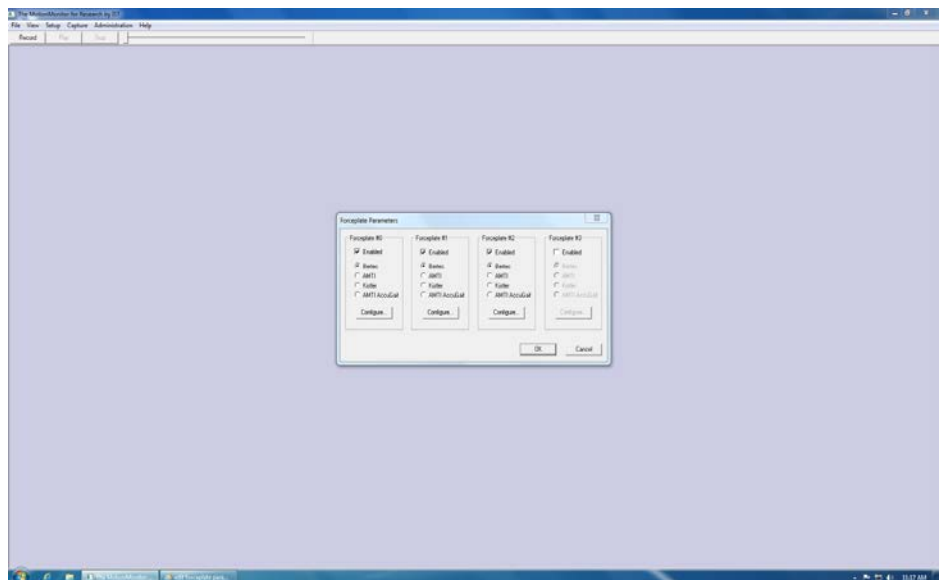
ii. Initializing Sensors >> wait for few seconds until initializing done.

6. **Sensor Attachment:** We cleaned the identified sensors site using alcohol pads. Then we attached the EMG sensors and Motion Sensors at identified sensor sites using double sided tape. We attached EMG Strober unit to participant pant or pocket.

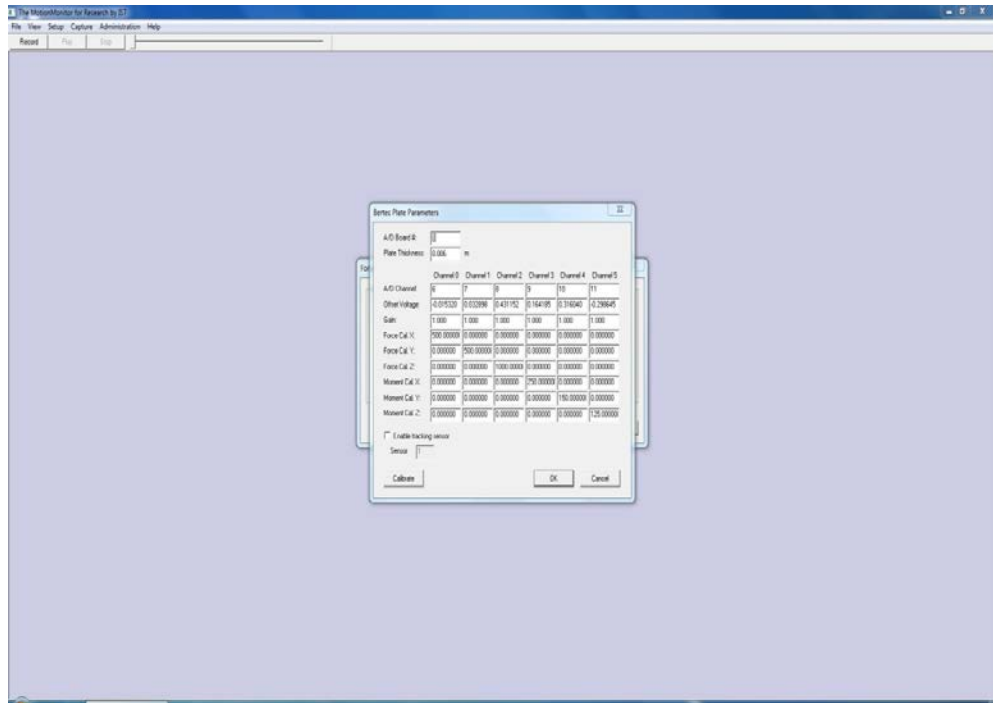


7. **Reconfigure the force plate:**

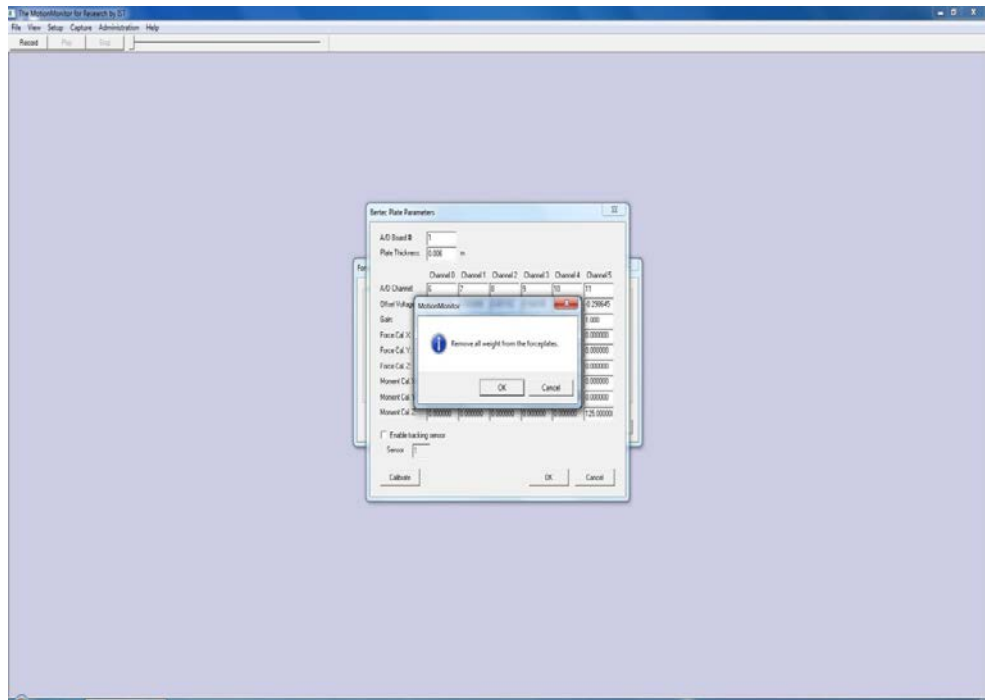
- i. Go to Administration >> Edit force plate parameter.
- ii. New window pop – up: Force plate parameters.



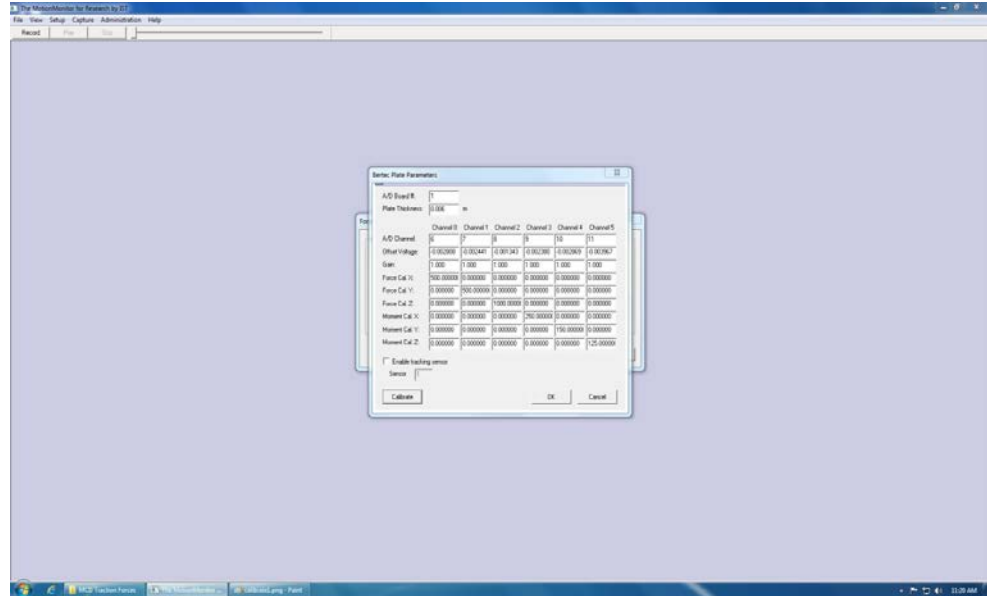
- iii. Force plate 0: click on Configure>> New window will pop-up: Bertec Plate Parameters >> click on calibrate.



- iv. new window will pop up: Remove all weight from force plate >> Ok

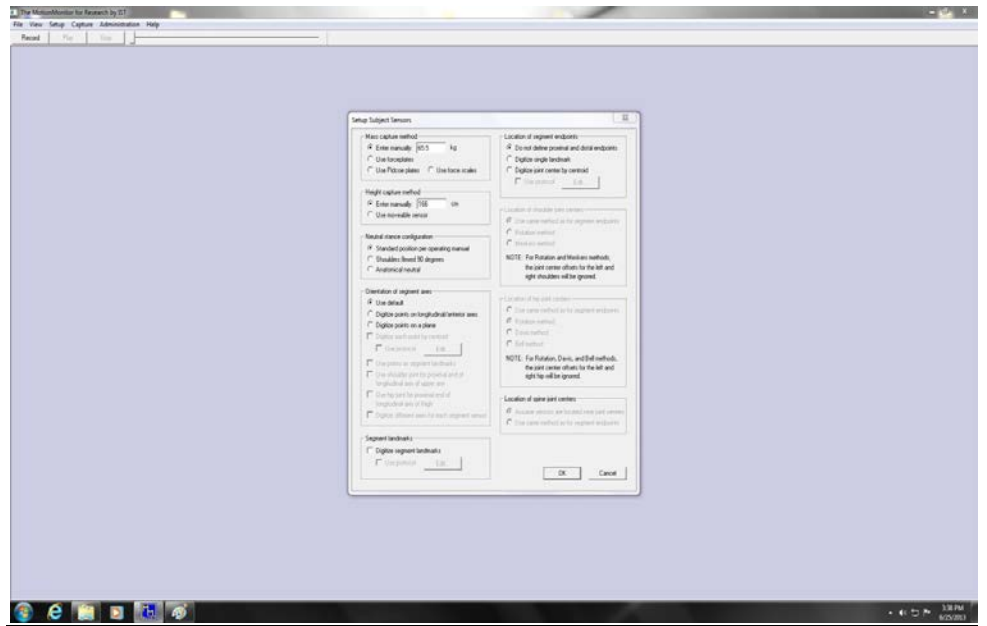


- v. Wait until Offset voltage values change.



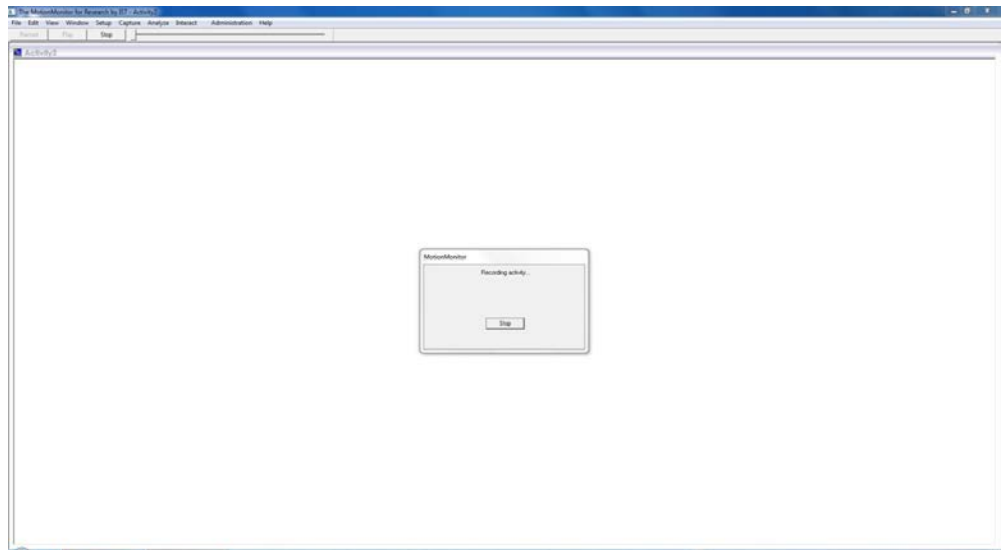
8. Set up Subject Sensors: (participant must stand still and straight position during setup subjects sensors)

- i. Go to Set up Menu >> Click on Setup Subject Sensor.
- ii. New window will pop-up: Setup Subject Sensor >> Enter weight and height of participant manually >> OK



9. Data Recording:

- i. Press Record
- ii. Recording activity >> when done: Click on **Stop**.

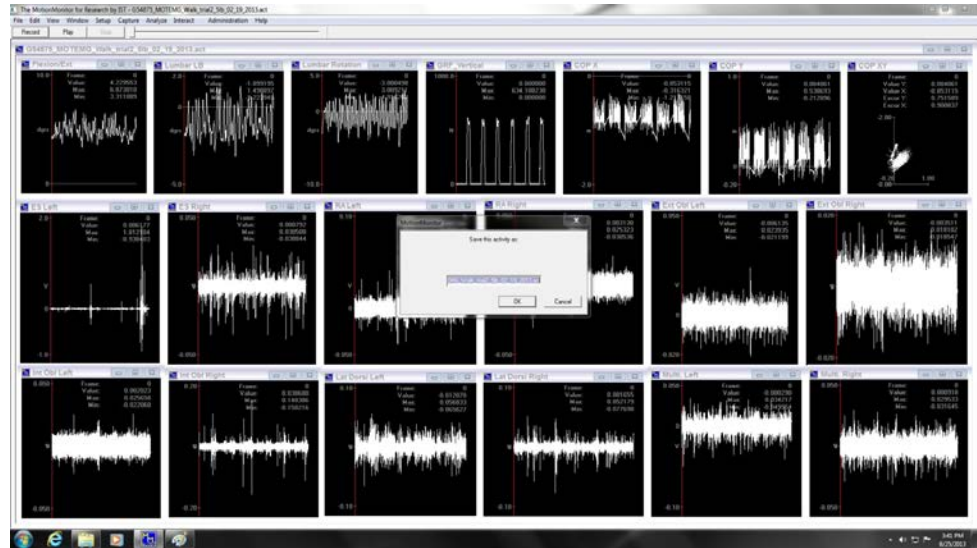


10. Result Window:



11. Save Data As:

- i. Go to File menu >> Save as
- ii. Save as activity >> Select user activity >> OK.
- iii. Save this activity as: Filename >> Ok.



Filename: “ParticipantID_MOTEMG_Walk_Trial_load_Date”.

For Example: “G54704_MOTEMG_Walk_trial1_0lb_11_16_2012”.

12. Repeat Step 9-11 for Different trials.

13. Close The Motion Monitor.

D. Data Exporting:

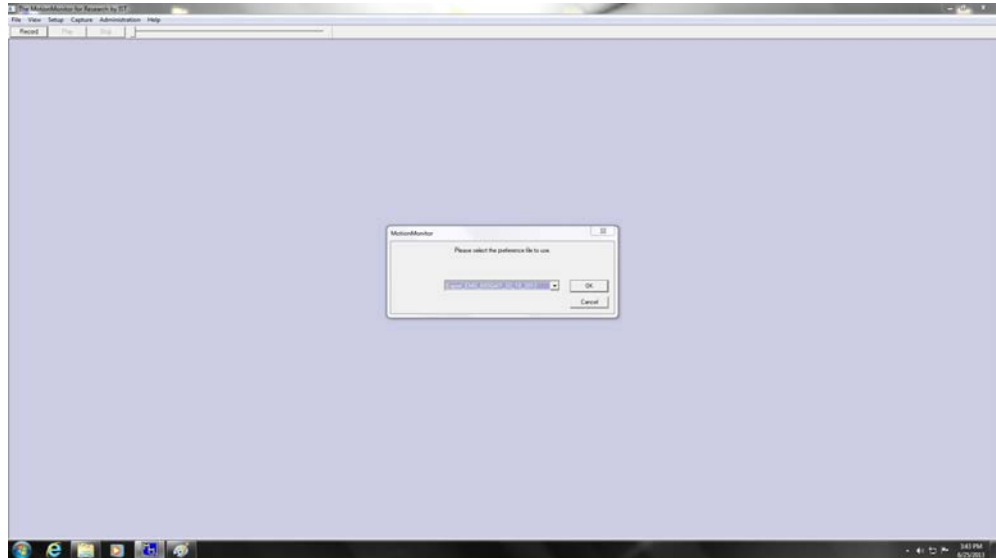
1. **Open Motion Monitor** >> Please select your User ID >> Test >> Ok.
2. **Select data to collect:**
 - i. Select Data-acquisition board data,
 - ii. Force/torque transducer data,
 - iii. Force scale data,
 - iv. EMG data.

3. **Load Preference File:** File >> Load Preference File >> Click on Setup and analysis.

i. Preference File Option >> Ok.

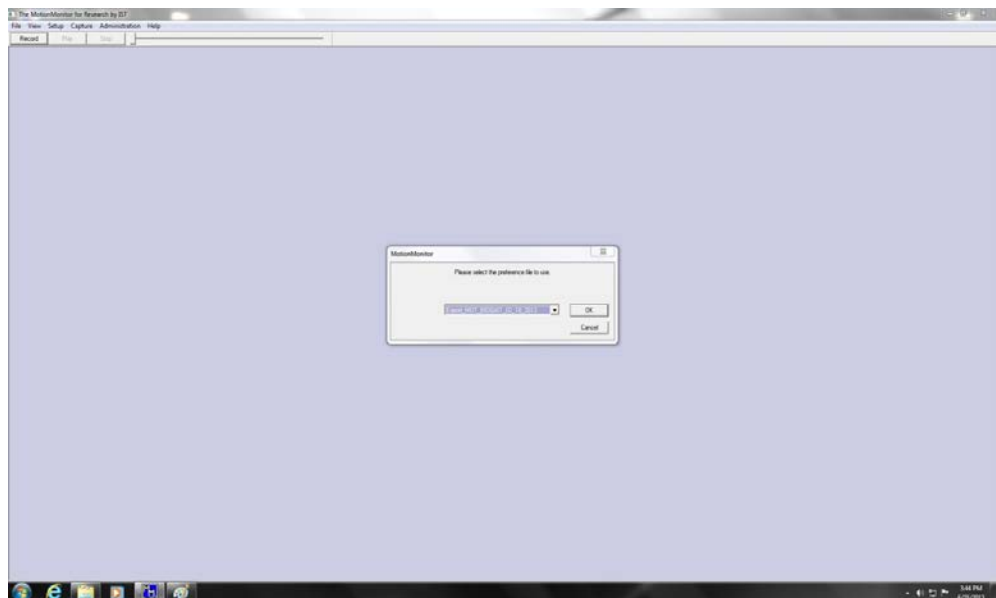
ii. Please select the preference file to use: For EMG Data:

EXPORT_EMG_BIOGAI_02_18_2013.

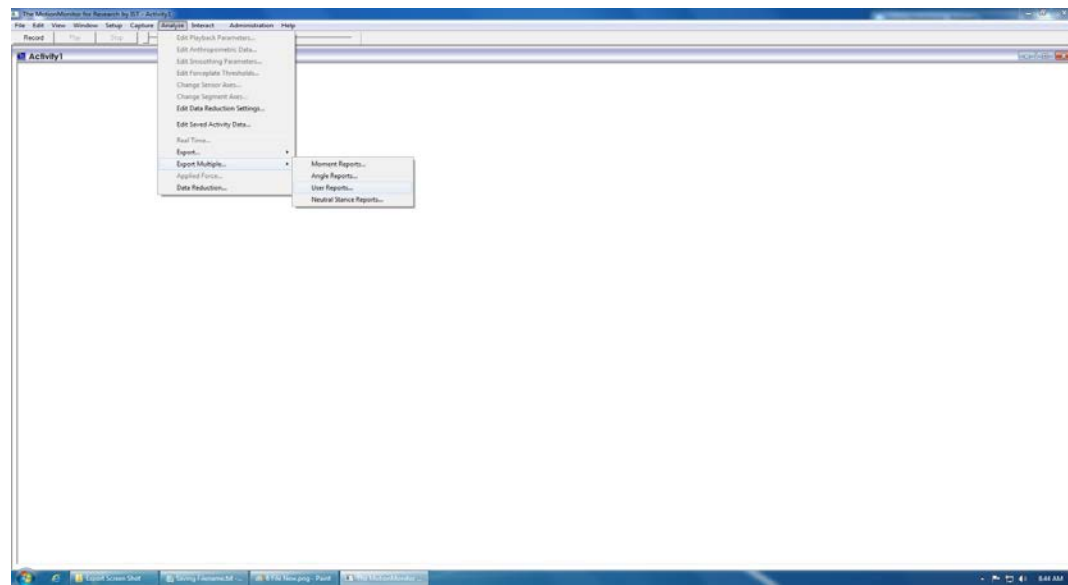


For Motion and Force Plate Data:

EXPORT_MOT_BIOGAI_02_18_2013.



4. **File >> Click on New.**
5. **Export: Analyze >> Export Multiple >> Click on User Reports.**



Select Orthopedic Angle Data

Please select the orthopedic angle data you want to analyze:

	NAME	ORTHOPEDIC ANGLE	DOMAIN		MIN	MAX	HIDE
<input checked="" type="checkbox"/>	Flexion/Ext	Lumbar Flex	Time	<input type="checkbox"/>	0.000	0.000	<input type="checkbox"/>
<input checked="" type="checkbox"/>	Lumbar LB	Lumbar Right Lateral Flex	Time	<input type="checkbox"/>	0.000	0.000	<input type="checkbox"/>
<input checked="" type="checkbox"/>	Lumbar Rotation	Lumbar Rotation	Time	<input type="checkbox"/>	0.000	0.000	<input type="checkbox"/>
<input checked="" type="checkbox"/>	Thorax flexion	Thoracic Flex	Time	<input type="checkbox"/>	0.000	0.000	<input checked="" type="checkbox"/>
<input checked="" type="checkbox"/>	Thoracic LB	Thoracic Right Lateral Flex	Time	<input type="checkbox"/>	0.000	0.000	<input checked="" type="checkbox"/>
<input checked="" type="checkbox"/>	Thoracic Rotation	Thoracic Rotation	Time	<input type="checkbox"/>	0.000	0.000	<input checked="" type="checkbox"/>
<input type="checkbox"/>		Cervical Flex	Time	<input type="checkbox"/>	0.000	0.000	<input type="checkbox"/>
<input type="checkbox"/>		Cervical Flex	Time	<input type="checkbox"/>	0.000	0.000	<input type="checkbox"/>
<input type="checkbox"/>		Cervical Flex	Time	<input type="checkbox"/>	0.000	0.000	<input type="checkbox"/>
<input type="checkbox"/>		Cervical Flex	Time	<input type="checkbox"/>	0.000	0.000	<input type="checkbox"/>
<input type="checkbox"/>		Cervical Flex	Time	<input type="checkbox"/>	0.000	0.000	<input type="checkbox"/>
<input type="checkbox"/>		Cervical Flex	Time	<input type="checkbox"/>	0.000	0.000	<input type="checkbox"/>
<input type="checkbox"/>		Cervical Flex	Time	<input type="checkbox"/>	0.000	0.000	<input type="checkbox"/>
<input type="checkbox"/>		Cervical Flex	Time	<input type="checkbox"/>	0.000	0.000	<input type="checkbox"/>
<input type="checkbox"/>		Cervical Flex	Time	<input type="checkbox"/>	0.000	0.000	<input type="checkbox"/>
<input type="checkbox"/>		Cervical Flex	Time	<input type="checkbox"/>	0.000	0.000	<input type="checkbox"/>
<input type="checkbox"/>		Cervical Flex	Time	<input type="checkbox"/>	0.000	0.000	<input type="checkbox"/>

Reset Page Reset All Back More... OK Cancel

Figure: Orthopedic Angle Selection

Select Forceplate Data

Please select the forceplate data you want to analyze:

----- REFERENCE FRAME -----

	NAME	FORCEPLATE	SEGMENT	SENSOR	POINT	DATA TYPE	DATA ELEMENT	DOMAIN	MIN	MAX	HIDE
<input checked="" type="checkbox"/>	GRF_Vertical	Forceplate #0	World			Force	Z	Time	600.000	1000.000	<input checked="" type="checkbox"/>
<input checked="" type="checkbox"/>	COP_X	Forceplate #0	World			Center Of Pressure	X	Time	0.000	0.000	<input type="checkbox"/>
<input checked="" type="checkbox"/>	COP_Y	Forceplate #0	World			Center Of Pressure	Y	Time	0.000	0.000	<input type="checkbox"/>
<input checked="" type="checkbox"/>	COP_XY	Forceplate #0	World			Center Of Pressure		Time	0.000	0.000	<input checked="" type="checkbox"/>
<input type="checkbox"/>		Forceplate #0	World			Force	X	Time	0.000	0.000	<input type="checkbox"/>
<input type="checkbox"/>		Forceplate #0	World			Force	X	Time	0.000	0.000	<input type="checkbox"/>
<input type="checkbox"/>		Forceplate #0	World			Force	X	Time	0.000	0.000	<input type="checkbox"/>
<input type="checkbox"/>		Forceplate #0	World			Force	X	Time	0.000	0.000	<input type="checkbox"/>
<input type="checkbox"/>		Forceplate #0	World			Force	X	Time	0.000	0.000	<input type="checkbox"/>
<input type="checkbox"/>		Forceplate #0	World			Force	X	Time	0.000	0.000	<input type="checkbox"/>
<input type="checkbox"/>		Forceplate #0	World			Force	X	Time	0.000	0.000	<input type="checkbox"/>
<input type="checkbox"/>		Forceplate #0	World			Force	X	Time	0.000	0.000	<input type="checkbox"/>
<input type="checkbox"/>		Forceplate #0	World			Force	X	Time	0.000	0.000	<input type="checkbox"/>
<input type="checkbox"/>		Forceplate #0	World			Force	X	Time	0.000	0.000	<input type="checkbox"/>
<input type="checkbox"/>		Forceplate #0	World			Force	X	Time	0.000	0.000	<input type="checkbox"/>
<input type="checkbox"/>		Forceplate #0	World			Force	X	Time	0.000	0.000	<input type="checkbox"/>
<input type="checkbox"/>		Forceplate #0	World			Force	X	Time	0.000	0.000	<input type="checkbox"/>
<input type="checkbox"/>		Forceplate #0	World			Force	X	Time	0.000	0.000	<input type="checkbox"/>
<input type="checkbox"/>		Forceplate #0	World			Force	X	Time	0.000	0.000	<input type="checkbox"/>

Reset Page Reset All Back More... OK Cancel

Figure: Force Plate Data

Select EMG Data

Please specify the EMG data you want to analyze:

	NAME	BOARD	CHANNEL	TRANSDUCER GAIN	LOWPASS FILTER (Hz)	HIGHPASS FILTER (Hz)	NOTCH FILTERS (Hz)										SIGNAL TYPE	RMS PD. (ms)	EVA	MIN	MAX	HIDE	
						
<input checked="" type="checkbox"/>	ES Left	0	6	1	<input checked="" type="checkbox"/> 500	<input checked="" type="checkbox"/> 20	<input type="checkbox"/>	<input type="checkbox"/>	<input type="checkbox"/>	<input type="checkbox"/>	<input type="checkbox"/>	<input type="checkbox"/>	<input type="checkbox"/>	<input type="checkbox"/>	<input type="checkbox"/>	<input type="checkbox"/>	Raw	100.000	EVA	<input type="checkbox"/>	0	0	<input type="checkbox"/>
<input checked="" type="checkbox"/>	ES Right	0	7	1	<input checked="" type="checkbox"/> 500	<input checked="" type="checkbox"/> 20	<input type="checkbox"/>	<input type="checkbox"/>	<input type="checkbox"/>	<input type="checkbox"/>	<input type="checkbox"/>	<input type="checkbox"/>	<input type="checkbox"/>	<input type="checkbox"/>	<input type="checkbox"/>	<input type="checkbox"/>	Raw	50.0000	EVA	<input type="checkbox"/>	0	0	<input type="checkbox"/>
<input checked="" type="checkbox"/>	RA Left	0	8	1	<input checked="" type="checkbox"/> 500	<input checked="" type="checkbox"/> 20	<input type="checkbox"/>	<input type="checkbox"/>	<input type="checkbox"/>	<input type="checkbox"/>	<input type="checkbox"/>	<input type="checkbox"/>	<input type="checkbox"/>	<input type="checkbox"/>	<input type="checkbox"/>	<input type="checkbox"/>	Raw	0	EVA	<input type="checkbox"/>	0	0	<input type="checkbox"/>
<input checked="" type="checkbox"/>	RA Right	0	9	1	<input checked="" type="checkbox"/> 500	<input checked="" type="checkbox"/> 20	<input type="checkbox"/>	<input type="checkbox"/>	<input type="checkbox"/>	<input type="checkbox"/>	<input type="checkbox"/>	<input type="checkbox"/>	<input type="checkbox"/>	<input type="checkbox"/>	<input type="checkbox"/>	<input type="checkbox"/>	Raw	0	EVA	<input type="checkbox"/>	0	0	<input type="checkbox"/>
<input checked="" type="checkbox"/>	Ext Obl Left	0	10	1	<input checked="" type="checkbox"/> 500	<input checked="" type="checkbox"/> 20	<input type="checkbox"/>	<input type="checkbox"/>	<input type="checkbox"/>	<input type="checkbox"/>	<input type="checkbox"/>	<input type="checkbox"/>	<input type="checkbox"/>	<input type="checkbox"/>	<input type="checkbox"/>	<input type="checkbox"/>	Raw	0	EVA	<input type="checkbox"/>	0	0	<input type="checkbox"/>
<input checked="" type="checkbox"/>	Ext Obl Right	0	11	1	<input checked="" type="checkbox"/> 500	<input checked="" type="checkbox"/> 20	<input checked="" type="checkbox"/>	<input type="checkbox"/>	Raw	9.99999	EVA	<input type="checkbox"/>	0	0	<input type="checkbox"/>								
<input checked="" type="checkbox"/>	Int Obl Left	0	12	1	<input checked="" type="checkbox"/> 500	<input checked="" type="checkbox"/> 20	<input checked="" type="checkbox"/>	<input type="checkbox"/>	Raw	9.99999	EVA	<input type="checkbox"/>	-0.5	0.5	<input type="checkbox"/>								
<input checked="" type="checkbox"/>	Int Obl Right	0	13	1	<input checked="" type="checkbox"/> 500	<input checked="" type="checkbox"/> 20	<input checked="" type="checkbox"/>	<input type="checkbox"/>	Raw	200.000	EVA	<input type="checkbox"/>	0	0	<input type="checkbox"/>								
<input checked="" type="checkbox"/>	Lat Dorsi Left	0	14	1	<input checked="" type="checkbox"/> 500	<input checked="" type="checkbox"/> 20	<input checked="" type="checkbox"/>	<input type="checkbox"/>	Raw	200.000	EVA	<input type="checkbox"/>	0	0.2	<input type="checkbox"/>								
<input checked="" type="checkbox"/>	Lat Dorsi Right	0	15	1	<input checked="" type="checkbox"/> 500	<input checked="" type="checkbox"/> 20	<input type="checkbox"/>	<input type="checkbox"/>	<input type="checkbox"/>	<input type="checkbox"/>	<input type="checkbox"/>	<input type="checkbox"/>	<input type="checkbox"/>	<input type="checkbox"/>	<input type="checkbox"/>	<input type="checkbox"/>	Raw	0	EVA	<input type="checkbox"/>	0	0	<input type="checkbox"/>
<input checked="" type="checkbox"/>	ES Left	0	6	1	<input checked="" type="checkbox"/> 500	<input checked="" type="checkbox"/> 20	<input type="checkbox"/>	<input type="checkbox"/>	<input type="checkbox"/>	<input type="checkbox"/>	<input type="checkbox"/>	<input type="checkbox"/>	<input type="checkbox"/>	<input type="checkbox"/>	<input type="checkbox"/>	<input type="checkbox"/>	RMS	250	EVA	<input type="checkbox"/>	0	0	<input checked="" type="checkbox"/>
<input checked="" type="checkbox"/>	ES Right	0	7	1	<input checked="" type="checkbox"/> 500	<input checked="" type="checkbox"/> 20	<input type="checkbox"/>	<input type="checkbox"/>	<input type="checkbox"/>	<input type="checkbox"/>	<input type="checkbox"/>	<input type="checkbox"/>	<input type="checkbox"/>	<input type="checkbox"/>	<input type="checkbox"/>	<input type="checkbox"/>	RMS	250	EVA	<input type="checkbox"/>	0	0	<input checked="" type="checkbox"/>
<input checked="" type="checkbox"/>	RA Left	0	8	1	<input checked="" type="checkbox"/> 500	<input checked="" type="checkbox"/> 20	<input type="checkbox"/>	<input type="checkbox"/>	<input type="checkbox"/>	<input type="checkbox"/>	<input type="checkbox"/>	<input type="checkbox"/>	<input type="checkbox"/>	<input type="checkbox"/>	<input type="checkbox"/>	<input type="checkbox"/>	RMS	250	EVA	<input type="checkbox"/>	0	0	<input checked="" type="checkbox"/>
<input checked="" type="checkbox"/>	RA Right	0	9	1	<input checked="" type="checkbox"/> 500	<input checked="" type="checkbox"/> 20	<input type="checkbox"/>	<input type="checkbox"/>	<input type="checkbox"/>	<input type="checkbox"/>	<input type="checkbox"/>	<input type="checkbox"/>	<input type="checkbox"/>	<input type="checkbox"/>	<input type="checkbox"/>	<input type="checkbox"/>	RMS	250	EVA	<input type="checkbox"/>	0	0	<input checked="" type="checkbox"/>
<input checked="" type="checkbox"/>	Ext Obl Left	0	10	1	<input checked="" type="checkbox"/> 500	<input checked="" type="checkbox"/> 20	<input type="checkbox"/>	<input type="checkbox"/>	<input type="checkbox"/>	<input type="checkbox"/>	<input type="checkbox"/>	<input type="checkbox"/>	<input type="checkbox"/>	<input type="checkbox"/>	<input type="checkbox"/>	<input type="checkbox"/>	RMS	250	EVA	<input type="checkbox"/>	0	0	<input checked="" type="checkbox"/>
<input checked="" type="checkbox"/>	Ext Obl Right	0	11	1	<input checked="" type="checkbox"/> 500	<input checked="" type="checkbox"/> 20	<input type="checkbox"/>	<input type="checkbox"/>	<input type="checkbox"/>	<input type="checkbox"/>	<input type="checkbox"/>	<input type="checkbox"/>	<input type="checkbox"/>	<input type="checkbox"/>	<input type="checkbox"/>	<input type="checkbox"/>	RMS	250	EVA	<input type="checkbox"/>	0	0	<input checked="" type="checkbox"/>

Reset Page Reset All Notch Settings... Back More OK Cancel

Select EMG Data ☰

Please specify the EMG data you want to analyze:

NAME	BOARD	CHANNEL	TRANSDUCER GAIN	LOWPASS FILTER (Hz)	HIGHPASS FILTER (Hz)	NOTCH FILTERS (Hz)										SIGNAL TYPE	RMS PD. (ms)	EVA	MIN	MAX	HIDE		
						1	2	3	4	5	6	7	8	9	10							11	12
<input checked="" type="checkbox"/> Int Obl Left	0	12	1	<input checked="" type="checkbox"/> 500	<input checked="" type="checkbox"/> 20	<input type="checkbox"/>	RMS	250	EVA	<input type="checkbox"/>	0	0	<input checked="" type="checkbox"/>										
<input checked="" type="checkbox"/> Int Obl Right	0	13	1	<input checked="" type="checkbox"/> 500	<input checked="" type="checkbox"/> 20	<input type="checkbox"/>	RMS	250	EVA	<input type="checkbox"/>	0	0	<input checked="" type="checkbox"/>										
<input checked="" type="checkbox"/> Lat Dorsi Left	0	14	1	<input checked="" type="checkbox"/> 500	<input checked="" type="checkbox"/> 20	<input type="checkbox"/>	RMS	250	EVA	<input type="checkbox"/>	0	0	<input checked="" type="checkbox"/>										
<input checked="" type="checkbox"/> Lat Dorsi Right	0	15	1	<input checked="" type="checkbox"/> 500	<input checked="" type="checkbox"/> 20	<input type="checkbox"/>	RMS	250	EVA	<input type="checkbox"/>	0	0	<input checked="" type="checkbox"/>										
<input checked="" type="checkbox"/> ES Left	0	6	1	<input checked="" type="checkbox"/> 500	<input checked="" type="checkbox"/> 20	<input type="checkbox"/>	PSD	0	EVA	<input type="checkbox"/>	0	0	<input checked="" type="checkbox"/>										
<input checked="" type="checkbox"/> ES Right	0	7	1	<input checked="" type="checkbox"/> 500	<input checked="" type="checkbox"/> 20	<input type="checkbox"/>	PSD	0	EVA	<input type="checkbox"/>	0	0	<input checked="" type="checkbox"/>										
<input checked="" type="checkbox"/> RA Left	0	8	1	<input checked="" type="checkbox"/> 500	<input checked="" type="checkbox"/> 20	<input type="checkbox"/>	PSD	0	EVA	<input type="checkbox"/>	0	0	<input checked="" type="checkbox"/>										
<input checked="" type="checkbox"/> RA Right	0	9	1	<input checked="" type="checkbox"/> 500	<input checked="" type="checkbox"/> 20	<input type="checkbox"/>	PSD	0	EVA	<input type="checkbox"/>	0	0	<input checked="" type="checkbox"/>										
<input checked="" type="checkbox"/> Ext Obl Left	0	10	1	<input checked="" type="checkbox"/> 500	<input checked="" type="checkbox"/> 20	<input type="checkbox"/>	PSD	0	EVA	<input type="checkbox"/>	0	0	<input checked="" type="checkbox"/>										
<input checked="" type="checkbox"/> Ext Obl Right	0	11	1	<input checked="" type="checkbox"/> 500	<input checked="" type="checkbox"/> 20	<input type="checkbox"/>	PSD	0	EVA	<input type="checkbox"/>	0	0	<input checked="" type="checkbox"/>										
<input checked="" type="checkbox"/> Int Obl Left	0	12	1	<input checked="" type="checkbox"/> 500	<input checked="" type="checkbox"/> 20	<input type="checkbox"/>	PSD	0	EVA	<input type="checkbox"/>	0	0	<input checked="" type="checkbox"/>										
<input checked="" type="checkbox"/> Int Obl Right	0	13	1	<input checked="" type="checkbox"/> 500	<input checked="" type="checkbox"/> 20	<input type="checkbox"/>	PSD	0	EVA	<input type="checkbox"/>	0	0	<input checked="" type="checkbox"/>										
<input checked="" type="checkbox"/> Lat Dorsi Left	0	14	1	<input checked="" type="checkbox"/> 500	<input checked="" type="checkbox"/> 20	<input type="checkbox"/>	PSD	0	EVA	<input type="checkbox"/>	0	0	<input checked="" type="checkbox"/>										
<input checked="" type="checkbox"/> Lat Dorsi Right	0	15	1	<input checked="" type="checkbox"/> 500	<input checked="" type="checkbox"/> 20	<input type="checkbox"/>	PSD	0	EVA	<input type="checkbox"/>	0	0	<input checked="" type="checkbox"/>										
<input checked="" type="checkbox"/> Multi Left	1	0	1	<input checked="" type="checkbox"/> 500	<input checked="" type="checkbox"/> 20	<input type="checkbox"/>	Raw	0	EVA	<input type="checkbox"/>	0	0	<input type="checkbox"/>										
<input checked="" type="checkbox"/> Multi Right	1	1	1	<input checked="" type="checkbox"/> 500	<input checked="" type="checkbox"/> 20	<input type="checkbox"/>	Raw	0	EVA	<input type="checkbox"/>	0	0	<input type="checkbox"/>										

Reset Page Reset All Notch Settings... Back More OK Cancel

Select EMG Data ☰

Please specify the EMG data you want to analyze:

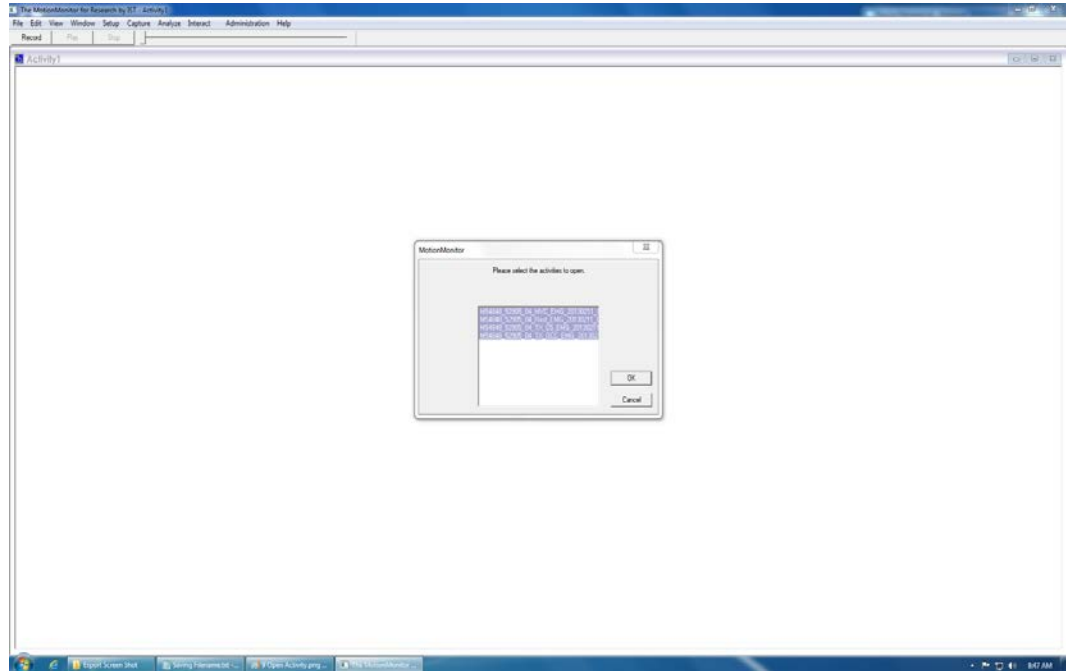
NAME	BOARD	CHANNEL	TRANSDUCER GAIN	LOWPASS FILTER (Hz)	HIGHPASS FILTER (Hz)	NOTCH FILTERS (Hz)										SIGNAL TYPE	RMS PD. (ms)	EVA	MIN	MAX	HIDE		
						1	2	3	4	5	6	7	8	9	10							11	12
<input checked="" type="checkbox"/> Multi Left	1	0	1	<input checked="" type="checkbox"/> 500	<input checked="" type="checkbox"/> 20	<input type="checkbox"/>	RMS	250	EVA	<input type="checkbox"/>	0	0	<input checked="" type="checkbox"/>										
<input checked="" type="checkbox"/> Multi Right	1	1	1	<input checked="" type="checkbox"/> 500	<input checked="" type="checkbox"/> 20	<input type="checkbox"/>	RMS	250	EVA	<input type="checkbox"/>	0	0	<input checked="" type="checkbox"/>										
<input checked="" type="checkbox"/> Multi Left	1	0	1	<input checked="" type="checkbox"/> 500	<input checked="" type="checkbox"/> 20	<input type="checkbox"/>	PSD	0	EVA	<input type="checkbox"/>	0	0	<input checked="" type="checkbox"/>										
<input checked="" type="checkbox"/> Multi Right	1	1	1	<input checked="" type="checkbox"/> 500	<input checked="" type="checkbox"/> 20	<input type="checkbox"/>	PSD	0	EVA	<input type="checkbox"/>	0	0	<input checked="" type="checkbox"/>										
<input type="checkbox"/>	0	0	1	<input type="checkbox"/> 0	<input type="checkbox"/> 0	<input type="checkbox"/>	Raw	0	EVA	<input type="checkbox"/>	0	0	<input type="checkbox"/>										
<input type="checkbox"/>	0	0	1	<input type="checkbox"/> 0	<input type="checkbox"/> 0	<input type="checkbox"/>	Raw	0	EVA	<input type="checkbox"/>	0	0	<input type="checkbox"/>										
<input type="checkbox"/>	0	0	1	<input type="checkbox"/> 0	<input type="checkbox"/> 0	<input type="checkbox"/>	Raw	0	EVA	<input type="checkbox"/>	0	0	<input type="checkbox"/>										
<input type="checkbox"/>	0	0	1	<input type="checkbox"/> 0	<input type="checkbox"/> 0	<input type="checkbox"/>	Raw	0	EVA	<input type="checkbox"/>	0	0	<input type="checkbox"/>										
<input type="checkbox"/>	0	0	1	<input type="checkbox"/> 0	<input type="checkbox"/> 0	<input type="checkbox"/>	Raw	0	EVA	<input type="checkbox"/>	0	0	<input type="checkbox"/>										
<input type="checkbox"/>	0	0	1	<input type="checkbox"/> 0	<input type="checkbox"/> 0	<input type="checkbox"/>	Raw	0	EVA	<input type="checkbox"/>	0	0	<input type="checkbox"/>										
<input type="checkbox"/>	0	0	1	<input type="checkbox"/> 0	<input type="checkbox"/> 0	<input type="checkbox"/>	Raw	0	EVA	<input type="checkbox"/>	0	0	<input type="checkbox"/>										
<input type="checkbox"/>	0	0	1	<input type="checkbox"/> 0	<input type="checkbox"/> 0	<input type="checkbox"/>	Raw	0	EVA	<input type="checkbox"/>	0	0	<input type="checkbox"/>										
<input type="checkbox"/>	0	0	1	<input type="checkbox"/> 0	<input type="checkbox"/> 0	<input type="checkbox"/>	Raw	0	EVA	<input type="checkbox"/>	0	0	<input type="checkbox"/>										
<input type="checkbox"/>	0	0	1	<input type="checkbox"/> 0	<input type="checkbox"/> 0	<input type="checkbox"/>	Raw	0	EVA	<input type="checkbox"/>	0	0	<input type="checkbox"/>										
<input type="checkbox"/>	0	0	1	<input type="checkbox"/> 0	<input type="checkbox"/> 0	<input type="checkbox"/>	Raw	0	EVA	<input type="checkbox"/>	0	0	<input type="checkbox"/>										

Reset Page Reset All Notch Settings... Back More OK Cancel

Figure: EMG data

6. Open Activity >> User Activity >> Ok.

7. Please Select the activities to open >> choose activities >> Ok.



8. Export Location >> Default Folder >> Ok.

9. Export Done.